Human Metapneumovirus

Evolution And Interaction With The Innate Immune system

Kevin Groen

Human Metapneumovirus

Evolution and Interaction with the Innate Immune System

Kevin Groen

Author: Kevin Groen
Provided by thesis specialist Ridderprint, ridderprint.nl
Printing: Ridderprint
Layout and design: Jacolijn de Krom, persoonlijkproefschrift.nl
Cover art: BernArt Visuals

Human Metapneumovirus
Evolution and Interaction with the Innate Immune System.

Humaan metapneumovirus
Evolutie en interactie met het aangeboren immuunsysteem

Thesis

to obtain the degree of Doctor from the
Erasmus University Rotterdam
by command of the
rector magnificus

Prof. dr. A.L. Bredenoord

and in accordance with the decision of the Doctorate Board.
The public defence shall be held on

Wednesday 27 September 2023 at 15.30 hrs
by

Kevin Groen
born in Leiden, the Netherlands.

Erasmus University Rotterdam

Doctoral Committee:

Promotor:	Prof. dr. R.A.M. Fouchier
Other members:	Prof. dr. M.P.G. Koopmans Prof. dr. A.M.C. van Rossum Prof. dr. L. Bont
Copromotor:	Dr. B.G. van den Hoogen

Table of content

1

Thesis introduction

Human metapneumovirus

The Human metapneumovirus (HMPV), at first a member of the *Pneumoviridae* family, was first characterized in 2001 in the Netherlands (1). Although identified in 2001, retrospective serology studies demonstrated that the virus has been circulating for at least the past 65 years (1). After the identification, multiple studies worldwide demonstrated that between 515% of hospitalizations due to respiratory tract infections (RTI) in children and adults are caused by an HMPV infection (2–7). The most susceptible individuals for an HMPV infection are young children in which HMPV is the second leading causative agent of RTIs, only second after Respiratory Syncytial Virus (RSV), the closest related mammalian virus and also a member of the *Pneumoviridae* family (7–14). Young children between the age of 6-12 months are most at risk for HMPV infections, and virtually all children are infected with HMPV by the age of five (3, 9, 15–18). In addition to young children, the elderly and immunocompromised individuals have shown to be risk groups for severe HMPV infections (19–24). The clinical symptoms caused by HMPV infections are very similar to those caused by RSV infections, varying from mild respiratory illness including cough, throat soreness, wheezing, rhinorrhea, and fever, to more severe bronchiolitis and pneumonia (4, 7, 25, 26). For both HMPV and RSV infections (7, 27), asthma has been reported as risk factor for severe disease, while both viruses have also been indicated as risk factor for the development or exacerbation of asthma (28). Clearance of an HMPV infection does not necessarily result in long-lasting immunity against the virus, as reinfections with HMPV readily occur with either homologous or heterologous viruses (29, 30). These reinfections might be explained by waning antibody titers over time (29–31). HMPV has an annual seasonality similar to that of RSV, with most reported cases in the late winter and early spring, while the peak incidence of HMPV infections typically follows that of the RSV season (7).

Genome organization and virion structure

HMPV is a negative-sense, non-segmented, single-stranded RNA (-ssRNA) virus with a genome length of approximately 13,3kb (32). HMPV virions are pleomorphic and range in size between 150 and 600 nm (1). The genome contains eight genes that encode nine proteins: nucleoprotein (N), phosphoprotein (P), matrix protein (M), fusion protein (F), two matrix 2 proteins (M2-1 and M2-2), short hydrophobic protein (SH), glycoprotein (G), and large polymerase protein (L) (32). Although the genomes of HMPV and RSV are quite similar, the gene order is different and HMPV lacks the NS1 and NS2 genes that are present in the RSV genome, which encode non-structural proteins that function as interferon (IFN)antagonists (32). The core of the virion contains genomic RNA that is encapsidated by the N protein. While each N protein of RSV binds 7 bases of RNA (33, 34), data on the RNA binding capacity of the HMPV N protein is lacking.

The encapsidated RNA is associated with tetrameric P, M2-1, and L, collectively referred to as the ribonucleoprotein complex (RNP). The RNA-dependent RNA polymerase (RdRp) L protein harbors the catalytic activities required for two distinct roles: genome replication and transcription (35). The P protein acts as a polymerase co-factor (36). The RSV M2-1 protein has been described to function as transcription anti-termination factor that enhances polymerase read through at gene-end signal sequences (37), making the M2-1 protein essential for the synthesis of full-length viral mRNAs (37–40). The function of the HMPV M2-1 protein appears to differ from that of RSV, as HMPV M2-1 is not essential for virus replication, but rather improves transcription efficiency (41, 42). Viruses lacking M2-1 protein expression are highly attenuated (41), and phosphorylation of amino acid residues S57 and S60 of the M2-1 protein increases RNA replication and mRNA transcription (43). So far, little is known about the function of the HMPV M2-2 protein. Viruses lacking M2-2 protein expression were shown to have increased viral gene expression relative to the number of genome copies (41, 44), suggesting that the M2-2 protein functions as a regulator of the switch between transcription and replication, similar as described for the M2-2 protein of RSV. Interestingly, HMPV lacking M2-2 protein expression accumulated excessive mutations in parts of the virus genome (44), suggesting an additional function for the M22 protein in preventing accumulation of mutations.

The HMPV RNP is located within a layer of M protein, which is surrounded by an envelope derived from the host-cell. The envelope contains three viral surface glycoproteins: G, F, and SH. The G protein binds the receptor(s) on the hostcell, which are currently unknown, although there are implications for the use of heparin sulfate or glycosaminoglycans (GAGs) in 2D culture models (45, 46). It has been shown that the RSV G protein targets CX3CR1 on human airway epithelial cells to mediate viral attachment and subsequent infection (47, 48). As the HMPV and RSV G proteins share no discernible sequence homology, the cellular target of the HMPV G protein cannot be simply inferred from that of RSV (32). The F protein that is present on the virion as a homotrimer is responsible for fusion between the viral envelope and the host-cell membrane, mediating entry (49), and is the primary target of neutralizing antibodies (50, 51). The function of the SH protein is not fully understood (52), although it has been suggested to function as a viroporin (53). In addition to their primary functions, the G, SH, and M2-2 proteins were suggested to be involved in viral evasion of innate immune responses, which is later discussed in more detail.

Replication cycle

The HMPV replication cycle, which is strictly bound to the cytoplasm (depicted in Figure 1), begins with attachment of the G protein to cellular receptors, which brings the F protein in close proximity to the cell membrane. The F protein initiates fusion of the viral and cellular membranes independently

of other glycoproteins, which is a feature of *Pneumoviruses* that contrasts the fusion event of *Paramyxoviruses* ((54, 55), and reviewed in (56)). Deletion of the SH and G ORFs resulted in a virus that could replicate in cell culture models and in the respiratory tract of hamsters (57), demonstrating that the HMPV F protein is capable of both attachment and membrane fusion without involvement (or independent of) other glycoproteins**.** However, the G protein is clearly important, as viruses lacking G protein expression are attenuated in both cell culture models and *in vivo* models (57–59). Of note, many aspects of pneumovirus replication and transcription have been inferred from aspects of replication and transcription of paramyxoviruses. For example, after fusion of the viral and cellular membranes, the RNP is released into the cytoplasm which serves as template for the viral polymerase to initiate replication (reviewed in (60)). The viral RNA (vRNA) contains promoter sequences at both the 3′ leader and 5′ trailer sequences. Following entry, replication of the vRNA starts by recruitment of the L protein at the 3′ leader sequence, at which transcription of a positive stranded full-length genome copy of the RNA (cRNA) is initiated, also known as the antigenome. Transcription of the genome is initiated from a second promoter sequence at the 3′ leader region, which occurs through a

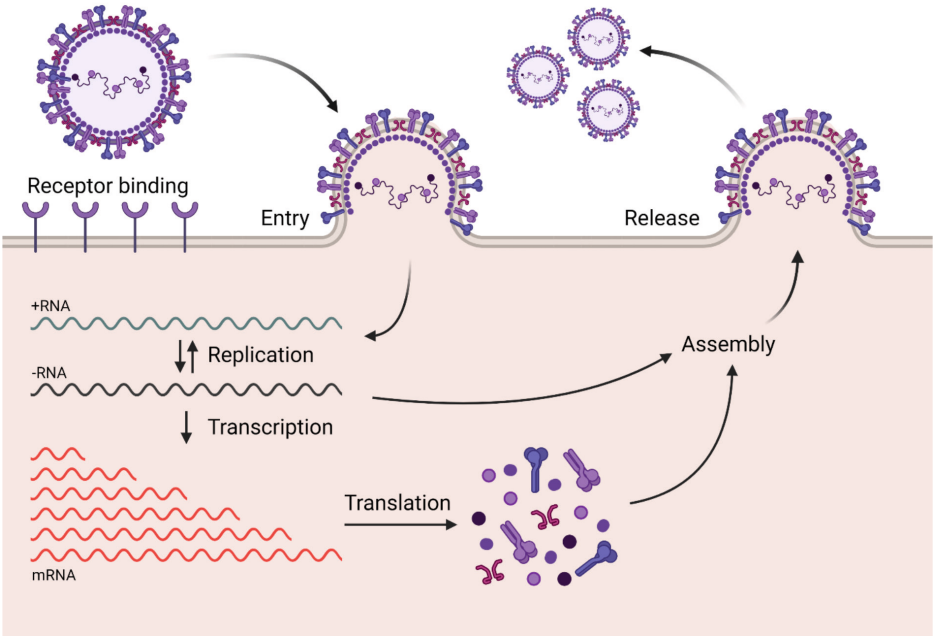

Figure 1. Schematic overview of the HMPV replication cycle. Image generated with Biorender.

sequential terminationreinitiation mechanism (37). This mechanism is regulated by genestart (GS) and geneend (GE) sequences present at each gene, resulting in transcription of subgenomic mRNAs (61), which are translated into each individual viral protein. These transcription and replication processes are suggested to occur in cellular membraneless organelles, called inclusion bodies (IBs), at which viral proteins required for replication are incorporated (N, P, M2-1, L)(62)(63). For HMPV, IBs were shown to incorporate vRNA, mRNA, and replication proteins N and P, while excluding the assembly proteins M and F (62). From these IBs, nascent vRNA strands that are replicated from the cRNA must be translocated to the cell membrane for virion assembly. While the mechanism for this is not fully understood, a role for the actin cytoskeleton has been implicated for this process (62, 64). At the cell membrane, new virions are assembled that leave the cell by budding, which are ready for transmission to new, uninfected cells. HMPV transmission can occur canonically through budding of virus particles from the host cell membrane, followed by attachment to a new cell. However, *in vitro* viral transmission through cell-to-cell fusion has also been described (64, 65). This process occurs through accumulation of the F protein at the cell surface of infected cells which subsequently bind to the membranes of neighboring cells, resulting in fusion of both cells and formation of large, multinucleated cells known as syncytia (reviewed in (66)). Another mechanism of viral spread is through intercellular extensions that have been observed during HMPV infection (64). These cellular extensions were shown to contain smaller filaments at which viral proteins as well as vRNA were present that could potentially be delivered to neighboring cells. This transmission route could present a favorable way of rapid viral spread without a potential interaction with extracellular, neutralizing antibodies, although evidence of this transmission route *in vivo* is lacking (65).

HMPV classification, nomenclature, and evolution

Monitoring virus evolution is crucial for keeping diagnostic assays up-to-date, studying virus epidemiology, identifying transmission events and nosocomial outbreaks, and design of vaccines or intervention strategies. Studies on HMPV evolution have focused on sequencing of the F and G genes (4, 67–73). The G protein is the most variable protein of HMPV, with amino acid (AA) sequence homologies between lineage A and B viruses as low as 30.0% (67). In contrast, the F protein is more conserved, with sequence homologies between lineage A and B viruses as low as 93.7% (74). Initial studies of the antigenic diversity of HMPV demonstrated circulation of two main lineages, A and B, that were antigenically distinct. These two main lineages genetically diverged into sublineages A1, A2, B1, and B2 (67). In 2006, lineage A2 was suggested to diverge into lineages A2a and A2b (75), followed by a suggested divergence within lineage A2b into lineages A2b1 and A2b2 (68). More recently, two separate duplication events in

the G gene of viruses within lineage A2b2 were reported, with a length of 111 or 180 nucleotides (69, 70). Although first reported in Japan, these viruses were later also detected in Spain and China (71, 76). Viruses carrying a 111-nucleotide duplication in the G gene became the dominant circulating viruses in Yokohama city in Japan (71). Additionally, viruses carrying a duplication in the G gene increased in prevalence in Spain from 2014-2017 (77). Although the function of these duplications in the G gene have not been studied yet, similar duplication events have been described for RSV (78–80). One RSV study suggested that viruses with a duplication in the G gene have an improved attachment efficiency to target cells (81). These evolutionary events highlight the importance to monitor HMPV evolution.

Despite the need to easily classify both RSV and HMPV strains, a unified classification and nomenclature system for both of these viruses is lacking. Most of the methods used to classify RSV are based on pairwise distances between viral G gene sequences (*p*-distances) (82, 83). However, the length as well as the number of sequences affect *p*distance calculations and these calculations require regular updating due to increasing numbers of available sequences. In addition, RSV names represent the origin of the first isolate (e.g. BA for Buenos Aires or ON1 for Ontario 1), rather than providing information about the virus lineage (e.g. A2) (84). HMPV lineages have mostly been classified based on *p*-distances, or simply by visually inferring lineages from phylogenetic trees (67, 68, 85). For HMPV, the field of studying evolution is still in its infancy, which could facilitate implementing unified classification and nomenclature systems.

Innate immunity against RNA virus infection

Sensing of incoming viral pathogens starts by the recognition of pathogen associated molecular patterns (PAMPs) by Pattern Recognition Receptors (PRRs). Well described PRRs include three categories: Toll-like receptors (TLRs) (86), nucleotide binding oligomerization domain (NOD)-like receptors (NLRs) (87), and retinoic acid inducible-gene 1 (RIG-I)-like receptors (RLRs) (88). RLRs are the most important PRRs for RNA viruses (89). Sensing of PAMPs by PRRs activates a downstream signaling cascade that almost always results in the production and secretion of IFNs, which is the hallmark of innate immunity to viral infections.

RLRs are intracellular receptors that are known to recognize cytosolic RNAs (reviewed in (90)). Members of the RLR protein family include RIG-I and melanoma differentiation associated gene-5 (MDA-5), which are expressed in virtually all cell types (91–93)**.** RIG-I senses 5′-triphosporylated RNA and short dsRNA, while MDA-5 is activated by recognition of long, dsRNA that can be produced during RNA virus infection (93). As cellular mRNAs contain a 5′-cap and dsRNA is not produced during any stage of the cell cycle, RLRs can discriminate between foreign and cellular RNA species. Upon sensing of PAMPS, RIG-I or MDA-5 associates with the caspase activation and recruitment (CARD) domain

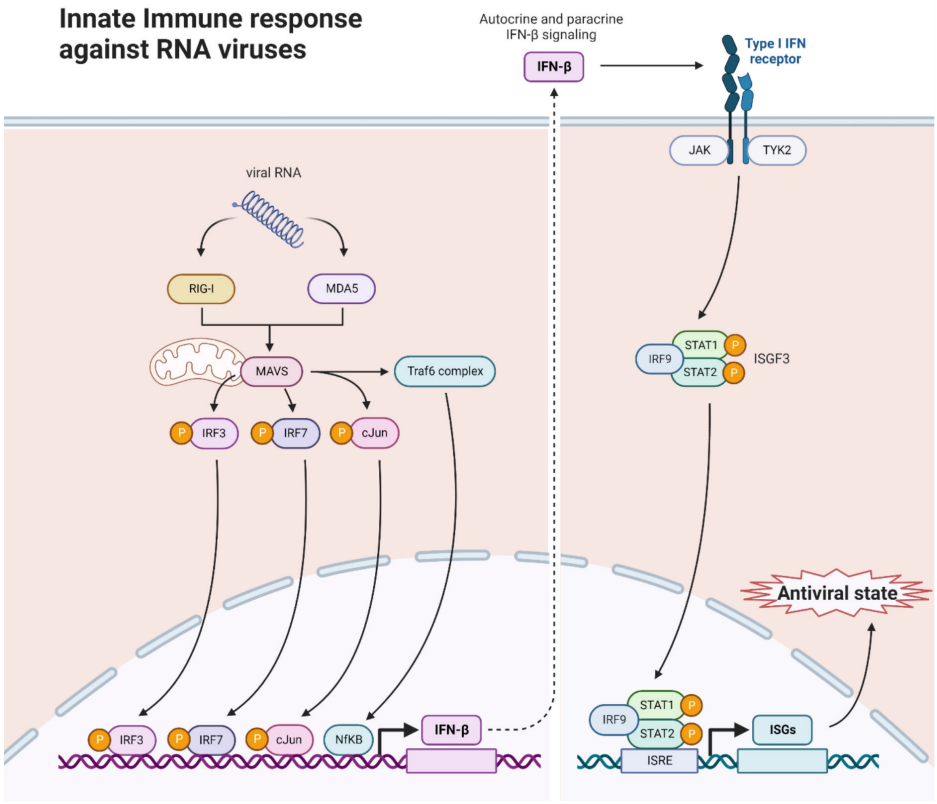

Figure 2. Simplified RLR signaling pathway upon sensing of RNA virus infections, leading to production of type-I IFNs. IFN-*β* production and signaling are shown. Type-I IFNs bind the receptor and signal through the Jak-STAT signaling pathway to induce expression of ISGs, causing the cell to enter an antiviral state. Image generated with Biorender.

of the downstream adaptor mitochondrial antiviral signaling (MAVS) protein. This leads to the activation of NF-κB, IRF3, and IRF7, subsequently leading to the expression cytokines, chemokines, and IFNs (Figure 2)(reviewed in (90)).

IFNs can be classified into three protein families: typeI, typeII, and typeIII IFNs. The type-I IFN protein family in humans, first identified in 1957 (94), includes IFN-α (divided into 13 subtypes), IFNβ, IFNε, IFNκ, and IFNω (reviewed in (95)). Of these, IFN-α and IFN-β have been elaborately described, while studies on IFNε, IFNκ, and IFNω are relatively limited. Most cell types produce IFNβ, while IFNα is predominantly produced by dendritic cells . The type-II IFN family consists of only IFN-γ and is mainly produced by natural killer cells and innate lymphoid cells (96, 97). IFN-γ plays an important role in orchestrating the transition from innate to adaptive immune responses against viruses. Type-III IFNs include four subtypes: IFNλ-1 (IL-29), IFN-λ2 (IL-28A), IFN-λ3 (IL-28B), and IFN-λ4 (98–100). While type-I IFNs are produced in most cell types, type-III IFNs

are limited to the respiratory and intestinal mucosa (101). Together, type-I and type-III IFN signaling provides the main barrier of vertebrate innate immunity against viral infections.

Once secreted, type-I IFNs bind to receptors present on the cell surface of the cell in which the IFNs were produced (autocrine signaling) as well as neighboring cells (paracrine signaling)(102). Dimerization of the receptors initiates the canonical IFN signaling pathway that starts with the activation of tyrosine kinase 2 (TYK2) and Janus kinase 1 (JAK1), which in turn phosphorylate and thereby activate the signal transducers and activators of transcription (STAT)1 and STAT2 proteins (103). These protein dimers form a complex together with IRF9, called IFN-stimulated gene factor 3 (ISGF3), which translocates to the nucleus where it binds interferon-stimulated response elements (ISRE) present in promoter regions of interferonstimulated genes (ISGs). This process activates the transcription of a wide variety of ISGs, which together cause the cell to enter an antiviral state to limit spread of the ongoing viral infection (104, 105).

Viral antagonism of the innate immune response

Most, if not all, mammalian pathogenic viruses have mechanisms to subvert the cellular innate immune responses. In most cases, viral proteins called IFNantagonists actively block one of the RLR signaling cascades to prevent the production of IFNs (106, 107). IFNantagonists are mostly conserved within virus families. For example, influenza A viruses (IAV) use the NS1 protein to interfere with the type-I IFN response at multiple levels (107, 108). Viruses belonging to the *Paramyxoviridae* family, the closest related virus family of *Pneumoviridae*, use the V and C proteins to interfere with RLR signaling and the IFN signaling pathway (109, 110). RSV encodes the NS1 and NS2 proteins as IFN antagonist (106, 111), which are absent in the genome of HMPV. Therefore, HMPV must contain other mechanisms to avoid the type-I IFN response.

For HMPV, several proteins have been described to act as IFNantagonists. However, these reports are sometimes conflicting. The G protein was suggested to inhibit TLR signaling by blocking TLR4mediated signaling in DCs and RLR signaling by interacting with RIG-I in epithelial cells (59, 112). However, another study, using siRNA knockdown of the G gene, did not find such a role for the G protein (113). Additionally, the SH protein was suggested to inhibit TLR7-MyD88-mediated signaling in DCs and to downregulate IFN signaling by preventing STAT1 phosphorylation in DCs (114, 115). However, another study, using a genomics approach, could not find a role for the SH protein (52). A third protein, the M2-2 protein, was suggested to act as IFN-antagonist in epithelial cells by physically interacting with MAVS and by inhibition of TLR7 and TLR9 signaling in DCs (116–118). However, yet another study demonstrated that viruses lacking M2-2 protein expression contained an increased mutation frequency in parts of the genome (44), of which the effect on induction of IFN production was

not investigated, but could result in a loss of function of other viral proteins or alter important secondary RNA structures. In 2014, it was reported that HMPV rapidly accumulates snapback defective interfering RNAs (DIs) upon passaging of the virus with a higher MOI (119). These DIs are potent inducers of the type-I IFN response (119), providing a possible explanation for the conflicting results of previous reports. Thus far, the role of the G, SH, and M2-2 proteins as IFNantagonist, or any other mechanism of HMPV to avoid the innate immune response, has not been firmly established.

Outline of the thesis

Most viruses that cause RTIs have a winter seasonality. However, as a result of alleviating lockdown measures during the SARS-CoV-2 pandemic, some respiratory viruses have resurged during months outside of their regular epidemic season (120–122). **Chapter 2** describes an offseason HMPV outbreak in the summer of 2021 in a hospitalized setting.

Since the discovery in 2001, many studies have focused on the evolution and genetic diversity of HMPV. While the F and G gene sequences have been used extensively for analysis of HMPV evolution, studies based on analyses of whole genome sequences remain limited, even though the cost and feasibility to generate whole viral genome sequences has improved considerably throughout the past decade. In **Chapter 3**, we report on the development of whole genome sequencing method for HMPV using Nanopore technologies. This method was used in **Chapter 4** to study HMPV evolution between 2005 and 2021 using sequences from samples obtained from hospitalized patients and people visiting general practitioners for RTIs. Additionally, analysis of these sequences was used to propose a robust HMPV classification system.

The second part of this thesis focuses on the interaction between HMPV and the innate immune system. In **Chapter 5,** the role of the G, SH, and M2-2 proteins as bona fide IFN antagonist was studied. In addition, as a previous report described genomic instability of M22 mutant viruses, the genomic stability of the G, SH, and M22 deletion mutant viruses was analyzed. Because a role for the M2-2 protein as IFNantagonist could not be confirmed, the function of the M22 protein in viral antagonism of the innate immune system, as well as its transcriptional function, was further studied in **Chapter 6**. Finally, in **Chapter 7,** key findings of this thesis are discussed in the context of the work of others.

References

1. Van Den Hoogen BG, De Jong JC, Groen J, Kuiken T, De Groot R, Fouchier RAM, Osterhaus ADME. 2001. A newly discovered human pneumovirus isolated from young children with respiratory tract disease. Nat Med 7(6):719–724.
2. Williams JV, Wang CK, Yang C, Tollefson SJ, House FS, Heck JM, Chu M, Brown JB, Lintao LD, Quinto JD, Chu D, Spaete RR, Edwards KM, Wright PF, Crowe, Jr. JE. 2006. The Role of Human Metapneumovirus in Upper Respiratory Tract Infections in Children: A 20-Year Experience. J Infect Dis 193(3):387–395.
3. Feuillet F, Lina B, Rosa-Calatrava M, Boivin G. 2012. Ten years of human metapneumovirus research. J Clin Virol 53(2):97–105.
4. Williams J v., Harris PA, Tollefson SJ, Halburnt-Rush LL, Pingsterhaus JM, Edwards KM, Wright PF, Crowe JE. 2004. Human Metapneumovirus and Lower Respiratory Tract Disease in Otherwise Healthy Infants and Children. N Engl J Med 350(5):687–696.
5. Schildgen V, van den Hoogen B, Fouchier R, Tripp RA, Alvarez R, Manoha C, Williams J, Schildgen O. 2011. Human metapneumovirus: Lessons learned over the first decade. Clin Microbiol Rev 24(4):734–754.
6. O'Brien KL, Baggett HC, Brooks WA, Feikin DR, Hammitt LL, Higdon MM, Howie SRC, Deloria Knoll M, Kotloff KL, Levine OS, Madhi SA, Murdoch DR, Prosperi C, Scott JAG, Shi Q, Thea DM, Wu Z, Zeger SL, Adrian P V., Akarasewi P, Anderson TP, Antonio M, Awori JO, Baillie VL, Bunthi C, Chipeta J, Chisti MJ, Crawley J, DeLuca AN, Driscoll AJ, Ebruke BE, Endtz HP, Fancourt N, Fu W, Goswami D, Groome MJ, Haddix M, Hossain L, Jahan Y, Kagucia EW, Kamau A, Karron RA, Kazungu S, Kourouma N, Kuwanda L, Kwenda G, Li M, Machuka EM, Mackenzie G, Mahomed N, Maloney SA, McLellan JL, Mitchell JL, Moore DP, Morpeth SC, Mudau A, Mwananyanda L, Mwansa J, Silaba Ominde M, Onwuchekwa U, Park DE, Rhodes J, Sawatwong P, Seidenberg P, Shamsul A, Simões EAF, Sissoko S, Wa Somwe S, Sow SO, Sylla M, Tamboura B, Tapia MD, Thamthitiwat S, Toure A, Watson NL, Zaman K, Zaman SMA. 2019. Causes of severe pneumonia requiring hospital admission in children without HIV infection from Africa and Asia: the PERCH multi-country case-control study. Lancet 394(10200):757–779.
7. van den Hoogen BG, Doornum GJJ van, Fockens JC, Cornelissen JJ, Beyer WEP, Groot R de, Osterhaus ADME, Fouchier RAM. 2003. Prevalence and clinical symptoms of human metapneumovirus infection in hospitalized patients. J Infect Dis 188(10):1571–1577.
8. Jiang D, Zhu W, Wang Y, Sun C, Zhang KQ, Yang J. 2013. Molecular tools for functional genomics in filamentous fungi: Recent advances and new strategies. Biotechnol Adv 31(8):1562–1574.
9. Zhang C, Zhu N, Xie Z, Lu R, He B, Liu C, Ma X, Tan W. 2013. Viral Etiology and Clinical Profiles of Children with Severe Acute Respiratory Infections in China. PLoS One 8(8):e72606.
10. Yi L, Zou L, Peng J, Yu J, Song Y, Liang L, Guo Q, Kang M, Ke C, Song T, Lu J, Wu J. 2019. Epidemiology, evolution and transmission of human metapneumovirus in Guangzhou China, 2013–2017. Sci Rep 9(1):14022.
11. Ren L, Gonzalez R, Wang Z, Xiang Z, Wang Y, Zhou H, Li J, Xiao Y, Yang Q, Zhang J, Chen L, Wang W, Li Y, Li T, Meng X, Zhang Y, Vernet G, Paranhos-Baccalà G, Chen J, Jin Q, Wang J. 2009. Prevalence of human respiratory viruses in adults with acute respiratory tract infections in Beijing, 2005-2007. Clin Microbiol Infect 15(12):1146–1153.

12. Wang Y, Chen Z, Yan YD, Guo H, Chu C, Liu J, Ding Y, Shao X, Xu J, Ji W. 2013. Seasonal distribution and epidemiological characteristics of human metapneumovirus infections in pediatric inpatients in Southeast China. Arch Virol 158(2):417–424.
13. García-García ML, Calvo C, Martín F, Pérez-Breña P, Acosta B, Casas I. 2006. Human metapneumovirus infections in hospitalised infants in Spain. Arch Dis Child 91(4):290–295.
14. Fabbiani M, Terrosi C, Martorelli B, Valentini M, Bernini L, Cellesi C, Cusi MG. 2009. Epidemiological and Clinical Study of Viral Respiratory Tract Infections in Children From Italy. J Med Virol 81(4):750-756.
15. Dunn SR, Ryder AB, Tollefson SJ, Xu M, Saville BR, Williams J V. 2013. Seroepidemiologies of human metapneumovirus and respiratory syncytial virus in young children, determined with a new recombinant fusion protein enzyme-linked immunosorbent assay. Clinical and Vaccine Immunology 20(10):1654–1656.
16. Lüsebrink J, Wiese C, Thiel A, Tillmann RL, Ditt V, Müller A, Schildgen O, Schildgen V. 2010. High seroprevalence of neutralizing capacity against human metapneumovirus in all age groups studied in Bonn, Germany. Clin Vaccine Immunol 17(3):481–484.
17. Pavlin JA, Hickey AC, Ulbrandt N, Chan Y-P, Endy TP, Boukhvalova MS, Chunsuttiwat S, Nisalak A, Libraty DH, Green S, Rothman AL, Ennis FA, Jarman R, Gibbons R V., Broder CC. 2008. Human Metapneumovirus Reinfection among Children in Thailand Determined by an Enzyme-Linked Immunosorbent Assay Using Purified Soluble Fusion Protein. J Infect Dis 198:836–842.
18. Wolf DG, Zakay-Rones Z, Fadeela A, Greenberg D, Dagan R. 2003. High Seroprevalence of Human Metapneumovirus among Young Children in Israel. J Infect Dis 188(12):1865–1867.
19. Laine O, Laine J, Säilä P, Huhtala H, Syrjänen J, Vuorinen T, Vuento R. 2015. An outbreak of human metapneumovirus in a rehabilitation center for alcoholics in Tampere, Finland. Infect Dis 47(7):499–503.
20. Tu CC, Chen LK, Lee YS, Ko CF, Chen CM, Yang HH, Lee JJ. 2009. An outbreak of human metapneumovirus infection in hospitalized psychiatric adult patients in Taiwan. Scandinavian J Infect Dis 41(5):363–367.
21. Cheng VCC, Wu AKL, Cheung CHY, Lau SKP, Woo PCY, Chan KH, Li KSM, Ip IKS, Dunn ELW, Lee RA, Yam LYC, Yuen KY. 2007. Outbreak of human metapneumovirus infection in psychiatric inpatients: implications for directly observed use of alcohol hand rub in prevention of nosocomial outbreaks. J Hosp Infect 67(4):336–343.
22. Seynaeve D, Augusseau-Rivière B, Couturier P, Morel-Baccard C, Landelle C, Bosson JL, Gavazzi G, Mallaret MR. 2020. Outbreak of Human Metapneumovirus in a Nursing Home: A Clinical Perspective. J Am Med Dir Assoc 21(1):104-109.e1.
23. Centers for Disease Control and Prevention (CDC). 2013. Outbreaks of Human Metapneumovirus in Two Skilled Nursing Facilities — West Virginia and Idaho, 2011–2012. MMWR Morb mortal wkly rep 62(46):909–13.
24. Liao RS, Appelgate DM, Pelz RK. 2012. An outbreak of severe respiratory tract infection due to human metapneumovirus in a long-term care facility for the elderly in Oregon. J Clin Virol 53(2):171–173.
25. Esper F, Martinello RA, Boucher D, Weibel C, Ferguson D, Landry ML, Kahn JS. 2004. A 1-year experience with human metapneumovirus in children aged <5 years. J Infect Dis 189(8):1388–1396.
26. Coverstone AM, Wilson BS, Burgdorf D, Schechtman KB, Storch GA, Holtzman MJ, Castro M, Bacharier LB, Sumino K. 2018. Recurrent Wheezing in Children Following Human Metapneumovirus Infection. J Allergy Clin Immunol 142(1):297–301.

27. Howard LM, Edwards KM, Zhu Y, Griffin MR, Weinberg GA, Szilagyi PG, Staat MA, Payne DC, Williams J V. 2018. Clinical features of human metapneumovirus infection in ambulatory children aged 5–13 years. J Pediatric Infect Dis Soc 7(2):165–168.
28. García-García ML, Calvo C, Casas I, Bracamonte T, Rellán A, Gozalo F, Tenorio T, Pérez-Breña P. 2007. Human metapneumovirus bronchiolitis in infancy is an important risk factor for asthma at age 5. Pediatr Pulmonol 42(5):458–464.
29. Falsey AR, Erdman D, Anderson LJ, Walsh EE. 2003. Human Metapneumovirus Infections in Young and Elderly Adults. J Infect Dis 187(5):785–790.
30. Boivin G, De Serres G, Hamelin ME, Côté S, Argouin M, Tremblay G, Maranda-Aubut R, Sauvageau C, Ouakki M, Boulianne N, Couture C. 2007. An outbreak of severe respiratory tract infection due to human metapneumovirus in a long-term care facility. Clin Infect Dis 44(9):1152–1158.
31. Herfst S, Schrauwen EJA, de Graaf M, van Amerongen G, van den Hoogen BG, de Swart RL, Osterhaus ADME, Fouchier RAM. 2008. Immunogenicity and efficacy of two candidate human metapneumovirus vaccines in cynomolgus macaques. Vaccine 26(33):4224–4230.
32. Van Den Hoogen BG, Bestebroer TM, Osterhaus ADME, Fouchier RAM. 2002. Analysis of the genomic sequence of a human metapneumovirus. Virology 295(1):119–132.
33. Tawar RG, Duquerroy S, Vonrhein C, Varela PF, Damier-Piolle L, Castagne N, MacLellan K, Bedouelle H, Bricogne G, Bhella D, Eléouët JF, Rey FA. 2009. Crystal structure of a nucleocapsid-like nucleoprotein-RNA complex of respiratory syncytial virus. Science 326(5957):1279–1283.
34. Renner M, Bertinelli M, Leyrat C, Paesen GC, de Oliveira LFS, Huiskonen JT, Grimes JM. 2016. Nucleocapsid assembly in pneumoviruses is regulated by conformational switching of the N protein. eLife 5:e12627.
35. Paesen GC, Collet A, Sallamand C, Debart F, Vasseur JJ, Canard B, Decroly E, Grimes JM. 2015. X-ray structure and activities of an essential Mononegavirales L-protein domain. Nat Commun 6:8749.
36. García-Barreno B, Delgado T, Melero JA. 1996. Identification of protein regions involved in the interaction of human respiratory syncytial virus phosphoprotein and nucleoprotein: significance for nucleocapsid assembly and formation of cytoplasmic inclusions. J Virol 70(2):801–808.
37. Fearns R, Collins PL. 1999. Role of the M2-1 Transcription Antitermination Protein of Respiratory Syncytial Virus in Sequential Transcription. J Virol 73(7):5852–5864.
38. Zhou H, Cheng X, Jin H. 2003. Identification of Amino Acids That Are Critical to the Processivity Function of Respiratory Syncytial Virus M2-1 Protein. J Virol 77(9):5046–5053.
39. Hardy RW, Wertz GW. 2000. The Cys 3 -His 1 Motif of the Respiratory Syncytial Virus M2-1 Protein Is Essential for Protein Function. J Virol 74(13):5880–5885.
40. Hardy RW, Wertz GW. 1998. The Product of the Respiratory Syncytial Virus M2 Gene ORF1 Enhances Readthrough of Intergenic Junctions during Viral Transcription. J Virol 72(1):520–526.
41. Buchholz UJ, Biacchesi S, Pham QN, Tran KC, Yang L, Luongo CL, Skiadopoulos MH, Murphy BR, Collins PL. 2005. Deletion of M2 Gene Open Reading Frames 1 and 2 of Human Metapneumovirus: Effects on RNA Synthesis, Attenuation, and Immunogenicity. J Virol 79(11):6588–6597.
42. Herfst S, de Graaf M, Schickli JH, Tang RS, Kaur J, Yang C-F, Spaete RR, Haller AA, van den Hoogen BG, Osterhaus ADME, Fouchier RAM. 2004. Recovery of Human Metapneumovirus Genetic Lineages A and B from Cloned cDNA. J Virol 78(15):8264–8270.

43. Cai H, Zhang Y, Lu M, Liang X, Jennings R, Niewiesk S, Li J. 2016. Phosphorylation of Human Metapneumovirus M2-1 Protein Upregulates Viral Replication and Pathogenesis. J Virol 90(16):7323–7338.
44. Schickli JH, Kaur J, MacPhail M, Guzzetta JM, Spaete RR, Tang RS. 2008. Deletion of human metapneumovirus M2-2 increases mutation frequency and attenuates growth in hamsters. Virol J 5:69.
45. Adamson P, Thammawat S, Muchondo G, Sadlon T, Gordon D. 2012. Diversity in glycosaminoglycan binding amongst hMPV G protein lineages. Viruses 4(12):3785–3803.
46. Thammawat S, Sadlon TA, Hallsworth PG, Gordon DL. 2008. Role of Cellular Glycosaminoglycans and Charged Regions of Viral G Protein in Human Metapneumovirus Infection. J Virol 82(23):11767–11774.
47. Anderson CS, Chu CY, Wang Q, Mereness JA, Ren Y, Donlon K, Bhattacharya S, Misra RS, Walsh EE, Pryhuber GS, Mariani TJ. 2020. CX3CR1 as a respiratory syncytial virus receptor in pediatric human lung. Pediatr Res 87(5):862–867.
48. Johnson SM, McNally BA, Ioannidis I, Flano E, Teng MN, Oomens AG, Walsh EE, Peeples ME. 2015. Respiratory Syncytial Virus Uses CX3CR1 as a Receptor on Primary Human Airway Epithelial Cultures. PLoS Pathog 11(12):e1005318.
49. Cox RG, Livesay SB, Johnson M, Ohi MD, Williams J V. 2012. The Human Metapneumovirus Fusion Protein Mediates Entry via an Interaction with RGD-Binding Integrins. J Virol 86(22):12148–12160.
50. Skiadopoulos MH, Biacchesi S, Buchholz UJ, Amaro-Carambot E, Surman SR, Collins PL, Murphy BR. 2006. Individual contributions of the human metapneumovirus F, G, and SH surface glycoproteins to the induction of neutralizing antibodies and protective immunity. Virology 345(2):492–501.
51. Battles MB, Más V, Olmedillas E, Cano O, Vázquez M, Rodríguez L, Melero JA, Mclellan JS. Structure and immunogenicity of pre-fusion-stabilized human metapneumovirus F glycoprotein. Nat Commun 8(1):1528.
52. de Graaf M, Herfst S, Aarbiou J, Burgers PC, Zaaraoui-Boutahar F, Bijl M, van IJcken W, Schrauwen EJA, Osterhaus ADME, Luider TM, Scholte BJ, Fouchier RAM, Andeweg AC. 2013. Small Hydrophobic Protein of Human Metapneumovirus Does Not Affect Virus Replication and Host Gene Expression In Vitro. PLoS One 8(3):e58572.
53. Masante C, El Najjar F, Chang A, Jones A, Moncman CL, Dutch RE. 2014. The Human Metapneumovirus Small Hydrophobic Protein Has Properties Consistent with Those of a Viroporin and Can Modulate Viral Fusogenic Activity. J Virol 88(11):6423–6433.
54. Herfst S, Mas V, Ver LS, Wierda RJ, Osterhaus ADME, Fouchier RAM, Melero JA. 2008. Low-pH-Induced Membrane Fusion Mediated by Human Metapneumovirus F Protein Is a Rare, Strain-Dependent Phenomenon. J Virol 82(17):8891–8895.
55. de Graaf M, Schrauwen EJA, Herfst S, van Amerongen G, Osterhaus ADME, Fouchier RAM. 2009. Fusion protein is the main determinant of metapneumovirus host tropism. J Gen Virol 90(Pt 6):1408–1416.
56. Cox RG, Williams J V. 2013. Breaking in: Human metapneumovirus fusion and entry. Viruses 5(1):192–210.
57. Biacchesi S, Skiadopoulos MH, Yang L, Lamirande EW, Tran KC, Murphy BR, Collins PL, Buchholz UJ. 2004. Recombinant Human Metapneumovirus Lacking the Small Hydrophobic SH and/or Attachment G Glycoprotein: Deletion of G Yields a Promising Vaccine Candidate. J Virol 78(23):12877–12887.

58. Biacchesi S, Pham QN, Skiadopoulos MH, Murphy BR, Collins PL, Buchholz UJ. 2005. Infection of Nonhuman Primates with Recombinant Human Metapneumovirus Lacking the SH, G, or M2-2 Protein Categorizes Each as a Nonessential Accessory Protein and Identifies Vaccine Candidates. J Virol 79(19):12608–12613.
59. Bao X, Liu T, Shan Y, Li K, Garofalo RP, Casola A. 2008. Human metapneumovirus glycoprotein G inhibits innate immune responses. PLoS Pathog 4(5):e1000077.
60. Norton SL, Fearns R. 2016. Initiation and Regulation of Paramyxovirus. Virology 479-480:545–554.
61. Iverson LE, Rose JK, Diego S. 1981. Localized Attenuation and Discontinuous Synthesis during Vesicular Stomatitis Virus Transcription. Cell 23(2):477–484.
62. Cifuentes-muñoz N, Branttie J, Slaughter KB, Dutch RE. 2017. Human Metapneumovirus Induces Formation of Inclusion Bodies for Efficient Genome Replication and Transcription. J Virol 91(24):e01282-17.
63. Derdowski A, Peters TR, Glover N, Qian R, Thomas J, Burnett A, Williams J V, Spearman P, Crowe JE. 2008. Human metapneumovirus nucleoprotein and phosphoprotein interact and provide the minimal requirements for inclusion body formation. J Gen Virol 89(Pt 11):2698–2708.
64. Chen J, Zhu H, Najjar F El, Buchholz J, Moncman CL, Dutch RE. 2016. Human metapneumovirus Induces Reorganization of the Actin Cytoskeleton for Direct Cell-to-Cell Spread. PLoS Pathog 12(9)e1005922.
65. Kinder JT, Moncman CL, Barrett C, Jin H, Kallewaard N. 2020. Respiratory Syncytial Virus and Human Metapneumovirus an Interesting Dichotomy in Viral Replication , Spread , and Inhibition by Neutralizing Antibodies. J Virol 94(20):e01068-20.
66. Sattentau Q. 2008. Avoiding the void: cell-to-cell spread of human viruses. Nat Rev Microbiol 6(11):815-26.
67. van den Hoogen BG, Herfst S, Sprong L, Cane PA, Forleo-Neto E, de Swart RL, Osterhaus ADME, Fouchier RAM. 2004. Antigenic and Genetic Variability of Human Metapneumoviruses. Emerg Infect Dis 10(4):658–666.
68. Nao N, Saikusa M, Sato K, Sekizuka T, Usuku S, Tanaka N, Nishimura H, Takeda M. 2020. Recent molecular evolution of human metapneumovirus (HMPV): Subdivision of HMPV a2b strains. Microorganisms 8(9):1280.
69. Saikusa M, Nao N, Kawakami C, Usuku S, Sasao T, Toyozawa T, Takeda M, Okubo I. 2017. A novel 111-nucleotide duplication in the G gene of human metapneumovirus. Microbiol Immunol 61(11):507–512.
70. Saikusa M, Kawakami C, Nao N, Takeda M, Usuku S, Sasao T, Nishimoto K, Toyozawa T. 2017. 180-nucleotide duplication in the G Gene of Human metapneumovirus A2b subgroup strains circulating in Yokohama City, Japan, since 2014. Front Microbiol 8:402.
71. Saikusa M, Nao N, Kawakami C, Usuku S, Tanaka N, Tahara M, Takeda M, Okubo I. 2019. Predominant detection of the subgroup a2b human metapneumovirus strain with a 111-nucleotide duplication in the g gene in Yokohama city, Japan in 2018. Jpn J Infect Dis 72(5):350–352.
72. Arshad Y, Rana MS, Ikram A, Salman M, Aamir UB, Zaidi SSZ, Alam MM, Sharif S, Shaukat S, Khurshid A, Hakim R, Mujtaba G, Umair M, Sattar S, Bostan N. 2022. Molecular detection and genetic characterization of human metapneumovirus strains circulating in Islamabad, Pakistan. Sci Rep 12(1):2790.
73. Boivin G, Mackay I, Sloots TP, Madhi S, Freymuth F, Wolf D, Shemer-Avni Y, Ludewick H, Gray GC, LeBlanc É. 2004. Global genetic diversity of human metapneumovirus fusion gene. Emerg Infect Dis 10(6):1154–1157.

74. Yang CF, Wang CK, Tollefson SJ, Piyaratna R, Lintao LD, Chu M, Liem A, Mark M, Spaete RR, Crowe JE, Williams J V. 2009. Genetic diversity and evolution of human metapneumovirus fusion protein over twenty years. Virol J 6:138.
75. Huck B, Scharf G, Neumann-Haefelin D, Puppe W, Weigl J, Falcone V. 2006. Novel human metapneumovirus sublineage. Emerg Infect Dis 12(1):147–150.
76. Piñana M, Vila J, Gimferrer L, Valls M, Andrés C, Codina MG, Ramón J, Martín MC, Fuentes F, Saiz R, Rodrigo PAC, Pumarola T, Antón A. 2017. Novel human metapneumovirus with a 180-nucleotide duplication in the G gene. Future Microbiol 12:565–571.
77. Pinana M, Vila J, Maldonado C, Galano-Frutos JJ, Valls M, Sancho J, Andres FXNC, Martín-Gomez MT, Esperalba J, Codina MG, Pumarola T, Anton A. 2020. Insights into immune evasion of human metapneumovirus: novel 180- and 111-nucleotide duplications within viral G gene throughout 2014-2017 seasons in Barcelona, Spain. Journal of Clinical Virology 132:104590.
78. Schobel SA, Stucker KM, Moore ML, Anderson LJ, Larkin EK, Shankar J, Bera J, Puri V, Shilts MH, Rosas-Salazar C, Halpin RA, Fedorova N, Shrivastava S, Stockwell TB, Peebles RS, Hartert T v., Das SR. 2016. Respiratory Syncytial Virus whole-genome sequencing identifies convergent evolution of sequence duplication in the C-terminus of the G gene. Sci Rep 6:26311.
79. Nidaira M, Taira K, Hamabata H, Kawaki T, Gushi K, Mahoe Y, Maeshiro N, Azama Y, Okano S, Kyan H, Kudaka J, Hiroyuki T, Noda M, Kimura H. 2013. Molecular Epidemiology of Human Metapneumovirus from 2009 to 2011 in Okinawa, Japan. Jpn J Infect Dis 65(4):337-40.
80. Eshaghi AR, Duvvuri VR, Lai R, Nadarajah JT, Li A, Patel SN, Low DE, Gubbay JB. 2012. Genetic variability of human respiratory syncytial virus A strains circulating in Ontario: A novel genotype with a 72 nucleotide G gene duplication. PLoS One 7(3):e32807.
81. Hotard AL, Laikhter E, Brooks K, Hartert T v., Moore ML. 2015. Functional Analysis of the 60-Nucleotide Duplication in the Respiratory Syncytial Virus Buenos Aires Strain Attachment Glycoprotein. J Virol 89(16):8258–8266.
82. Trento A, Ábrego L, Rodriguez-Fernandez R, González-Sánchez MI, González-Martínez F, Delfraro A, Pascale JM, Arbiza J, Melero JA. 2015. Conservation of G-Protein Epitopes in Respiratory Syncytial Virus (Group A) Despite Broad Genetic Diversity: Is Antibody Selection Involved in Virus Evolution? J Virol 89(15):7776–7785.
83. Agoti CN, Mayieka LM, Otieno JR, Ahmed JA, Fields BS, Waiboci LW, Nyoka R, Eidex RB, Marano N, Burton W, Montgomery JM, Breiman RF, Nokes DJ. 2014. Examining strain diversity and phylogeography in relation to an unusual epidemic pattern of respiratory syncytial virus (RSV) in a long-term refugee camp in Kenya. BMC Infect Dis 14:178.
84. Chen J, Qiu X, Avadhanula V, Shepard SS, Kim DK, Hixson J, Piedra PA, Bahl J. 2022. Novel and extendable genotyping system for human respiratory syncytial virus based on whole-genome sequence analysis. Influenza other Respir Viruses 16(3):492–500.
85. Carr MJ, Waters A, Fenwick F, Toms GL, Hall WW, O'Kelly E. 2008. Molecular Epidemiology of Human Metapneumovirus in Ireland. J Med Virol 80(3):510–516.
86. Xagorari A, Chlichlia K. 2008. Toll-Like Receptors and Viruses: Induction of Innate Antiviral Immune Responses. Open Microbiol J 2:49–59.
87. Jacobs SR, Damania B. 2012. NLRs, inflammasomes, and viral infection. J Leukoc Biol 92(3):469–477.

88. Li D, Wu M. 2021. Pattern recognition receptors in health and diseases. Signal Transduct Target Ther 6(1):129.
89. Kikkert M. 2020. Innate Immune Evasion by Human Respiratory RNA Viruses. J Innate Immun 12(1):4–20.
90. Rehwinkel J, Gack MU. 2020. RIG-I-like receptors: their regulation and roles in RNA sensing. Nat Rev Immunol 20(9):537-551.
91. Jensen S, Thomsen AR. 2012. Sensing of RNA Viruses: a Review of Innate Immune Receptors Involved in Recognizing RNA Virus Invasion. J Virol 86(6):2900–2910.
92. Loo YM, Gale M. 2011. Immune Signaling by RIG-I-like Receptors. Immunity 34:680–692.
93. Patel JR, García-Sastre A. 2014. Activation and regulation of pathogen sensor RIG-I. Cytokine Growth Factor Rev 25(5):513–523.
94. Isaacs A, Lindenmann J. 1957. Virus interference. I. The interferon. Proc R Soc B Biol Sci 147(927):258-67
95. Ivashkiv LB, Donlin LT. 2014. Regulation of type I interferon responses. Nat Rev Immunol 14(1):36–49.
96. Trent JM, Olson S, Lawn RM. 1982. Chromosomal localization of human leukocyte, fibroblast, and immune interferon genes by means of in situ hybridization. Proc Natl Acad Sci U S A 79(24):7809–7813.
97. Sanceau J, Sondermeyer P, Beranger F, Falcoff R, Falcoff R, Sanctau J, Sondermeyert P. 1986. Intracellular Human γ -interferon Triggers an Antiviral State in Transformed Murine L Cells. Proc Natl Acad Sci U S A 84(9):2906–2910.
98. Kotenko S V, Gallagher G, Baurin V V, Lewis-antes A, Shen M, Shah NK, Langer JA, Sheikh F, Dickensheets H, Donnelly RP. 2003. IFN-λs mediate antiviral protection through a distinct class II cytokine receptor complex. Nat Immunol 4(1):69-77.
99. Sheppard P, Kindsvogel W, Xu W, Henderson K, Schlutsmeyer S, Whitmore TE, Kuestner R, Garrigues U, Birks C, Roraback J, Ostrander C, Dong D, Shin J, Presnell S, Fox B, Haldeman B, Cooper E, Taft D, Gilbert T, Grant FJ, Tackett M, Krivan W, Mcknight G, Clegg C, Foster D, Klucher KM. 2003. IL-28, IL-29 and their class II cytokine receptor IL-28R. Nat Immunol 4(1):63–68.
100. Ye L, Schnepf D, Staeheli P. 2019. Interferon-λ orchestrates innate and adaptive mucosal immune responses. Nat Rev Immunol 19(10):614-625.
101. Mordstein M, Neugebauer E, Ditt V, Jessen B, Rieger T, Falcone V, Sorgeloos F, Ehl S, Mayer D, Kochs G, Schwemmle M, Gunther S, Drosten C, Michiels T, Staeheli P. 2010. Lambda Interferon Renders Epithelial Cells of the Respiratory and Gastrointestinal Tracts Resistant to Viral Infections. J Virol 84(11):5670–5677.
102. Novick D, Cohen B, Rubinstein M. 1994. The human interferon α β receptor: Characterization and molecular cloning. Cell 77(3):391–400.
103. Darnell JE, Kerr IM, Stark GR. 1994. Jak-STAT pathways and transcriptional activation in response to IFNs and other extracellular signaling proteins. Science 264(5164):1415–1421.
104. Larner AC, Jonak G, Cheng YS, Korant B, Knight E, Darnell JE. 1984. Transcriptional induction of two genes in human cells by β interferon. Proc Natl Acad Sci U S A 81(21):6733–6737.
105. Schoggins JW. 2019. Interferon-Stimulated Genes: What Do They All Do? Annu Rev Virol 6(1):567–584.
106. Spann KM, Tran KC, Collins PL. 2005. Effects of nonstructural proteins NS1 and NS2 of human respiratory syncytial virus on interferon regulatory factor 3, NF-kappaB, and proinflammatory cytokines. J Virol 79(9):5353–5362.

107. Gack MU, Albrecht RA, Urano T, Inn K-S, Huang I-C, Carnero E, Farzan M, Inoue S, Jung JU, García-Sastre A. 2009. Influenza A virus NS1 targets the ubiquitin ligase TRIM25 to evade recognition by RIG-I. Cell Host Microbe 5(5):439–449.
108. Ayllon J, Garcia-Sastre A. 2014. The NS1 Protein: A Multitasking Virulence Factor. Curr Top Microbiol Immunol 386:73–107.
109. Andrejeva J, Childs KS, Young DF, Carlos TS, Stock N, Goodbourn S, Randall RE. 2004. The V proteins of paramyxoviruses bind the IFN-inducible RNA helicase, mda-5, and inhibit its activation of the IFN-β promoter. Proc Natl Acad Sci U S A 101(49):17264–17269.
110. Strähle L, Marq J-B, Brini A, Hausmann S, Kolakofsky D, Garcin D. 2007. Activation of the Beta Interferon Promoter by Unnatural Sendai Virus Infection Requires RIG-I and Is Inhibited by Viral C Proteins. J Virol 81(22):12227–12237.
111. Ban J, Lee NR, Lee NJ, Lee JK, Quan FS, Inn KS. 2018. Human respiratory syncytial virus NS 1 targets TRIM25 to suppress RIG-I ubiquitination and subsequent RIG-I-mediated antiviral signaling. Viruses 10(12):716.
112. Kolli D, Bao X, Liu T, Hong C, Wang T, Garofalo RP, Casola A. 2011. Human Metapneumovirus Glycoprotein G Inhibits TLR4-Dependent Signaling in Monocyte-Derived Dendritic Cells. J Immunol 187(1):47–54.
113. Preston FM, Straub CP, Ramirez R, Mahalingam S, Spann KM. 2012. SiRNA against the G gene of human metapneumovirus. Virol J 9:105.
114. Bao X, Kolli D, Esham D, Velayutham TS, Casola A. 2018. Human metapneumovirus small hydrophobic protein inhibits interferon induction in plasmacytoid dendritic cells. Viruses 10(6):278.
115. Hastings AK, Amato KR, Wen SC, Peterson LS, Williams V. 2016. Human metapneumovirus small hydrophobic (SH) protein downregulates type I IFN pathway signaling by affecting STAT1 expression and phosphorylation. Virology 494:248–256.
116. Kitagawa Y, Sakai M, Funayama M, Itoh M, Gotoh B. 2017. Human Metapneumovirus M2-2 Protein Acts as a Negative Regulator of Alpha Interferon Production by Plasmacytoid Dendritic Cells 91(20):e00579-17.
117. Ren J, Wang Q, Kolli D, Prusak DJ, Tseng C-TK, Chen ZJ, Li K, Wood TG, Bao X. 2012. Human Metapneumovirus M2-2 Protein Inhibits Innate Cellular Signaling by Targeting MAVS. J Virol 86(23):13049–13061.
118. Chen Y, Deng X, Deng J, Zhou J, Ren Y, Prusak DJ, Wood TG, Bao X, Hospital T, First T, Hospital A. 2017. Functional Motifs Responsible for Human Metapneumovirus M2-2-mediated Innate Immune Evasion. Virology 499:361–368.
119. van den Hoogen BG, van Boheemen S, de Rijck J, van Nieuwkoop S, Smith DJ, Laksono B, Gultyaev A, Osterhaus ADME, Fouchier RAM. 2014. Excessive production and extreme editing of human metapneumovirus defective interfering RNA is associated with type I IFN induction. J Gen Virol 95(Pt 8):1625–1633.
120. Nott R, Fuller TL, Brasil P, Nielsen-Saines K. 2022. Out-of-Season Influenza during a COVID-19 Void in the State of Rio de Janeiro, Brazil: Temperature Matters. Vaccines (Basel) 10(5):821.
121. Eden J-S, Sikazwe C, Xie R, Deng Y-M, Sullivan SG, Michie A, Levy A, Cutmore E, Blyth CC, Britton PN, Crawford N, Dong X, Dwyer DE, Edwards KM, Horsburgh BA, Foley D, Kennedy K, Minney-Smith C, Speers D, Tulloch RL, Holmes EC, Dhanasekaran V, Smith DW, Kok J, Barr IG, Alafaci A, Carter I, Daley A, Francis M, Kesson A, Moore H, Ngo C, Tran T. 2022. Off-season RSV epidemics in Australia after easing of COVID-19 restrictions. Nat Commun 13(1):2884.
122. Jones N. 2020. How COVID-19 is changing the cold and flu season. Nature 588(7838):388–390.

2

An off-season outbreak of human metapneumovirus infections after ending of a COVID-19 lockdown

C.M.H.J. Kivit [a], K. Groen [e], M. Jongbloed [a b], C.F.M. Linssen [c], A. van Loo [d], E.C.M. van Gorp [e], S. van Nieuwkoop [e], B.G. van den Hoogen [e], M.D. de Kruif [a]*.

[a] *Department of Pulmonology, Zuyderland Hospital, Henri Dunantstraat 5, Heerlen 6419, PC, Netherlands*
[b] *Faculty of Health, Medicine and Life Sciences, Maastricht University, Universiteitssingel 60, Maastricht 6229, ER, Netherlands*
[c] *Department of Medical Microbiology, Zuyderland Hospital, Henri Dunantstraat 5, Heerlen 6419, PC, Netherlands*
[d] *Department of Paediatrics, Zuyderland Hospital, Henri Dunantstraat 5, Heerlen 6419, PC, Netherlands*
[e] *Department of Viroscience, Erasmus MC, University Medical Center Rotterdam the Netherlands, Department of Infectious diseases, Erasmus MC, University Medical Center Rotterdam, Rotterdam, Netherlands*

J Infect. 2022 May;84(5):722-746.

Dear Editor,

We read with great interest the article by Lumley et al.[1] who described changes in pediatric respiratory infections at a British hospital after ending of a national COVID-19 lockdown. They showed off-season increased infection rates with Respiratory Syncytial Virus (RSV), rhinovirus and adenovirus, whereas influenza virus infection rates remained low. Here, we report that in addition, also a change in human metapneumovirus (HMPV) epidemiology has been observed in our hospital. Normally, the peak incidence of HMPV infections is found in late winter and early spring in the northern hemisphere.[2] In our hospital, this pattern has always been very stable with a peak incidence in March. Among 239 patients hospitalized with HMPV, we have previously observed only one infection in June.[3] In contrast, in 2021, we observed an off-season outbreak of HMPV in June and July among both adults and children. The outbreak occurred just after national lockdown measures due to coronavirus disease 2019 (COVID-19) had been lifted. To characterize the outbreak further, clinical characteristics were studied of the patients and phylogenetic analysis of the viral samples was performed in order to investigate the relationship of the viruses.

Between June and July 2021, 28 patients were hospitalized with an HMPV infection in the Zuyderland Medical Center, which is a large teaching hospital situated in Heerlen in the south of The Netherlands. After exclusion of two patients who refused informed consent and three patients who were unable to communicate, 23 patients were analyzed. None of the patients had known relationships with each other. Twelve patients were children ranging from 0 to 4 years and the 11 adult patients were between 20 and 90 years old. None of the patients were immunocompromised. The most prominent comorbidity in adults was chronic obstructive pulmonary disease (COPD) in 5 (46%) of the patients. In general, the clinical disease severity at presentation and the course of disease was not different from that observed in other cohorts.[3] Temperature in children and adults was 38.4 ± 1.1 °C and 37.9 ± 0.8 °C, respectively, heart rate 146 ± 17 and 100 ± 22 min^{-1} and respiratory rate 24 ± 12 and 23 ± 7 min^{-1}. Antibiotics were administered to 3 (25%) children and 9 (82%) adults. No patient was admitted to the intensive care unit. Mean length of hospital stay was 4.0 ± 4.0 days for children and 4.4 ± 2.9 days for adults. One adult patient died after hospital dismissal but within 30 days after admission. This patient had severe comorbidity (end-stage neuroendocrine tumor and ileus).

For the purpose of this study, surplus samples initially tested for routine clinical care were obtained. For sequence analysis 14 samples were selected, in which HMPV could be detected by routine diagnostic qRT-PCR assays at a cycle threshold less than 27. For all samples, full length F sequences, and for 8 of these samples that of the attachment protein (G), were obtained with sanger sequencing as described previously.[4] Phylogenetic analysis of complete F gene

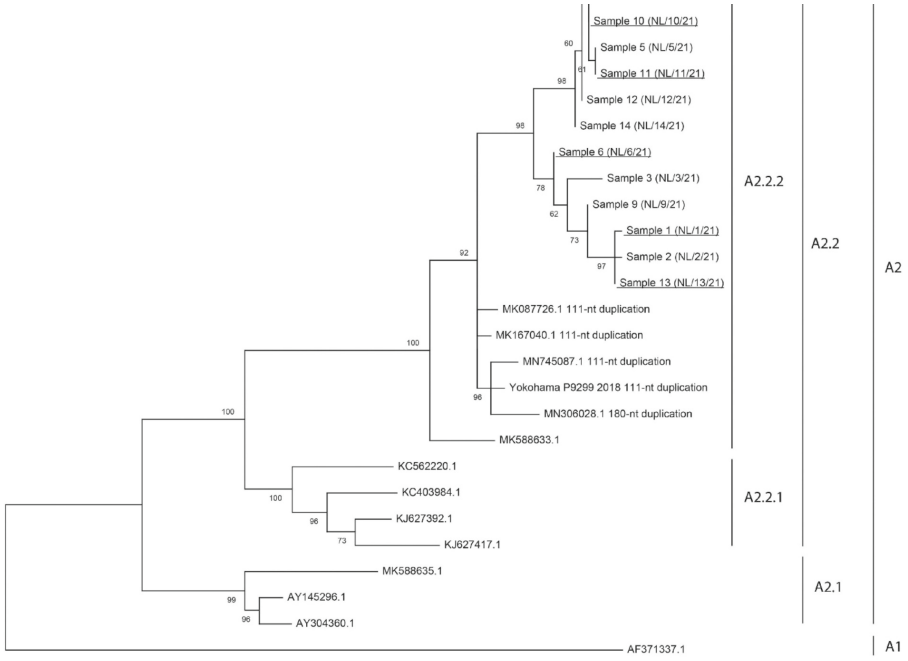

Figure 1. Maximum likelihood phylogenetic tree reconstructed from HMPV complete F gene sequences. The tree was reconstructed using the GTR *+G + I* substitution model with 1000 bootstraps. Fourteen complete F gene sequences (thirteen from GenBank, indicated with accession numbers, and one from[10]) were included for the tree topology. Viruses sequenced in this study that contain a 111-nucleotide duplication in the G gene that was confirmed by Sanger sequencing of the G gene are underlined.

nucleotide sequences was performed using the MEGA 10 software with the best fit DNA model determined by the MEGA software with 1000 bootstraps. This phylogenetic analysis demonstrated that all viruses clustered in two smaller clusters within the A2.2.2 lineage (Fig. 1). All eight viruses, for which sequences were obtained for the G gene, had a 111 nt duplication in that gene.

Taken together, this study described an off-season outbreak of infections with HMPV in both adults and children caused by viruses belonging to the HMPV A2.2.2 lineage. Because all 8 viruses for which sequences of the G gene could be obtained showed a 111-nt duplication in the G gene, it may be considered likely that this variant has been responsible for most infections during the outbreak. This variant was first described in 2016 and has gradually become the dominating strain worldwide but is not the only circulating variant.[5] Some authors initially postulated that this strain may be more virulent;[6] however, in time, HMPV incidence has not changed significantly.[3] The cause of the unusual summer outbreak of HMPV infections is likely related to reopening of the society

after a severe COVID-19 lockdown, thus enabling the spread of HMPV. During the first COVID-19 wave in 2020, both SARS-CoV2 and HMPV had circulated independently, which suggested that there was no competition between the viruses at the time.[3] During subsequent lockdowns HMPV incidence was very low, like that of RSV.[7] Together these data suggest that public health measures were probably more important drivers for the shift in HMPV incidence than viral interference. Whether the currently identified clusters of patients, all hospitalized with the same HMPV genotype, were limited to local transmission only or spread to the region, country or continent remains to be determined. However, because the cluster was further divided into two smaller clusters within the same A2.2.2 lineage and because the patients in our study did not have known relationships with each other, the HMPV outbreak probably did not occur locally only. Of note, whereas the incidence of HMPV in this cohort and the previously reported incidence of RSV in the study by Lumley et al.[1] and others[8,9] both peaked after ending of the COVID-19 lockdown, the incidence of influenza viruses was not affected at that time.[1, 9] Hence, different factors drive seasonal variation among different viruses and this concurrent outbreak of HMPV and RSV suggests that outbreaks of these viruses may be less depending on weather conditions.

Declaration of Competing Interest

None.

Ethical statement

The study protocol was approved by the board of the METC-Z (medical-ethics board of Zuyderland Medical Center; approval number: METCZ20190153).

Acknowledgements

None.

Funding

This research did not receive any specific grant from funding agencies in the public, commercial, or not-for-profit sectors.

Supplementary materials

Supplementary material associated with this article can be found, in the online version, at doi:10.1016/j.jinf.2022.01.042.

References

1. Lumley S.F., Richens N., Lees E., Cregan J., Kalimeris E., Oakley S., et al. Changesin paediatric respiratory infections at a UK teaching hospital 2016-2021; impactof the SARS-CoV-2 pandemic. J Infect 2022;84(1):40–7. doi:10.1016/j.jinf.2021.10.022.
2. Li Y., Reeves R.M., Wang X., Bassat Q., Brooks W.A., Cohen C., et al. Global patterns in monthly activity of influenza virus, respiratory syncytial virus, parainfluenza virus, and metapneumovirus: a systematic analysis. Lancet Glob Health2019;7(8):e1031–45. doi:10.1016/S2214-109X(19)30264-5.
3. Jongbloed M., Leijte W.T., Linssen C.F.M., van den Hoogen B.G., van Gorp E.C.M.,de Kruif M.D.. Clinical impact of human metapneumovirus infections before andduring the COVID-19 pandemic. Infect Dis (Lond) 2021;53(7):488–97. doi:10.1080/23744235.2021.1887510.
4. Groen K., van Nieuwkoop S., Bestebroer T.M., Fraaij P.L., Fouchier R.A.M.,van den Hoogen B.G.. Whole genome sequencing of human metapneu-moviruses from clinical specimens using MinION nanopore technology. VirusRes 2021;302:198490. doi:10.1016/j.virusres.2021.198490.5. Xie Z., Xu J., Ren Y., Cui A., Wang H., Song J., et al. Emerging human metap-neumovirus gene duplication variants in patients with severe acute respiratoryinfection, China, 2017-2019. Emerg Infect Dis 2021;27(1):275–7. doi:10.3201/eid2701.201043.
6. Saikusa M., Nao N., Kawakami C., Usuku S., Sasao T., Toyozawa T., et al. A novel111-nucleotide duplication in the G gene of human metapneumovirus. MicrobiolImmunol 2017;61(11):507–12. doi:10.1111/1348-0421.12543.
7. van Summeren J., Meijer A., Aspelund G., Casalegno J.S., Erna G., Hoang U., et al.Low levels of respiratory syncytial virus activity in Europe during the 2020/21season: what can we expect in the coming summer and autumn/winter? EuroSurveill 2021;26(29). doi:10.2807/1560-7917.ES.2021.26.29.2100639.
8. Weinberger Opek M., Yeshayahu Y., Glatman-Freedman A., Kaufman Z.,Sorek N., Brosh-Nissimov T. Delayed respiratory syncytial virus epidemic inchildren after relaxation of COVID-19 physical distancing measures, Ashdod,Israel, 2021. Euro Surveill 2021;26(29). doi:10.2807/1560-7917.ES.2021.26.29.2100706.
9. Hodjat P., Christensen P.A., Subedi S., Bernard D.W., Olsen R.J., Long S.W.. The reemergence of seasonal respiratory viruses in Houston, Texas, after relaxing COVID-19 restrictions. Microbiol Spectr 2021;9(2):e0043021. doi:10.1128/Spectrum.00430-21.
10. Nao N., Saikusa M., Sato K., Sekizuka T., Usuku S., Tanaka N., et al. Recentmolecular evolution of human metapneumovirus (HMPV): subdivision of HMPVA2b strains. microorganisms. 2020;8(9). doi:10.3390/microorganisms8091280.

3

Whole genome sequencing of human metapneumoviruses from clinical specimens using MinION nanopore technology

Kevin Groen[1], Stefan van Nieuwkoop[1], Theo M. Bestebroer[1], Pieter L. Fraaij[1], Ron A.M. Fouchier[1] and Bernadette G. van den Hoogen[1]*

[1]*Department of Viroscience, Erasmus MC, Wijtemaweg 80, 3015 CN Rotterdam, The Netherlands*

Virus Res. 2021 Sep;302:198490

Abstract

Human metapneumovirus (HMPV), a member of the *Pneumoviridae* family, is a causative agent of respiratory illness in young children, the elderly, and immunocompromised individuals. Globally, viruses belonging to two main genetic lineages circulate, A and B, which are further divided into four genetic sublineages (A1, A2, B1, B2). Classical genotyping of HMPV is based on the sequence of the fusion (F) and attachment (G) glycoprotein genes, which are under direct antibody-mediated immune pressure. Whole genome sequencing provides more information than sequencing of subgenomic fragments and is therefore a powerful tool for studying virus evolution and disease epidemiology and for identifying transmission events and nosocomial outbreaks. Here, we report a robust method to obtain whole genome sequences for HMPV using MinION Nanopore technology. This assay is able to generate HMPV whole genome sequences from clinical specimens with good coverage of the highly variable G gene and is equally sensitive for strains of all four genetic HMPV sublineages. This method can be used for studying HMPV genetics, epidemiology, and evolutionary dynamics.

Keywords

human metapneumovirus, whole genome sequencing, Nanopore technology; MinION sequencing

Introduction

After its identification in 2001, human metapneumovirus (HMPV), a member of the *Pneumoviridae* family, was shown to have a large clinical impact on human health, especially in young children, the elderly, and immunocompromised individuals (Falsey et al., 2003; Van Den Hoogen et al., 2001; Williams et al., 2006). Globally, HMPV accounts for approximately 5-15% of all respiratory tract infections (RTI) with a peak of infections in infants between 6 and 12 months of age (Jain et al., 2015; O'Brien et al., 2019; Van Den Hoogen et al., 2001; Williams et al., 2004).

HMPV is a non-segmented negative-strand RNA virus with a genome of ±13,300 nucleotides containing 8 genes encoding nine open reading frames (ORF), including three surface glycoproteins: the fusion protein (F), the small hydrophobic protein (SH) and the attachment protein (G). Of these, F is the major target of neutralizing and protective antibodies (Skiadopoulos et al., 2006; Herfst et al., 2007). However, antibody titers rapidly wane over time and therefore reinfections with HMPV can occur throughout life (Ebihara et al., 2004; van den Hoogen et al., 2007). Genetically, HMPV strains cluster in two major lineages (A and B) which are subdivided in four sublineages (A1, A2, B1, B2) (Van Den Hoogen et al., 2004). Viruses from multiple HMPV sublineages can co-circulate in a single season, but in general, viruses from one sublineage predominate per season (Boivin et al., 2004; Mackay et al., 2006; Van Den Hoogen et al., 2004). Phylogenetic analyses of HMPV strains have suggested that the A2 sublineage may be further divided in two clades, A2a and A2b, or rather A2.1 and A2.2, following nomenclature as used for Influenza viruses and the international committee on taxonomy of Viruses (ICTV) (Huck et al., 2006; Lefkowitz et al., 2018; Nao et al., 2020). Additionally, two different sizes of duplications in the open reading frame (ORF) of G of the virus belonging to lineage A2 were detected of 111 or 180 nucleotides, in Japan, followed by reports of the occurrence of these duplications in viruses circulating in Spain, Vietnam and China (Saikusa et al., 2019, 2017b, 2017a). One of these strains, with a 111 nucleotide duplication in G, became the predominant circulating strain in Yokohoma city suggesting a beneficial role for the duplication (Saikusa et al., 2019). Furthermore, studies reported variability in the length of the G ORF due to changes in the position of the stop codon (Kamau et al., 2020; Van Den Hoogen et al., 2004). These evolutionary events highlight the need to carefully monitor HMPV evolutionary dynamics, which is critical towards the design of diagnostic assays and future intervention strategies that can lead towards epidemiological containment strategies of the virus.

Thus far, studying HMPV genetic variation and evolution has been mainly based on the genetic variability of F and G (Boivin et al., 2004; Saikusa et al., 2019, 2017b, 2017a; Van Den Hoogen et al., 2004). Whole genome sequences

could provide additional genomic information about virus evolution that will remain undiscovered by sequencing of subgenomic fragments (Dudas and Bedford, 2019). With rapidly developing next generation sequencing (NGS) techniques, the time and cost efficiency to sequence entire viral genomes is improving considerably. NGS technologies, such as Ion Torrent, Illumina and the relatively new Oxford Nanopore Technologies MinION sequencing, are used in a wide range of applications such as population surveillance of viral outbreaks, tracking nosocomial infections and the design of vaccine strategies (Radford et al., 2012). While all three platforms can be used for viral whole genome sequencing, MinION sequencing has the advantage that it does not require additional amplification steps during the sequencing procedure (Quick et al., 2018; Siddle et al., 2018). The cost of MinION sequencing provides an additional benefit of MinION sequencing over Ion Torrent and Illumina sequencing (Van Nimwegen et al., 2016), and the scale of MinION sequencing is very suitable for virus-sized genomes.

Here, we introduce a sensitive HMPV whole genome sequencing method by MinION sequencing of multiplexed PCR amplicons. As the G is highly variable between viruses from the different lineages (nucleotide identity: 50%-57%), and therefore used for classification, a good genomic coverage of this gene is desirable (Van Den Hoogen et al., 2004). However, this high variability makes it challenging to design primers that can detect the G gene of HMPV strains from all sublineages with the same assay. With the method described here, HMPV whole genome sequences can be generated from viruses in clinical specimens belonging to all sublineages, with good genomic coverage of the entire genome including the highly variable G gene. This rapid whole genome sequencing technique facilitates HMPV genomic and evolution studies and can be used to monitor HMPV epidemiology.

Methods

HMPV reference strains

HMPV strains NL/00/1 (Genbank accession number AF371337), NL/00/17 (Genbank accession number AY304360.1), NL/99/1 (Genbank accession number AY525843) and NL/94/1 (Genbank accession number AY304362.1) were used as reference strains for HMPV sublineages A1, A2, B1 and B2, respectively. The HMPV reference strains were isolated and cultured as described previously (Herfst et al., 2004).

Patient materials

Table 1. List of primer sequences used for the uneven amplicons (primer pool 1) and their optimized concentrations used for HMPV whole genome MinION sequencing. For degenerate primers, Y = C or T, W = A or T , R = A or G, M = A or C, S = C or G, K = G or T, D = A, G or T, N = any base.

Amplicon	Primer	Nucleotide sequence (5'-3')	µM primer per PCR reaction
1	FW 1	ACGCGAAAAAAACGCGTATA	40
	REV 1	CCAGAYTCWGGRCCCATYTC	
3	FW 3A	CMARCAACCAAAACAACAGATCC	10
	FW 3B	CAANYAAYCAAARYYATGGATCC	
	REV 3A	GAAGTACAGACATNGCWGCACC	
	E	GAAGTACMGACATNGCWGCACC	
5	FW 5A	GCAAGACTTGGAGCCATCAAGG	30
	FW 5B	GCAAGAGCTGGAGTCACCAAGG	
	REV 5	CAAGGYGTRYTATNACNCCAAAGAT	
7	FW 7A	TTGAAAACAGTCAAGCACTAGT	40
	FW 7B	TTYCCTGARGATCARTTYAATGT	
	REV 7	CATCYAATGTTWTCATTGTCAYTTATC	
9	FW 9A	GGAAAATAAGYAGAAAYCAATGCAC	50
	FW 9B	GGRAARTAAGYANAAATCAATGYAC	
	REV 9A	CATTRAGAGGATCCATTGYYATTT	
	REV 9B	CACARARNGGATCCATTGYYATTT	
11	FW 11A	AACCCACCTCAGATAACACATCAATYCT	10
	FW 11B	ACCCAACCTCAGATAACACATCAATTCT	
	REV 11A	AGTTGACTGGGGTAAYTTTTWGCTT	
	REV 11B	AGTTGGCTRGGGTAACTTTTRGCTT	
13	FW 13A	GGAAATSAAATCRGAACTTTCTTCYAYTAAAAC	5
	FW 13B	GGAAATRAAATCAGAACTTTCYTCYATTAAAAC	
	REV 13A	TCTCCYCCWCCAAAYTGCATTG	
	REV 13B	TCTCCTCCWCCAAAYTGCATCG	
15	FW 15	AATGGTAGGCTGATATGCTGYCAG	5
	REV 15A	YGATAYRAACCCRTCACCCCAGTC	
	REV 15B	TGARATGAACCCATCACCCCARTC	

Table 1. *Continued.*

Amplicon	Primer	Nucleotide sequence (5'-3')	µM primer per PCR reaction
17	FW 17A	AYCAGTTCRGAYTACAACAAAGGG	5
	FW 17B	TCCCYAAGATAACATTYGAAAGGCTAAAAA	
	REV 17	CTTRCTRCCNCCAACTGTTGCT	

For the purpose of this study surplus samples initially tested for routine clinical care were obtained from the diagnostics unit of the Viroscience department of the Erasmus MC. Only samples in which HMPV could be detected by routine diagnostic qRT-PCR assays at a cycle times less than 25 were selected. A volume of 200 µl was used for RNA extraction using the MagnaPureLC (Roche Diagnostics) that was eluted in a volume of 100 µl. qRT-PCR was performed as described previously (Hoek et al., 2013). Data collection and analyses were conducted in an anonymized matter, which does not require further medical ethics review as consented by our Medical ethical board (MEC-2015-306).

RNA extraction, cDNA synthesis and multiplexed PCR amplification of clinical HMPV samples

RNA extraction was performed using the High Pure RNA Isolation Kit (Roche). Briefly, 200 µl of HMPV-positive clinical material or diluted virus reference strain culture supernatant was lysed in 400 µl RNA lysis buffer. RNA was extracted according to the manufacturer's instructions and eluted in 50 µl elution buffer. For each sample, two separate cDNA reactions (1 for each primer pool) and subsequently two separate multiplexed PCR reactions were performed. cDNA synthesis was performed using the SuperScript IV First-Strand cDNA Synthesis kit (Invitrogen) in a total volume of 20 µl containing 6 µl eluted RNA, 10 mM dNTPs and 20 U RNAse OUT (Invitrogen), 10 µM of each forward primer from primer pool 1 or primer pool 2, 4 µl 5x First Strand Buffer, 100 mM DTT, 20 U RNAse OUT and 200 U SuperScript IV Reverse Transcriptase. The cDNA reaction was carried out for 15 minutes at 50ºC followed by 10 minutes at 80ºC. The cDNA was amplified by PCR in a total volume of 50 µl containing 4 µl cDNA, 5 µl 10x PFU DNA polymerase buffer (Agilent Technologies), 12.5 mM dNTPs, 1 µl PFU DNA polymerase (Agilent Technologies) and primer concentrations as indicated in Table 1 and 2. Thermocycling was performed with the following parameters: 95ºC for 2 minutes, 40 cycles of 95ºC for 20 seconds, 50ºC for 30 seconds and 72ºC for 90 seconds, followed by 72ºC for 3 minutes.

Table 2. List of primer sequences used for the even amplicons (primer pool 2) and their optimized concentrations used for HMPV whole genome MinION sequencing. For degenerate primers, Y = C or T, W = A or T , R = A or G, M = A or C, S = C or G, K = G or T, D = A, G or T, N = any base.

Amplicon	FW/RV	Nucleotide sequence (5'-3')	µM primer per PCR reaction
2	FW 2	CWACAGGMAGCAAAGCAGAAAG	10
	REV 2	GARAGCAARTCTAGRGCATCTT	
4	FW 4	AYACAGCYGCTGTTCAAGTTGA	40
	REV 4	ACCARCCTGTYCTYARAACACT	
6	FW 6	GTGCGGCARTTTTCAGACAATG	10
	REV 6	ACACCAYTYAGCTCYGGAGG	
8	FW 8	AGTGRCATGGTCCTGTYTTCA	30
	FW 8A	GACAGTGAARGCAYTAATCAAGTGC	
	REV 8	ACYTCCATRRCYACTTGTCCCA	
10	FW 10A	YCRCAYRAGCAGCAYARGRRAAAGA	20
	FW 10B	CCGCACKAGCAGCRCAAKAAGGAGA	
	FW 10C	CAACCARAYCAGMAATGNAAGNGAGRCA	
	FW10D	CAACCAAACCAGCAATGGAAGAGAGGCG	
	FW 10E	CAACCARAYCAGMAATGNAAGNGAG	
	REV 10A	CTYAYTCTTYTRCTTTTGTTGCT	
	REV 10B	GCTYAYTCTTYTRCTTTTGTTGCT	
12	FW 12	TYGGWCAYCCDATGGTAGATGA	10
	REV 12	ACCYYTTGTTTCYGGTGGTGCA	
14	FW 14	RGGRGARAGYATRYTAGTTAGTYTGATA	5
	REV 14A	TGAGTGCTTGATCCTACCCAGG	
	REV 14B	AGGGCTYTTTGGACCTCTTTGA	
16	FW 16	ACAYTRGGRAARATGCTYATGC	10
	REV 16	CARTTWCCTGCYCCTTCTCCAA	
18	FW 18	GAYCTTGAYCAYCATTAYCCNYTRGAATAYCA	40
	REV 18	ACGGCAAAAAAACCGTATACAWTCAA	

PCR purification and MinION sequencing

For each primer pool, 5 µl PCR product was analyzed on a 1% agarose gel. When bands were visible, the remaining PCR products from both primer pools were pooled and purified using Agencourt AMPure XP beads (Beckman Coulter). Upon measurement of sample concentrations with the Qubit dsDNA HS assay kit (Thermo Fisher) on a Qubit fluorometer (Thermo Fisher), 1000 ng DNA was used per sample for library preparation. A maximum of twelve purified samples

were barcoded using the 1D Native barcoding genomic DNA kit (EXP-NBD104 and SQK-LSK109) according to the manufacturer's instructions and sequenced using a R9.4 FLO-MIN106 flowcell (Oxford Nanopore Technologies) on a GridION Mk1 (Oxford Nanopore Technologies) for 16 hours.

Sequence data analysis

Obtained sequence data was demultiplexed using the Porechop algorithm (https://github.com/rrwick/Porechop) as described previously (Oude Munnink et al., 2019). The demultiplexed sequence data was analyzed using CLC Genomics Workbench version 12.0 (Qiagen). After trimming the 30-nt primer sequences from the ends of the reads, the samples were genotyped by mapping the reads of an individual sample against the full genome sequences of the 4 reference strains (HMPV A1, A2, B1, B2). The HMPV reference sequence to which most of the reads were mapped was considered the genotype of that sample. If an equal number of reads mapped to two different reference strains, the genotype was determined based on homology of the F and G sequences of the sample compared to the reference strains. Subsequently, all reads were mapped against one reference genome. A consensus sequence was extracted with a minimum threshold of 25 read coverage per nucleotide. Gaps in homopolymeric regions of the obtained consensus sequences where checked and resolved by consulting reference genomes. A schematic overview of the complete HMPV MinION sequencing workflow is depicted in Figure 1.

Quantitative reverse-transcription PCR

RNA extraction was performed as described above and quantitative reverse-transcription PCR on the HMPV N gene was performed as described previously (Maertzdorf et al., 2004).

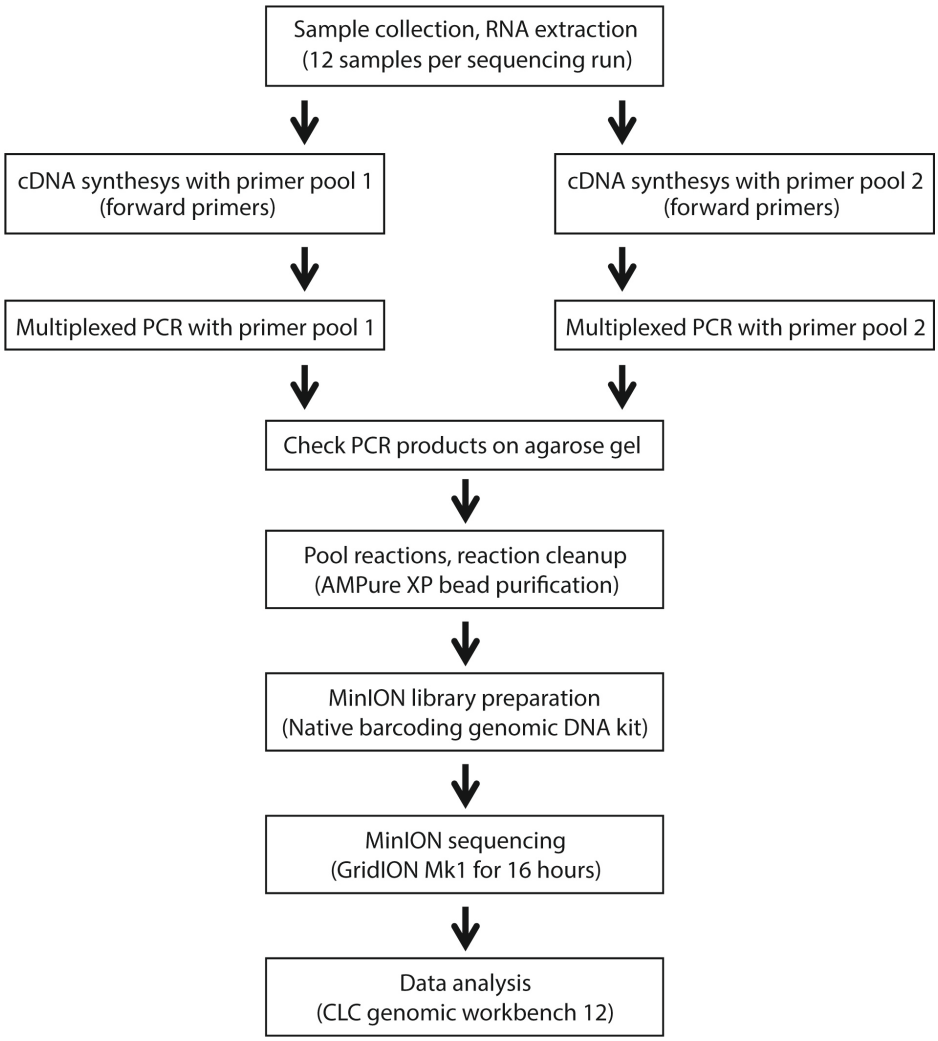

Figure 1. Schematic representation of the HMPV whole genome MinION sequencing workflow.

PCR and Sanger sequencing for genotyping of HMPV strains

RNA extracted from HMPV-positive clinical samples was subjected to PCR amplification of a region covering the HMPV F gene as previously described (Van Den Hoogen et al., 2004). PCR products were purified and Sanger sequencing was performed using the BigDye Terminator v3.1 Cycle Sequencing Kit (Applied Biosystems) according to the manufacturer's protocol. The sequencing products were purified using a Performa V3 96-well short plate (EdgeBio) according to the

manufacturer's protocol. Nucleotide sequences were determined using a 3130xl Genetic Analyzer (Applied Biosystems). The HMPV genotype was determined from the sequence of the F gene as described previously (Van Den Hoogen et al., 2004).

Results

Primer design for HMPV whole genome sequencing

To obtain amplicons with a size of 1000 nucleotides and a 200 nucleotide overlap with neighboring amplicons, primers were designed using Primalscheme (Quick et al., 2018). A total of 183 available HMPV whole genome sequences from GenBank were aligned using MAFFT (https://mafft.cbrc.jp/alignment/server/). Two separate alignments were generated for HMPV lineage A and B strains, respectively, based on the information supplied on GenBank or, in case the information was lacking, by analysis of the sequence of the F gene as described previously (Van Den Hoogen et al., 2004). Area's containing gaps in the alignments were removed manually, the designed primers were added to the alignment and primers sequences directed against these manipulated alignments were optimized using Primer3 plus (http://www.bioinformatics.nl/cgi-bin/primer3plus/primer3plus.cgi). The designed primers were imported in the MAFFT alignment containing all full genome sequences for both genotype A and B, including the gaps. Only primers that matched sequences of both HMPV-A and HMPV-B viruses were selected and, if necessary, degeneracies were introduced into the primer sequences to increase primer sensitivity for viruses of both HMPV lineages. In case degenerate primers could not be designed that would align to both genotype A and B viruses, multiple primers for that position were designed. Primers were designed to yield 18 PCR fragments, each of approximately 1,000 nucleotides in length with average overlap of approximately 260 nucleotides with neighboring amplicons (Figure 2a). The average amplicon length was 970 nucleotides, with the exception of amplicon 9, with a length of ± 1,250 nucleotides to span the entire G gene. The amplicons were divided over two pools (Table 1 and 2). Primer pool 1 contained the primers of the uneven numbered amplicons and primer pool two contained the primers of even numbered amplicons to prevent the generation of small PCR products from the overlapping part of neighboring amplicons.

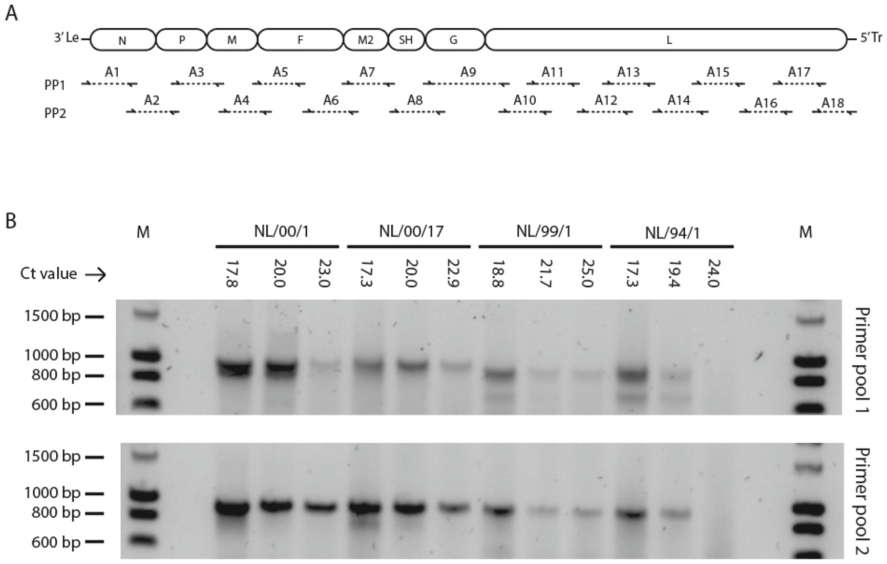

Figure 2. (a) Schematic overview of the 18 amplicons used to cover the HMPV genome by MinION sequencing. Le: leader sequence, Tr: trailer sequence, N: nucleoprotein, P: phosphoprotein, M: matrix protein, F: fusion protein, M2: Matrix protein 2, SH: small hydrophobic protein, G: glycoprotein, L: polymerase, PP1: primer pool 1, PP2: primer pool 2, A: amplicon. (b) Gel electrophoresis of multiplexed PCR products of serially diluted RNA from four HMPV reference strains NL/00/1, NL/00/17, NL/99/1, and NL/94/1. PCR products were run on a 1% agarose gel to validate the presence of PCR products. M: Molecular marker.

Validation and optimization of HMPV MinION whole genome sequencing

The sensitivity and specificity of primers for individual amplicons was first determined using full genome HMPV NL/00/1 (A1) and HMPV NL/99/1 (B1) plasmid DNA [30]. Dilution series ranging from 50 to 0.005 pg plasmid were used as template DNA for PCR amplification of all described amplicons. The PCR products were run on an agarose gel to confirm the presence of PCR product (data not shown). Next, the primers were used for cDNA synthesis and PCR amplification of viral RNA isolated from reference strains NL/00/1 (genotype A1), NL/00/17 (genotype A2), NL/99/1 (genotype B1) and NL/94/1 (genotype B2). To obtain equal input for all strains, viral RNA was subjected to quantitative reverse-transcription PCR (qRT-PCR) and RNA samples were diluted in order to match a Ct value of 20. From these samples, cDNA was generated using the forward primers of primer pool 1 or primer pool 2 separately, followed by a PCR reaction with primers for each individual PCR amplicon. The presence of PCR product for each amplicon was validated on an agarose gel and primer

concentrations were optimized by increasing primer concentrations for those PCR products that had a low intensity. Next, the cDNA was subjected to multiplexed PCR using the primers from primer pool 1 or primer pool 2 in two separate reactions (Figure 1). The multiplexed PCR products were then subjected to MinION sequencing and coverage plots were generated for each HMPV reference strains (data not shown). Primer concentrations from amplicons which yielded a genomic coverage <100 reads per nucleotide were increased in the multiplexed PCR reaction and the new primer concentrations were validated by MinION sequencing. This process was repeated until all amplicons had a minimum genomic coverage of at least 100 reads per nucleotide throughout the entire genome, including the highly variable G gene. The finally selected primer concentrations are listed in table 1 (pool 1) and 2 (pool 2).

To validate the sensitivity of the HMPV whole genome MinION sequencing assay, three dilutions of the RNA extracted from each HMPV reference strain were generated. The input of viral RNA varied based on Ct values obtained by qRT-PCR, with a range of Ct values from 17.8 to 23.7. The presence of bands from the multiplexed PCR products was validated on an agarose gel (Figure 2b). Samples were subjected to MinION sequencing using the selected primer concentrations from table 1 and 2. Whole genome consensus sequences were obtained from all dilutions of the reference strains (Figure 3). The PCR product of amplicon 9 had a size of 1,200 nucleotides and should run higher than the other amplicons but was not visible on the agarose gel (Figure 2b). Despite this, good genomic coverage of this region was obtained for all sample dilutions for viruses of all lineages (Figure 3). For the viruses belonging to the A1 and B2 lineages, the genomic coverage was lower for the samples with higher Ct values (23.0 and 24.0, respectively) (Figure 3a and 3d). However, a consensus sequence with a minimum coverage of 100 reads per nucleotide throughout the genome, including the G gene, was obtained for all dilutions. For the viruses belonging to the A2 and B1 lineages, similar genomic coverages were obtained for the different dilutions of these samples, with the exception of the 5' end of the genome. For all three dilutions of these viruses a coverage of at least 100 reads per nucleotide was obtained, including good coverage of the G gene (Figure 3b and 3c). Although multiplexed PCR amplification for NL/94/01 (lineage B2) with a Ct value of 24.0 resulted in bands with lower intensities on the agarose gel (Figure 2b), a whole genome sequence was still obtained (Figure 3d). Thus, we were able to obtain HMPV whole genome sequences of viruses from all four HMPV lineages with good genomic coverage throughout the genome using RNA with Ct values obtained by qRT-PCR up to at least 25.0.

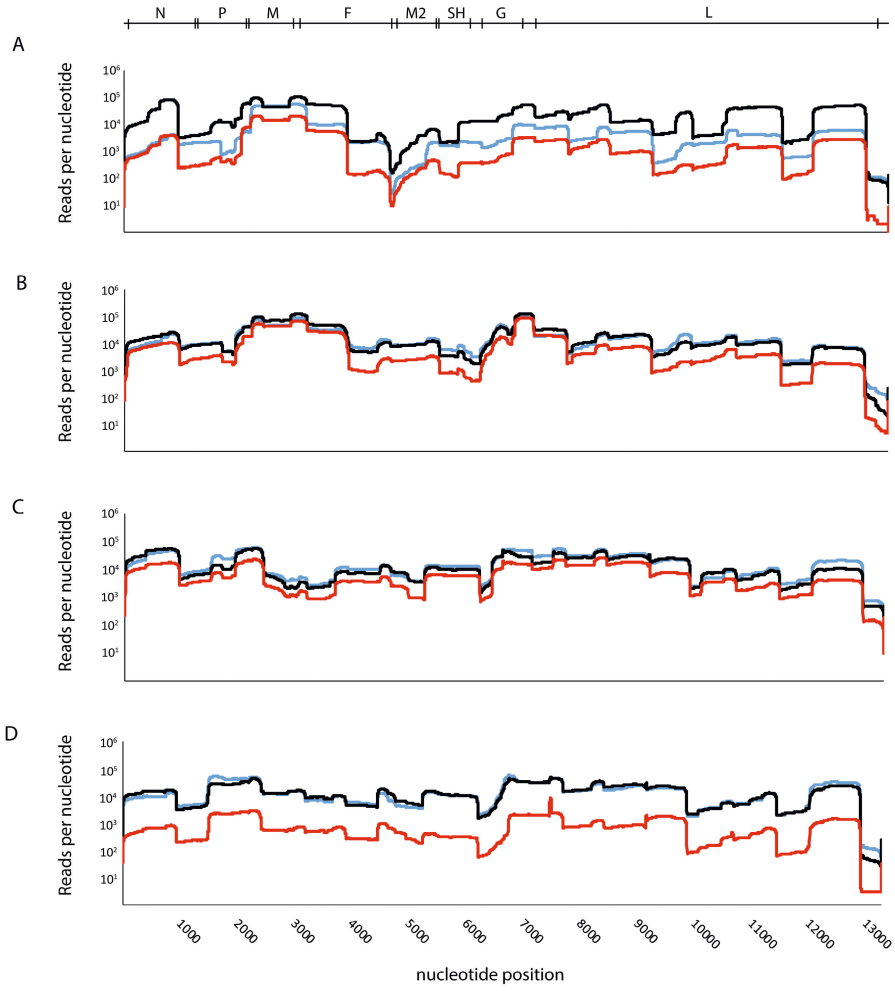

Figure 3. Coverage plots generated by MinION sequencing of serially diluted HMPV reference strains. Three dilutions of each reference strain were sequenced, with Ct values ranging from 17.3 to 25.0 obtained by qRT-PCR. Coverage indicated on the y-axis is expressed as the number of reads per nucleotide. (a) Coverage plots of serially diluted HMPV NL/00/1. Blue line: Ct 17.8, black line: Ct 20.0, red line: Ct 23.0. (b) Coverage plots of serially diluted HMPV NL/17/00. Blue line: Ct 17.3, black line: Ct 20.0, red line: Ct 22.9. (c) Coverage plots of serially diluted HMPV NL/99/1. Blue line: Ct 18.8, black line: Ct 21.7, red line: Ct 25.0. (d) Coverage plots of serially diluted HMPV NL/94/1. Blue line: Ct 17.3, black line: Ct 19.4, red line: Ct 24.0.

Table 3. Summary of MinION sequencing results of HMPV-positive clinical samples. The mean genomic coverage is expressed as the mean number of reads per nucleotide in the genome.

Clinical sample	Material	Ct value	Genotype	Total reads obtained (x1000)	mapped reads (x1000)	Mean genomic coverage (x1000)
1	Throat swab	20.1	A1	393	292 (74.3%)	18.5
2	Nasal wash	22.4	A2	580	362 (62.4%)	16.2
3	Sputum	19.5	A2	365	307 (83.8%)	8.4
4	Sputum	21	A2	400	316 (79%)	8.1
5	Nasal wash	21.1	B1	376	206 (54.9%)	12.5
6	Sputum	18.7	B1	163	133 (81.6%)	6.1
7	Throath swab	22.5	B1	110	58 (52.7%)	2.5
8	Lung Lavage	21.6	B2	208	78 (37,7%)	4.9
9	Lung Lavage	21.6	B2	208	78 (37,7%)	4.9
10	Nasal wash	22.7	B2	391	269 (68,7%)	9.0

MinION sequencing of HMPV-positive clinical samples

The HMPV whole genome MinION sequencing assay was subsequently used to sequence HMPV genomes from clinical specimens. HMPV-positive clinical samples were obtained and their genotype was determined by sanger sequencing of the HMPV F gene. Three samples belonged to sublineage A2, three to B1, three to B2 and one to sublineage A1, and Ct values ranged from 18.7 to 22.7 (Table 3). A HMPV whole genome consensus sequence was obtained for all 10 selected clinical specimens with a minimum genomic coverage of 100 reads per nucleotide, with the exception of the 5' and 3' ends of the genome and a small region of the virus belonging to the A1 sublineage (Figure 4). The genomic coverage, expressed as the mean number of reads per nucleotide in total number of reads ranged from 110,000 to 580,000 per sample. The mean

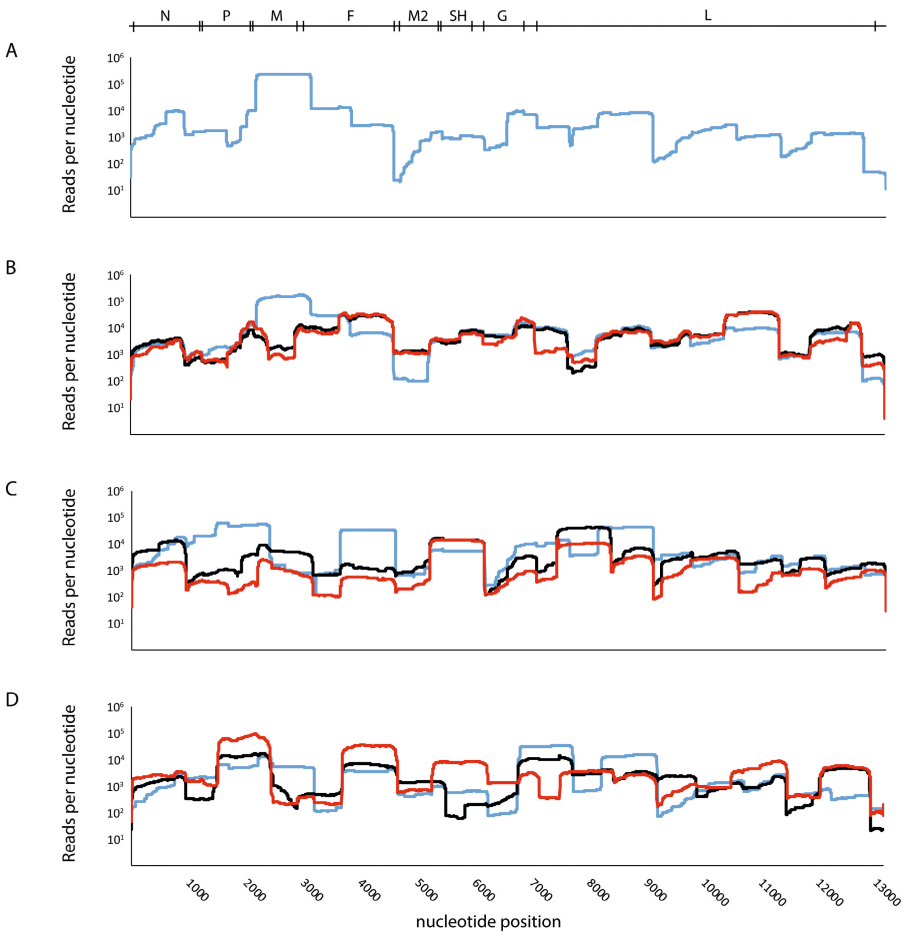

Figure 4. Coverage plots generated by MinION sequencing of 10 HMPV-positive clinical isolates. Ct values of HMPV clinical samples ranged from 18.7 to 22.7. Coverage indicated on the y-axis is expressed as the number of reads per nucleotide. (a) Coverage plot for a virus belonging to the A1 sublineage with a Ct of 20.1 (b) Coverage plots for viruses belonging to the A2 sublineage. Blue line: sample 2 (Ct 22.4), black line: sample 3 (Ct 19.5), red line: sample 4 (Ct 21.0). (c) Coverage plots for viruses belonging to the B1 sublineage. Blue line: sample 5 (Ct 21.1), black line: sample 6 (Ct 18.7), red line: sample 7 (Ct 22.5). (d) Coverage plots for viruses belonging to the B2 sublineage. Blue line: sample 8 (Ct 21.6), black line: sample 9 (Ct 22.4), red line: sample 10 (Ct 22.7).

genomic coverage, expressed as the mean number of reads per nucleotide in the genome, ranged from 2,500 to 18,500. The total reads and mean genomic coverage for HMPV A lineage viruses (total reads: 365,000-580,000, mean coverage in reads per nucleotide: 8,100-18,500) was somewhat higher than for the HMPV B lineage viruses (total reads: 110,000-391,000, mean coverage

in reads per nucleotide: 2,500-12,500), a full-length consensus sequence with a minimum genomic coverage of 100 reads per nucleotide was obtained for viruses from both lineage A and B. The mean Ct value of lineage A viruses was similar to that of lineage B viruses (20,75 for HMPV A, 21,35 for HMPV B), therefore the difference in total reads and genomic coverage between the two genotypes were not attributable to differences in Ct values. The genomic coverage of the highly variable G gene was above 100 reads per nucleotide for viruses from all four sublineages. This was similar to the genomic coverage of other regions of the genome, which demonstrated that the high variability of the G gene was not problematic for this assay. In conclusion, this method can be used for sensitive whole genome sequencing of viruses from all four sublineages from clinical specimens.

Discussion

Monitoring genetic evolution of HMPV is crucial for the design of diagnostic assays, for studying virus epidemiology, for identifying transmission events and nosocomial outbreaks, and for the rational design of future vaccines or other intervention strategies. Monitoring HMPV genetic evolution is classically done by sequencing of the F and G genes, of which the HMPV G gene is the most variable gene of the virus and is therefore used to distinguish between HMPV sublineages (Van Den Hoogen et al., 2004). In contrast, the HMPV F gene is relatively conserved but contains a number of distinct amino acids that can be used to distinguish between viruses from lineage A, B1 and B2 (Van Den Hoogen et al., 2004).

HMPV whole genome sequencing will provide additional important information about virus evolution which could be missed by partial genome sequencing (Radford et al., 2012). Here, we introduce a method to obtain whole genomes from HMPV positive clinical specimens that is equally sensitive to all four genetic sublineages. This method was optimized based on the intensity of PCR products on agarose gels and based on optimal genomic coverage obtained by MinION sequencing. However, a low band intensity of PCR products on gel did not translate to poor genomic coverage, as a whole genome consensus sequence with a 100 reads per nucleotide threshold was still obtained from samples with a low band intensity on gel. Adjustments to the primer concentrations did affect genomic coverage, as higher primer concentrations resulted in higher genomic coverage obtained by MinION sequencing. Using this method, a HMPV whole genome sequence was obtained from samples with an RNA input that equals a Ct value up to 25.0. However, the genomic coverage of the 5' end of the genome from samples with Ct values above 23.0 was relatively low. Additionally, we used our assay to sequence one clinical specimen with a Ct value of 28.0. This sample

had reduced genomic coverage as well as regions with poor genomic coverage (in comes cases even below 10 reads per nt).

A number of studies explored the option of HMPV whole genome sequencing, either by Illumina sequencing, Ion Torrent, or Nanopore technology (Kamau et al., 2020; Pollett et al., 2018; Xu et al., 2020, 2018). All three methods can be used to generate whole genome sequences, but the cost and scale of MinION sequencing is a benefit of the Nanopore technology for sequencing of viral genomes (Oude Munnink et al., 2019; Van Nimwegen et al., 2016). While metagenomics Nanopore sequencing of HMPV-positive clinical specimens can yield HMPV whole genome sequences, the sensitivity of metagenomic sequencing, as well as the coverage of the G gene, was sub-optimal in general (Xu et al., 2020, 2018). As the HMPV G gene is used for virus classification, good coverage of this gene in HMPV whole genome sequencing techniques is desired, but this can be challenging due to the high genetic variability (between 50%-57% nucleotide identity between lineages A and B) (Xu et al., 2018). We aimed to develop a whole genome sequencing method that detects HMPV from genotype A and B with equal sensitivity and with good coverage of the G gene. To this end, degeneracies were introduced in primer sequences or multiple primers were used for each PCR amplicon to improve the sensitivity of this assay. The introduction of multiple degenerate primers per amplicon resulted in an optimal coverage of the G gene for strain of all lineages.

A recent study, analyzing 2212 sequences, highlighted a notable difference between partial and whole genome sequences of respiratory syncytial virus (Ramaekers et al., 2020). Phylogenetic analyses of ten whole genome sequences obtained in our study, combined with 70 sequences obtained from Genbank, revealed no differences with phylogenetic analysis of only the fusion protein gene of these sequences (data not shown). This could be due to the limited availability of HMPV whole-genome sequences.

In conclusion, we introduce a HMPV whole genome sequencing technique using a MinION platform with virus-specific PCR amplicons. This assay is able to generate HMPV whole genome sequences from clinical specimens of all HMPV genotypes with good genomic coverage throughout the genome, including the variable G gene. This method can be used for in-depth studies of HMPV epidemiology and virus evolution, for following transmission routes during virus outbreaks, and can provide the foundation for the design of novel intervention strategies.

Acknowledgements

The authors would like to thank Dr. B. B. Oude Munnink for helping with troubleshooting during the optimization process of the assay and the ErasmusMC virology diagnostic department for carrying out the qRT-PCR on clinical specimens.

Author contributions

Conceptualization: B.H., R.F.

Data curation: K.G., S.N.
Formal analysis: K.G., S.N.
Funding acquisition: B.H., R.F.
Investigation: K.G., T.B., S.N.
Methodology: B.H., K.G., T.B., S.N.
Project administration: K.G., S.N.
Resources: P.F., B.H., R.F.
Software: K.G., S.N.
Supervision: B.H., R.F.
Validation: K.G., S.N.
Visualization: K.G., S.N.
Writing – original draft: K.G., S.N.
Writing – review & editing: K.G., S.N., B.H., R.F, P.F..

Funding

This research did not receive any specific grant from funding agencies in the public, commercial, or not-for-profit sectors.

Data Statement

The data generated during this study are available from the corresponding author upon request

References

Boivin, G., Mackay, I., Sloots, T.P., Madhi, S., Freymuth, F., Wolf, D., Shemer-Avni, Y., Ludewick, H., Gray, G.C., LeBlanc, É., 2004. Global genetic diversity of human metapneumovirus fusion gene. Emerg. Infect. Dis. 10, 1154–1157. https://doi.org/10.3201/eid1006.031097

Dudas, G., Bedford, T., 2019. The ability of single genes vs full genomes to resolve time and space in outbreak analysis. BMC Evol. Biol. 19, 1–27. https://doi.org/10.1186/s12862-019-1567-0

Ebihara, T., Endo, R., Kikuta, H., Ishiguro, N., Ishiko, H., Hara, M., Takahashi, Y., Kobayashi, K., 2004. Human Metapneumovirus Infection in Japanese Children. J. Clin. Microbiol. 42, 126–132. https://doi.org/10.1128/JCM.42.1.126-132.2004

Falsey, A.R., Erdman, D., Anderson, L.J., Walsh, E.E., 2003. Human Metapneumovirus Infections in Young and Elderly Adults. J. Infect. Dis. 187, 785–790. https://doi.org/10.1086/367901

Herfst, S., de Graaf, M., Schickli, J.H., Tang, R.S., Kaur, J., Yang, C.-F., Spaete, R.R., Haller, A.A., van den Hoogen, B.G., Osterhaus, A.D.M.E., Fouchier, R.A.M., 2004. Recovery of Human Metapneumovirus Genetic Lineages A and B from Cloned cDNA. J. Virol. 78, 8264–8270. https://doi.org/10.1128/jvi.78.15.8264-8270.2004

Herfst, S., de Graaf, M., Schrauwen, E.J.A., Ulbrandt, N.D., Barnes, A.S., Senthil, K., Osterhaus, A.D.M.E., Fouchier, R.A.M., van den Hoogen, B.G., 2007. Immunization of Syrian golden hamsters with F subunit vaccine of human metapneumovirus induces protection against challenge with homologous or heterologous strains. J. Gen. Virol. 88, 2702–2709. https://doi.org/10.1099/vir.0.83084-0

Hoek, R.A.S., Paats, M.S., Pas, S.D., Bakker, M., Hoogsteden, H.C., Boucher, C.A.B., Van Der Eerden, M.M., 2013. Incidence of viral respiratory pathogens causing exacerbations in adult cystic fibrosis patients. Scand. J. Infect. Dis. 45, 65–69. https://doi.org/10.3109/00365548.2012.708942

Huck, B., Scharf, G., Neumann-Haefelin, D., Puppe, W., Weigl, J., Falcone, V., 2006. Novel human metapneumovirus sublineage. Emerg. Infect. Dis. 12, 147–150. https://doi.org/10.3201/eid1201.050772

Jain, S., Self, W.H., Wunderink, R.G., Fakhran, S., Balk, R., Bramley, A.M., Reed, C., Grijalva, C.G., Anderson, E.J., Courtney, D.M., Chappell, J.D., Qi, C., Hart, E.M., Carroll, F., Trabue, C., Donnelly, H.K., Williams, D.J., Zhu, Y., Arnold, S.R., Ampofo, K., Waterer, G.W., Levine, M., Lindstrom, S., Winchell, J.M., Katz, J.M., Erdman, D., Schneider, E., Hicks, L.A., McCullers, J.A., Pavia, A.T., Edwards, K.M., Finelli, L., 2015. Community-Acquired Pneumonia Requiring Hospitalization among U.S. Adults. N. Engl. J. Med. 373, 415–427. https://doi.org/10.1056/nejmoa1500245

Kamau, E., Oketch, J.W., De Laurent, Z.R., Phan, M.V.T., Agoti, C.N., Nokes, D.J., Cotten, M., 2020. Whole genome sequencing and phylogenetic analysis of human metapneumovirus strains from Kenya and Zambia. BMC Genomics 21, 1–10. https://doi.org/10.1186/s12864-020-6498-z

Lefkowitz, E.J., Dempsey, D.M., Hendrickson, R.C., Orton, R.J., Siddell, S.G., Smith, D.B., 2018. Virus taxonomy: The database of the International Committee on Taxonomy of Viruses (ICTV). Nucleic Acids Res. 46, D708–D717. https://doi.org/10.1093/nar/gkx932

Mackay, I.M., Bialasiewicz, S., Jacob, K.C., McQueen, E., Arden, K.E., Nissen, M.D., Sloots, T.P., 2006. Genetic diversity of human metapneumovirus over 4 consecutive years in Australia. J. Infect. Dis. 193, 1630–1633. https://doi.org/10.1086/504260

Maertzdorf, J., Wang, C.K., Brown, J.B., Quinto, J.D., Chu, M., De Graaf, M., Van Den Hoogen, B.G., Spaete, R., Osterhaus, A.D.M.E., Fouchier, R.A.M., 2004. Real-Time Reverse Transcriptase PCR Assay for Detection of Human Metapneumoviruses from All Known Genetic Lineages. J. Clin. Microbiol. 42, 981–986. https://doi.org/10.1128/JCM.42.3.981-986.2004

Nao, N., Saikusa, M., Sato, K., Sekizuka, T., Usuku, S., Tanaka, N., Nishimura, H., Takeda, M., 2020. Recent molecular evolution of human metapneumovirus (HMPV): Subdivision of HMPV a2b strains. Microorganisms 8, 1–14. https://doi.org/10.3390/microorganisms8091280

O'Brien, K.L., Baggett, H.C., Brooks, W.A., Feikin, D.R., Hammitt, L.L., Higdon, M.M., Howie, S.R.C., Deloria Knoll, M., Kotloff, K.L., Levine, O.S., Madhi, S.A., Murdoch, D.R., Prosperi, C., Scott, J.A.G., Shi, Q., Thea, D.M., Wu, Z., Zeger, S.L., Adrian, P. V., Akarasewi, P., Anderson, T.P., Antonio, M., Awori, J.O., Baillie, V.L., Bunthi, C., Chipeta, J., Chisti, M.J., Crawley, J., DeLuca, A.N., Driscoll, A.J., Ebruke, B.E., Endtz, H.P., Fancourt, N., Fu, W., Goswami, D., Groome, M.J., Haddix, M., Hossain, L., Jahan, Y., Kagucia, E.W., Kamau, A., Karron, R.A., Kazungu, S., Kourouma, N., Kuwanda, L., Kwenda, G., Li, M., Machuka, E.M., Mackenzie, G., Mahomed, N., Maloney, S.A., McLellan, J.L., Mitchell, J.L., Moore, D.P., Morpeth, S.C., Mudau, A., Mwananyanda, L., Mwansa, J., Silaba Ominde, M., Onwuchekwa, U., Park, D.E., Rhodes, J., Sawatwong, P., Seidenberg, P., Shamsul, A., Simões, E.A.F., Sissoko, S., Wa Somwe, S., Sow, S.O., Sylla, M., Tamboura, B., Tapia, M.D., Thamthitiwat, S., Toure, A., Watson, N.L., Zaman, K., Zaman, S.M.A., 2019. Causes of severe pneumonia requiring hospital admission in children without HIV infection from Africa and Asia: the PERCH multi-country case-control study. Lancet 394, 757–779. https://doi.org/10.1016/S0140-6736(19)30721-4

Oude Munnink, B.B., Kik, M., de Bruijn, N.D., Kohl, R., van der Linden, A., Reusken, C.B.E.M., Koopmans, M., 2019. Towards high quality real-time whole genome sequencing during outbreaks using Usutu virus as example. Infect. Genet. Evol. 73, 49–54. https://doi.org/10.1016/j.meegid.2019.04.015

Pollett, S., Trovão, N.S., Tan, Y., Eden, J.S., Halpin, R.A., Bera, J., Das, S.R., Wentworth, D., Ocaña, V., Mendocilla, S.M., Álvarez, C., Calisto, M.E., Garcia, J., Halsey, E., Ampuero, J.S., Nelson, M.I., Leguia, M., 2018. The transmission dynamics and diversity of human metapneumovirus in Peru. Influenza Other Respi. Viruses 12, 508–513. https://doi.org/10.1111/irv.12537

Quick, J., Grubaugh, N.D., Pullan, S.T., Claro, I.M., Smith, A.D., Gangavarapu, K., Oliveira, G., Robles-Sikisaka, R., Rogers, T.F., Beutler, N.A., Burton, D.R., Lewis-Ximenez, L.L., Jesus, J.G. de, Giovanetti, M., Hill, S., Black, A., Bedford, T., Carroll, M.W., Nunes, M., Alcantara Jr, L.C., Sabino, E.C., Baylis, S.A., Faria, N., Loose, M., Simpson, J.T., Pybus, O.G., Andersen, K.G., Loman, N.J., 2018. Multiplex PCR method for MinION and Illumina sequencing of Zika and other virus genomes directly from clinical samples. Nat. Protoc. 12, 1261–1276. https://doi.org/10.1038/nprot.2017.066.Multiplex

Radford, A.D., Chapman, D., Dixon, L., Chantrey, J., Darby, A.C., Hall, N., 2012. Application of next-generation sequencing technologies in virology. J. Gen. Virol. 93, 1853–1868. https://doi.org/10.1099/vir.0.043182-0

Ramaekers, K., Rector, A., Cuypers, L., Lemey, P., Keyaerts, E., van Ranst, M., 2020. Towards a unified classification for human respiratory syncytial virus genotypes. Virus Evol. 6, 1–11. https://doi.org/10.1093/ve/veaa052

Saikusa, M., Kawakami, C., Nao, N., Takeda, M., Usuku, S., Sasao, T., Nishimoto, K., Toyozawa, T., 2017a. 180-nucleotide duplication in the G Gene of Human metapneumovirus A2b subgroup strains circulating in Yokohama City, Japan, since 2014. Front. Microbiol. 8, 1–11. https://doi.org/10.3389/fmicb.2017.00402

Saikusa, M., Nao, N., Kawakami, C., Usuku, S., Sasao, T., Toyozawa, T., Takeda, M., Okubo, I., 2017b. A novel 111-nucleotide duplication in the G gene of human metapneumovirus. Microbiol. Immunol. 61, 507–512. https://doi.org/10.1111/1348-0421.12543

Saikusa, M., Nao, N., Kawakami, C., Usuku, S., Tanaka, N., Tahara, M., Takeda, M., Okubo, I., 2019. Predominant detection of the subgroup a2b human metapneumovirus strain with a 111-nucleotide duplication in the g gene in Yokohama city, Japan in 2018. Jpn. J. Infect. Dis. 72, 350–352. https://doi.org/10.7883/yoken.JJID.2019.124

Siddle, K.J., Eromon, P., Barnes, K.G., Mehta, S., Oguzie, J.U., Odia, I., Schaffner, S.F., Winnicki, S.M., Shah, R.R., Qu, J., Wohl, S., Brehio, P., Iruolagbe, C., Aiyepada, J., Uyigue, E., Akhilomen, P., Okonofua, G., Ye, S., Kayode, T., Ajogbasile, F., Uwanibe, J., Gaye, A., Momoh, M., Chak, B., Kotliar, D., Carter, A., Gladden-Young, A., Freije, C.A., Omoregie, O., Osiemi, B., Muoebonam, E.B., Airende, M., Enigbe, R., Ebo, B., Nosamiefan, I., Oluniyi, P., Nekoui, M., Ogbaini-Emovon, E., Garry, R.F., Andersen, K.G., Park, D.J., Yozwiak, N.L., Akpede, G., Ihekweazu, C., Tomori, O., Okogbenin, S., Folarin, O.A., Okokhere, P.O., MacInnis, B.L., Sabeti, P.C., Happi, C.T., 2018. Genomic Analysis of Lassa Virus during an Increase in Cases in Nigeria in 2018. N. Engl. J. Med. 379, 1745–1753. https://doi.org/10.1056/nejmoa1804498

Skiadopoulos, M.H., Biacchesi, S., Buchholz, U.J., Amaro-Carambot, E., Surman, S.R., Collins, P.L., Murphy, B.R., 2006. Individual contributions of the human metapneumovirus F, G, and SH surface glycoproteins to the induction of neutralizing antibodies and protective immunity. Virology 345, 492–501. https://doi.org/10.1016/j.virol.2005.10.016

Van Den Hoogen, B.G., De Jong, J.C., Groen, J., Kuiken, T., De Groot, R., Fouchier, R.A.M., Osterhaus, A.D.M.E., 2001. A newly discovered human pneumovirus isolated from young children with respiratory tract disease. Nat. Med. 7, 719–724. https://doi.org/10.1038/89098

van den Hoogen, B.G., Herfst, S., de Graaf, M., Sprong, L., van Lavieren, R., van Amerongen, G., Yüksel, S., Fouchier, R.A.M., Osterhaus, A.D.M.E., de Swart, R.L., 2007. Experimental infection of macaques with human metapneumovirus induces transient protective immunity. J. Gen. Virol. 88, 1251–1259. https://doi.org/10.1099/vir.0.82663-0

Van Den Hoogen, B.G., Herfst, S., Sprong, L., Cane, P.A., Forleo-Neto, E., De Swart, R.L., Osterhaus, A.D.M.E., Fouchier, R.A.M., 2004. Antigenic and Genetic Variability of Human Metapneumoviruses. Emerg. Infect. Dis. 10, 658–666. https://doi.org/10.3201/eid1004.030393

Van Nimwegen, K.J.M., Van Soest, R.A., Veltman, J.A., Nelen, M.R., Van Der Wilt, G.J., Vissers, L.E.L.M., Grutters, J.P.C., 2016. Is the 1000 genome as near as we think? A cost analysis of next-generation sequencing. Clin. Chem. 62, 1458–1464. https://doi.org/10.1373/clinchem.2016.258632

Williams, J.V., Wang, C.K., Yang, C., Tollefson, S.J., House, F.S., Heck, J.M., Chu, M., Brown, J.B., Lintao, L.D., Quinto, J.D., Chu, D., Spaete, R.R., Edwards, K.M., Wright, P.F., Crowe, Jr., J.E., 2006. The Role of Human Metapneumovirus in Upper Respiratory Tract Infections in Children: A 20-Year Experience. J. Infect. Dis. 193, 387–395. https://doi.org/10.1086/499274

Williams, J. V., Harris, P.A., Tollefson, S.J., Halburnt-Rush, L.L., Pingsterhaus, J.M., Edwards, K.M., Wright, P.F., Crowe, J.E., 2004. Human Metapneumovirus and Lower Respiratory Tract Disease in Otherwise Healthy Infants and Children. N. Engl. J. Med. 350, 687–696. https://doi.org/10.1056/NEJMoa1505949

Xu, Y., Lewandowski, K., Jeffery, K., Downs, L.O., Foster, D., Sanderson, N.D., Kavanagh, J., Vaughan, A., Salvagno, C., Vipond, R., Carroll, M., Danby, R., Peto, T., Crook, D., Walker, A.S., Matthews, P.C., Pullan, S.T., 2020. Nanopore metagenomic sequencing to investigate nosocomial transmission of human metapneumovirus from a unique genetic group among haematology patients in the United Kingdom. J. Infect. 80, 571–577. https://doi.org/10.1016/j.jinf.2020.02.003

Xu, Y., Lewandowski, K., Lumley, S., Sanderson, N., Ali, V., Vipond, R., Carroll, M., Jeffery, K., Foster, D., Walker, A.S., Peto, T., Crook, D., Pullan, S.T., Matthews, P.C., 2018. Nanopore metagenomic sequencing of full length human metapneumovirus (HMPV) within a unique sub-lineage. bioRxiv.

Boivin, G., Mackay, I., Sloots, T.P., Madhi, S., Freymuth, F., Wolf, D., Shemer-Avni, Y., Ludewick, H., Gray, G.C., LeBlanc, É., 2004. Global genetic diversity of human metapneumovirus fusion gene. Emerg. Infect. Dis. 10, 1154–1157. https://doi.org/10.3201/eid1006.031097

Dudas, G., Bedford, T., 2019. The ability of single genes vs full genomes to resolve time and space in outbreak analysis. BMC Evol. Biol. 19, 1–27. https://doi.org/10.1186/s12862-019-1567-0

Ebihara, T., Endo, R., Kikuta, H., Ishiguro, N., Ishiko, H., Hara, M., Takahashi, Y., Kobayashi, K., 2004. Human Metapneumovirus Infection in Japanese Children. J. Clin. Microbiol. 42, 126–132. https://doi.org/10.1128/JCM.42.1.126-132.2004

Falsey, A.R., Erdman, D., Anderson, L.J., Walsh, E.E., 2003. Human Metapneumovirus Infections in Young and Elderly Adults. J. Infect. Dis. 187, 785–790. https://doi.org/10.1086/367901

Herfst, S., de Graaf, M., Schickli, J.H., Tang, R.S., Kaur, J., Yang, C.-F., Spaete, R.R., Haller, A.A., van den Hoogen, B.G., Osterhaus, A.D.M.E., Fouchier, R.A.M., 2004. Recovery of Human Metapneumovirus Genetic Lineages A and B from Cloned cDNA. J. Virol. 78, 8264–8270. https://doi.org/10.1128/jvi.78.15.8264-8270.2004

Herfst, S., de Graaf, M., Schrauwen, E.J.A., Ulbrandt, N.D., Barnes, A.S., Senthil, K., Osterhaus, A.D.M.E., Fouchier, R.A.M., van den Hoogen, B.G., 2007. Immunization of Syrian golden hamsters with F subunit vaccine of human metapneumovirus induces protection against challenge with homologous or heterologous strains. J. Gen. Virol. 88, 2702–2709. https://doi.org/10.1099/vir.0.83084-0

Hoek, R.A.S., Paats, M.S., Pas, S.D., Bakker, M., Hoogsteden, H.C., Boucher, C.A.B., Van Der Eerden, M.M., 2013. Incidence of viral respiratory pathogens causing exacerbations in adult cystic fibrosis patients. Scand. J. Infect. Dis. 45, 65–69. https://doi.org/10.3109/00365548.2012.708942

Huck, B., Scharf, G., Neumann-Haefelin, D., Puppe, W., Weigl, J., Falcone, V., 2006. Novel human metapneumovirus sublineage. Emerg. Infect. Dis. 12, 147–150. https://doi.org/10.3201/eid1201.050772

Jain, S., Self, W.H., Wunderink, R.G., Fakhran, S., Balk, R., Bramley, A.M., Reed, C., Grijalva, C.G., Anderson, E.J., Courtney, D.M., Chappell, J.D., Qi, C., Hart, E.M., Carroll, F., Trabue, C., Donnelly, H.K., Williams, D.J., Zhu, Y., Arnold, S.R., Ampofo, K., Waterer, G.W., Levine, M., Lindstrom, S., Winchell, J.M., Katz, J.M., Erdman, D., Schneider, E., Hicks, L.A., McCullers, J.A., Pavia, A.T., Edwards, K.M., Finelli, L., 2015. Community-Acquired Pneumonia Requiring Hospitalization among U.S. Adults. N. Engl. J. Med. 373, 415–427. https://doi.org/10.1056/nejmoa1500245

Kamau, E., Oketch, J.W., De Laurent, Z.R., Phan, M.V.T., Agoti, C.N., Nokes, D.J., Cotten, M., 2020. Whole genome sequencing and phylogenetic analysis of human metapneumovirus strains from Kenya and Zambia. BMC Genomics 21, 1–10. https://doi.org/10.1186/s12864-020-6498-z

Lefkowitz, E.J., Dempsey, D.M., Hendrickson, R.C., Orton, R.J., Siddell, S.G., Smith, D.B., 2018. Virus taxonomy: The database of the International Committee on Taxonomy of Viruses (ICTV). Nucleic Acids Res. 46, D708–D717. https://doi.org/10.1093/nar/gkx932

Mackay, I.M., Bialasiewicz, S., Jacob, K.C., McQueen, E., Arden, K.E., Nissen, M.D., Sloots, T.P., 2006. Genetic diversity of human metapneumovirus over 4 consecutive years in Australia. J. Infect. Dis. 193, 1630–1633. https://doi.org/10.1086/504260

Maertzdorf, J., Wang, C.K., Brown, J.B., Quinto, J.D., Chu, M., De Graaf, M., Van Den Hoogen, B.G., Spaete, R., Osterhaus, A.D.M.E., Fouchier, R.A.M., 2004. Real-Time Reverse Transcriptase PCR Assay for Detection of Human Metapneumoviruses from All Known Genetic Lineages. J. Clin. Microbiol. 42, 981–986. https://doi.org/10.1128/JCM.42.3.981-986.2004

Nao, N., Saikusa, M., Sato, K., Sekizuka, T., Usuku, S., Tanaka, N., Nishimura, H., Takeda, M., 2020. Recent molecular evolution of human metapneumovirus (HMPV): Subdivision of HMPV a2b strains. Microorganisms 8, 1–14. https://doi.org/10.3390/microorganisms8091280

O'Brien, K.L., Baggett, H.C., Brooks, W.A., Feikin, D.R., Hammitt, L.L., Higdon, M.M., Howie, S.R.C., Deloria Knoll, M., Kotloff, K.L., Levine, O.S., Madhi, S.A., Murdoch, D.R., Prosperi, C., Scott, J.A.G., Shi, Q., Thea, D.M., Wu, Z., Zeger, S.L., Adrian, P. V., Akarasewi, P., Anderson, T.P., Antonio, M., Awori, J.O., Baillie, V.L., Bunthi, C., Chipeta, J., Chisti, M.J., Crawley, J., DeLuca, A.N., Driscoll, A.J., Ebruke, B.E., Endtz, H.P., Fancourt, N., Fu, W., Goswami, D., Groome, M.J., Haddix, M., Hossain, L., Jahan, Y., Kagucia, E.W., Kamau, A., Karron, R.A., Kazungu, S., Kourouma, N., Kuwanda, L., Kwenda, G., Li, M., Machuka, E.M., Mackenzie, G., Mahomed, N., Maloney, S.A., McLellan, J.L., Mitchell, J.L., Moore, D.P., Morpeth, S.C., Mudau, A., Mwananyanda, L., Mwansa, J., Silaba Ominde, M., Onwuchekwa, U., Park, D.E., Rhodes, J., Sawatwong, P., Seidenberg, P., Shamsul, A., Simões, E.A.F., Sissoko, S., Wa Somwe, S., Sow, S.O., Sylla, M., Tamboura, B., Tapia, M.D., Thamthitiwat, S., Toure, A., Watson, N.L., Zaman, K., Zaman, S.M.A., 2019. Causes of severe pneumonia requiring hospital admission in children without HIV infection from Africa and Asia: the PERCH multi-country case-control study. Lancet 394, 757–779. https://doi.org/10.1016/S0140-6736(19)30721-4

Oude Munnink, B.B., Kik, M., de Bruijn, N.D., Kohl, R., van der Linden, A., Reusken, C.B.E.M., Koopmans, M., 2019. Towards high quality real-time whole genome sequencing during outbreaks using Usutu virus as example. Infect. Genet. Evol. 73, 49–54. https://doi.org/10.1016/j.meegid.2019.04.015

Pollett, S., Trovão, N.S., Tan, Y., Eden, J.S., Halpin, R.A., Bera, J., Das, S.R., Wentworth, D., Ocaña, V., Mendocilla, S.M., Álvarez, C., Calisto, M.E., Garcia, J., Halsey, E., Ampuero, J.S., Nelson, M.I., Leguia, M., 2018. The transmission dynamics and diversity of human metapneumovirus in Peru. Influenza Other Respi. Viruses 12, 508–513. https://doi.org/10.1111/irv.12537

Quick, J., Grubaugh, N.D., Pullan, S.T., Claro, I.M., Smith, A.D., Gangavarapu, K., Oliveira, G., Robles-Sikisaka, R., Rogers, T.F., Beutler, N.A., Burton, D.R., Lewis-Ximenez, L.L., Jesus, J.G. de, Giovanetti, M., Hill, S., Black, A., Bedford, T., Carroll, M.W., Nunes, M., Alcantara Jr, L.C., Sabino, E.C., Baylis, S.A., Faria, N., Loose, M., Simpson, J.T., Pybus, O.G., Andersen, K.G., Loman, N.J., 2018. Multiplex PCR method for MinION and Illumina sequencing of Zika and other virus genomes directly from clinical samples. Nat. Protoc. 12, 1261–1276. https://doi.org/10.1038/nprot.2017.066.Multiplex

Radford, A.D., Chapman, D., Dixon, L., Chantrey, J., Darby, A.C., Hall, N., 2012. Application of next-generation sequencing technologies in virology. J. Gen. Virol. 93, 1853–1868. https://doi.org/10.1099/vir.0.043182-0

Ramaekers, K., Rector, A., Cuypers, L., Lemey, P., Keyaerts, E., van Ranst, M., 2020. Towards a unified classification for human respiratory syncytial virus genotypes. Virus Evol. 6, 1–11. https://doi.org/10.1093/ve/veaa052

Saikusa, M., Kawakami, C., Nao, N., Takeda, M., Usuku, S., Sasao, T., Nishimoto, K., Toyozawa, T., 2017a. 180-nucleotide duplication in the G Gene of Human metapneumovirus A2b subgroup strains circulating in Yokohama City, Japan, since 2014. Front. Microbiol. 8, 1–11. https://doi.org/10.3389/fmicb.2017.00402

Saikusa, M., Nao, N., Kawakami, C., Usuku, S., Sasao, T., Toyozawa, T., Takeda, M., Okubo, I., 2017b. A novel 111-nucleotide duplication in the G gene of human metapneumovirus. Microbiol. Immunol. 61, 507–512. https://doi.org/10.1111/1348-0421.12543

Saikusa, M., Nao, N., Kawakami, C., Usuku, S., Tanaka, N., Tahara, M., Takeda, M., Okubo, I., 2019. Predominant detection of the subgroup a2b human metapneumovirus strain with a 111-nucleotide duplication in the g gene in Yokohama city, Japan in 2018. Jpn. J. Infect. Dis. 72, 350–352. https://doi.org/10.7883/yoken.JJID.2019.124

Siddle, K.J., Eromon, P., Barnes, K.G., Mehta, S., Oguzie, J.U., Odia, I., Schaffner, S.F., Winnicki, S.M., Shah, R.R., Qu, J., Wohl, S., Brehio, P., Iruolagbe, C., Aiyepada, J., Uyigue, E., Akhilomen, P., Okonofua, G., Ye, S., Kayode, T., Ajogbasile, F., Uwanibe, J., Gaye, A., Momoh, M., Chak, B., Kotliar, D., Carter, A., Gladden-Young, A., Freije, C.A., Omoregie, O., Osiemi, B., Muoebonam, E.B., Airende, M., Enigbe, R., Ebo, B., Nosamiefan, I., Oluniyi, P., Nekoui, M., Ogbaini-Emovon, E., Garry, R.F., Andersen, K.G., Park, D.J., Yozwiak, N.L., Akpede, G., Ihekweazu, C., Tomori, O., Okogbenin, S., Folarin, O.A., Okokhere, P.O., MacInnis, B.L., Sabeti, P.C., Happi, C.T., 2018. Genomic Analysis of Lassa Virus during an Increase in Cases in Nigeria in 2018. N. Engl. J. Med. 379, 1745–1753. https://doi.org/10.1056/nejmoa1804498

Skiadopoulos, M.H., Biacchesi, S., Buchholz, U.J., Amaro-Carambot, E., Surman, S.R., Collins, P.L., Murphy, B.R., 2006. Individual contributions of the human metapneumovirus F, G, and SH surface glycoproteins to the induction of neutralizing antibodies and protective immunity. Virology 345, 492–501. https://doi.org/10.1016/j.virol.2005.10.016

Van Den Hoogen, B.G., De Jong, J.C., Groen, J., Kuiken, T., De Groot, R., Fouchier, R.A.M., Osterhaus, A.D.M.E., 2001. A newly discovered human pneumovirus isolated from young children with respiratory tract disease. Nat. Med. 7, 719–724. https://doi.org/10.1038/89098

van den Hoogen, B.G., Herfst, S., de Graaf, M., Sprong, L., van Lavieren, R., van Amerongen, G., Yüksel, S., Fouchier, R.A.M., Osterhaus, A.D.M.E., de Swart, R.L., 2007. Experimental infection of macaques with human metapneumovirus induces transient protective immunity. J. Gen. Virol. 88, 1251–1259. https://doi.org/10.1099/vir.0.82663-0

Van Den Hoogen, B.G., Herfst, S., Sprong, L., Cane, P.A., Forleo-Neto, E., De Swart, R.L., Osterhaus, A.D.M.E., Fouchier, R.A.M., 2004. Antigenic and Genetic Variability of Human Metapneumoviruses. Emerg. Infect. Dis. 10, 658–666. https://doi.org/10.3201/eid1004.030393

Van Nimwegen, K.J.M., Van Soest, R.A., Veltman, J.A., Nelen, M.R., Van Der Wilt, G.J., Vissers, L.E.L.M., Grutters, J.P.C., 2016. Is the 1000 genome as near as we think? A cost analysis of next-generation sequencing. Clin. Chem. 62, 1458–1464. https://doi.org/10.1373/clinchem.2016.258632

Williams, J.V., Wang, C.K., Yang, C., Tollefson, S.J., House, F.S., Heck, J.M., Chu, M., Brown, J.B., Lintao, L.D., Quinto, J.D., Chu, D., Spaete, R.R., Edwards, K.M., Wright, P.F., Crowe, Jr., J.E., 2006. The Role of Human Metapneumovirus in Upper Respiratory Tract Infections in Children: A 20-Year Experience. J. Infect. Dis. 193, 387–395. https://doi.org/10.1086/499274

Williams, J. V., Harris, P.A., Tollefson, S.J., Halburnt-Rush, L.L., Pingsterhaus, J.M., Edwards, K.M., Wright, P.F., Crowe, J.E., 2004. Human Metapneumovirus and Lower Respiratory Tract Disease in Otherwise Healthy Infants and Children. N. Engl. J. Med. 350, 687–696. https://doi.org/10.1056/NEJMoa1505949

Xu, Y., Lewandowski, K., Jeffery, K., Downs, L.O., Foster, D., Sanderson, N.D., Kavanagh, J., Vaughan, A., Salvagno, C., Vipond, R., Carroll, M., Danby, R., Peto, T., Crook, D., Walker, A.S., Matthews, P.C., Pullan, S.T., 2020. Nanopore metagenomic sequencing to investigate nosocomial transmission of human metapneumovirus from a unique genetic group among haematology patients in the United Kingdom. J. Infect. 80, 571–577. https://doi.org/10.1016/j.jinf.2020.02.003

Xu, Y., Lewandowski, K., Lumley, S., Sanderson, N., Ali, V., Vipond, R., Carroll, M., Jeffery, K., Foster, D., Walker, A.S., Peto, T., Crook, D., Pullan, S.T., Matthews, P.C., 2018. Nanopore metagenomic sequencing of full length human metapneumovirus (HMPV) within a unique sub-lineage. bioRxiv.

4

Emergence and potential extinction of genetic lineages of human metapneumovirus between 2005 and 2021

Kevin Groen[a], Stefan van Nieuwkoop[a], Adam Meijer[b], Bas van der Veer[b], Jeroen J.A. van Kampen[a], Pieter L. Fraaij[a,c], Ron A.M. Fouchier[a], Bernadette G. van den Hoogen[a #]

[a] Department of Viroscience, Erasmus MC, Wijtemaweg 80, 3015 CN Rotterdam, The Netherlands
[b] Center for Infectious Disease Control, National Institute for Public Health and the Environment, Bilthoven, The Netherland
[c] Pediatric Infectious Diseases & Immunology, Erasmus MC-Sophia Children's Hospital, Rotterdam, The Netherlands.

mBio. 2023 Feb 28;14(1):e0228022

Abstract

Human metapneumovirus (HMPV) is one of the leading causes of respiratory illness (RI), primarily in infants. Worldwide, two genetic lineages (A and B) of HMPV are circulating that are antigenically distinct and can each be further divided into genetic sublineages. Surveillance combined with large-scale whole genome sequencing studies of HMPV are scarce but would help to identify viral evolutionary dynamics. Here, we analyzed 130 whole HMPV genome sequences obtained from samples collected from individuals hospitalized with RI and partial fusion (n=144) and attachment (n=123) protein gene sequences obtained from samples collected from patients with RI visiting general practitioners, from 2005 through 2021 in the Netherlands. Phylogenetic analyses demonstrated that HMPV continued to group in the four sublineages described in 2004 (A1, A2, B1, B2). However, one sublineage (A1) was no longer detected in the Netherlands after 2006, while the others continued to evolve. No differences were observed in dominant (sub)lineages between samples obtained from patients with RI being hospitalized and those consulting general practitioners. In both populations, viruses of lineage A2 carrying a 180-nucleotide or 111-nucleotide duplication in the attachment protein gene became the most frequently detected genotypes. In the past, different names for the newly emerging lineages have been, demonstrating the need for a consistent naming convention. Here, criteria are proposed for the designation of new genetic lineages to aid towards a systematic HMPV classification.

Importance

Human metapneumovirus is one of the major causative agents of human respiratory tract infections. Monitoring of virus evolution could aid towards the development of new antiviral treatments or vaccine designs. Here, we studied HMPV evolution between 2005 and 2021 with viruses obtained from samples collected from hospitalized individuals and patients consulting general practitioners with respiratory infections. Phylogenetic analyses demonstrated that HMPV continued to group in the four previously described sublineages (A1, A2, B1, B2). However, one sublineage (A1) was no longer detected after 2006, while the others continued to evolve. No differences were observed in dominant (sub)lineages between patients being hospitalized and those consulting general practitioners. In both populations, viruses of lineage A2 carrying a 180-nucleotide or 111-nucleotide duplication in the attachment protein gene became the most frequently detected genotypes. This data was used to propose criteria for the designation of new genetic lineages to aid towards a systematic HMPV classification.

Introduction

Human metapneumovirus (HMPV) is a non-segmented negative-strand RNA virus belonging to the *Pneumoviridae* family. Globally, HMPV is responsible for 5-15% of respiratory infections and one of the leading causative agents of respiratory illness in young children, only second to respiratory syncytial virus (RSV) (1–8). Clinical symptoms caused by HMPV range from mild respiratory illness to bronchiolitis and pneumonia, similar to those caused by RSV (reviewed in (9)).

HMPV has a genome of approximately 13,3 kb in size, containing 8 genes which encode 9 proteins. This includes three surface proteins: the short hydrophobic protein (SH), the attachment glycoprotein (G), and the fusion protein (F). These surface proteins can be used for virus genotyping, also in relation to antigenic variation of circulating HMPV (10, 11). In 2004 it was reported that HMPV isolates clustered in two main genetic lineages that are also antigenically distinct (A and B), and that each diverged in two sublineages (A1, A2, B1 and B2) (10). In 2006, a further split of sublineage A2 into A2a and A2b was reported (12). Although the presence of a third lineage (A2c) was reported, another study suggested that the A2b lineage should be further divided in A2b1 and A2b2 and that A2b2 can be mistaken for lineage A2c (13, 14). There were also suggestions that the B2 lineage should be further divided into lineages B2a and B2b, although a consensus on this matter has not been achieved (15). Recently, circulation of lineage A2 viruses carrying a 180-nucleotide or 111-nucleotide duplication in the G gene was reported for the first time in Japan in 2014 and 2017, respectively (16, 17). In the following years, these viruses were also detected in Spain, Vietnam and China (16–18). One of these genotypes, with a 111-nucleotide duplication, became the dominant circulating genotype in Yokohama city in Japan (16–18).

Studies on HMPV evolution have mainly focused on the genetic variation of the F and G genes (10, 11, 13, 16, 17, 19–21). However, whole genome sequencing of HMPV might provide insights into virus evolution that will be missed by analyzing (partial) F and G sequences. Recent genetic changes, such as sequence duplications in the HMPV G gene, highlight the importance to monitor HMPV evolutionary dynamics, but partial genome sequencing will miss any evolutionary events that occur in genes other than F and G. With next-generation sequencing (NGS) platforms rapidly improving, obtaining viral whole genome sequences has simplified considerably (22). Recent studies reported assays for HMPV whole genome sequencing, using either Illumina sequencing, Ion Torrent, or Nanopore technology (23–26). We recently introduced an HMPV whole genome sequencing method using MinION Nanopore technology (27). In this study, using this method, whole genome sequences were generated from 130 HMPV strains obtained from samples collected from hospitalized individuals suffering from respiratory tract infections (RTI) between 2005 and

2021. Additionally, partial F and G gene sequences were analyzed from 144 viruses obtained from patients with a RTI that visited general practitioners from 2005 through 2021, to compare circulation of viruses between the hospitalized patients and patients consulting general practitioners. Phylogenetic analyses were performed to study recent evolutionary patterns and used to propose a robust HMPV classification system for emerging virus lineages.

Results

Phylogenetic analyses of HMPV whole genome sequences

Full-length genome sequences were generated for 130 viruses obtained from hospitalized individuals between 2005 and 2021 and for 13 additional viruses from earlier years (1993-2004) that were also not sequenced previously. Phylogenetic analysis of these 143 whole genome sequences, in combination with all 56 whole genome sequences available from GenBank (total n=199), demonstrated clustering of the viruses in the two main genetic lineages A and B (Figure 1, Figure A1, Table A1). Within these lineages, separation into the four previously described sublineages A1, A2, B1 and B2 was still observed. Additional subdivisions within lineage A2 were clearly possible, as suggested before (12, 13), but clear criteria for such novel lineage designations are needed. Moreover, different names for the newly emerging lineages have been used in the past, demonstrating the need for a consistent naming convention. For simplicity, lineages from here on forward are referred to as A1, A2,A2.1, A2.2, A2.2.1, A2.2.2, B1, and B2. Hereby, A and B are used to distinguish between different phenotypes and phylogenetic clusters are defined numerically.

Table 1. Increase in incidence of viruses carrying a 180 and 111-nucleotide duplications in the G gene from samples obtained from hospitalized patients within lineage A2.2.2 between 2014 and 2021.

Year	180-nt duplication	111-nt duplication	No duplication	Total
2014	-	-	5 (100%)	5
2015	-	2 (29%)	5 (71%)	7
2016	3 (38%)	2 (25%)	3 (38%)	8
2017	2 (29%)	3 (43%)	2 (29%)	7
2018	1 (50%)	1 (50%)	-	2
2019	-	2 (100%)	-	2
2020	-	-	-	-
2021	-	4 (100%)	-	4

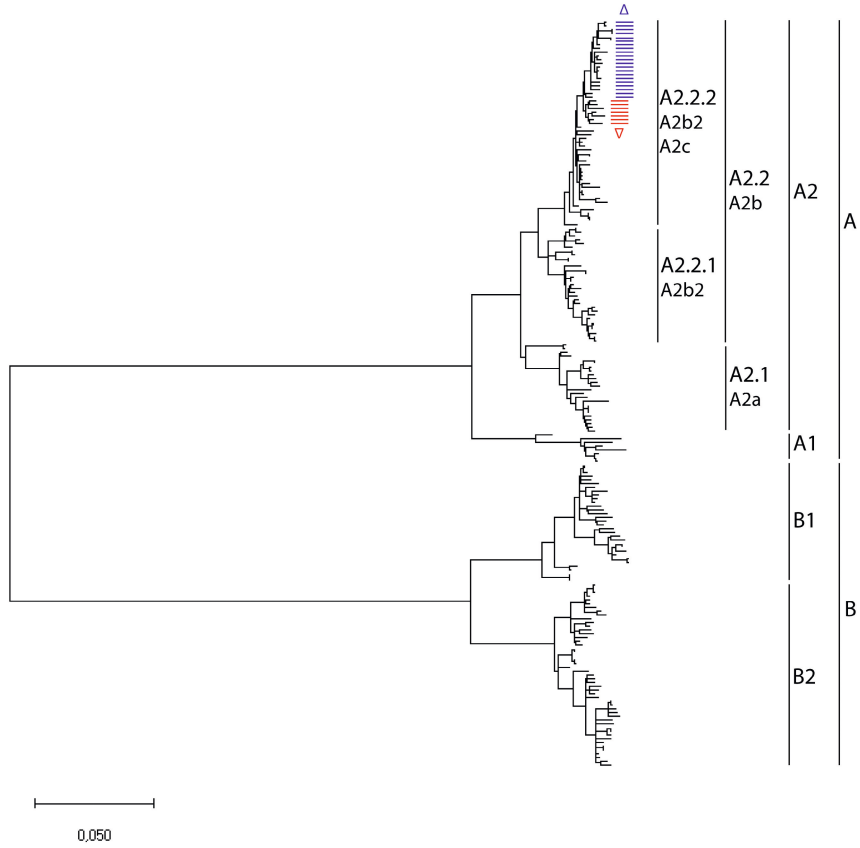

Figure 1. Maximum likelihood phylogenetic tree based on 199 whole HMPV genome sequences. The tree was reconstructed using the GTR +G +I substitution model with 1000 bootstraps. The tree with bootstrap values and virus names is shown in Figure A1. Markers on the right indicate the main virus lineages A and B, which could be divided in 6 sublineages (A1, A2.1, A2.2.1, A2.2.2, B1, B2). Lineage A2.2.2 viruses with a 180nt-duplication (▽, red line) or a 111nt-duplication (△, blue line) in the G gene are highlighted. Different names that have been used for each lineage are shown.

In this sample set, viruses with a duplication in the G gene were detected for the first time in 2015 (Table 1). Viruses containing either a 111-nucleotide or a 180-nucleotide duplication in the G gene clustered within the A2.2.2 lineage in two smaller clusters (Figure 1). The most recent virus with a 180-nucleotide duplication in the G gene was detected in 2018, while from 2019 onwards only viruses with a 111-nucleotide duplication in the G gene were detected. After 2018, no more lineage A2.2.2 viruses without a duplication in the G gene were detected.

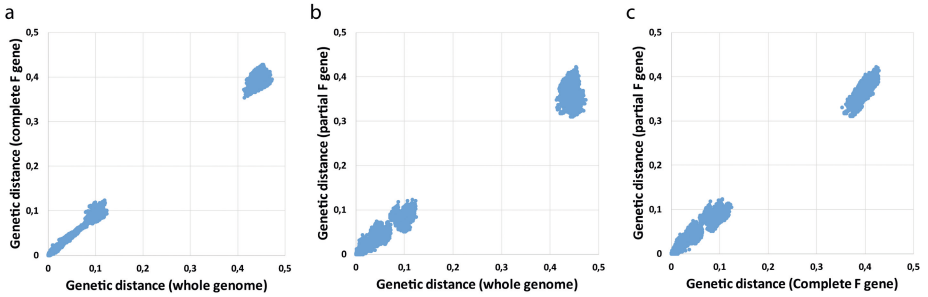

Figure 2. Scatterplots of p-distances between viruses from phylogenetic trees reconstructed from (a) whole genome sequences vs full-length F gene sequences, (b) whole genome sequences vs partial F gene sequences, (c) full-length F gene sequences vs partial F gene sequences. The trees from which pdistances were compared are shown in figures A1, A2, and A3.

Comparison of virus clustering based on whole genome, full-length F, or partial F gene sequences

The majority of reported phylogenetic analyses have been based on either full-length or partial F gene sequences (in general nt 778-1226 of the F gene (10)). To compare clustering of viruses based on full-length genome sequences with that based on full-length F or partial F gene sequences, phylogenetic trees were reconstructed from nucleotide alignments of full-length F gene and partial F gene sequences (nt 778-1226 of the F gene) derived from the 143 full genome sequences described above. No difference in clustering of the viruses was observed between the three analyses, which demonstrates the consistency of lineage topology (Figures A1, A2, and A3). Interestingly, viruses with a duplication in the G gene also clustered together based on full-length or partial F gene sequences, demonstrating that full-length or partial F gene sequences by themselves carry sufficient information to accurately genotype a virus. To assess whether the phylogenetic distances between viruses were similar in each of the three trees, scatterplots were generated from the *p*-distances (the proportion of nucleotide sites at which sequences differ) between all viruses from one tree plotted against those from another tree. The variation in *p*-distance between the trees reconstructed from whole genome sequences and full-length F gene sequences were the smallest (Figure 2a), while the variation in *p*-distances between trees reconstructed from partial F gene sequences and either full-length F gene sequences or whole genome sequences were slightly larger (Figure 2b and 2c), indicating that full-length F gene sequences can be used for phylogenetic analysis with similar accuracy as whole genome sequences.

Designation of HMPV lineages

Although the majority of HMPV evolution studies are based on analysis of F gene sequences, some studies rely on analysis of the more variable G gene, while the SH gene is rarely used for these studies. To compare genetic clustering based on the F, G, and SH genes, an alignment was generated from HMPV whole genome sequences obtained in this study combined with those available from GenBank (n=199). From this alignment, the F, G, and SH genes were selected and used to analyze genetic clustering. For all three proteins, genetic maps were constructed from the sequence alignments. Genetic maps were generated by multidimensional scaling of genetic distance matrixes, which contain all pairwise numbers of nucleotide substitutions between viruses. Distances in the map, represented by a grid, demonstrate the number of nucleotide substitutions between viruses, which each line of the grid representing 10 substitutions. The genetic maps demonstrated clear clustering into six distinct lineages: A1, A2.1, A2.2.1, A2.2.2, B1, and B2 (Figure A4). Clustering based on F gene sequences resulted in the highest resolution between these six lineages, which supported the use of F gene sequences for designation of lineages.

Table 2. Nucleotide substitutions within and between all HMPV lineages including the proposed A2.2.1 and A2.2.2 lineages.

Lineage	A1	A2.1	A2.2.1	A2.2.2	B1	B2
A1	0-57	68-114	68-122	84-129	234-275	236-264
A2.1		0-59	21-75	39-87	239-278	240-275
A2.2.1			0-45	26-70	247-288	248-284
A2.2.2				0-41	245-281	240-274
B1					0-88	62-126
B2						0-73

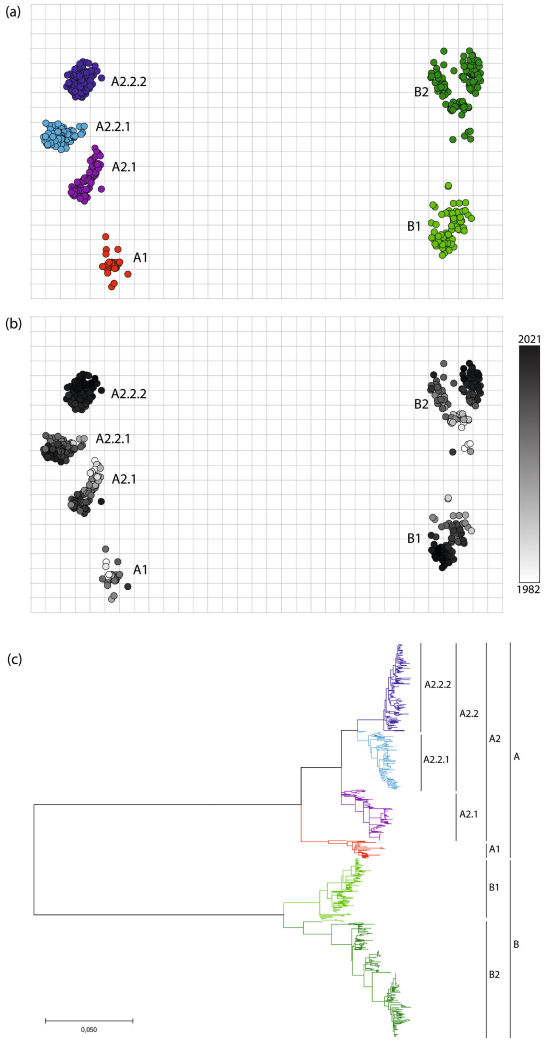

Figure 3. Genetic evolution of HMPV based on full-length F gene sequences. A genetic map was generated from full-length F gene sequences obtained in this study combined with those from GenBank (n=744) with color coding per (a) lineage or (b) year of isolation. The axes represent genetic distance, with each square of the grid representing a 10-nucleotide distance. Sequences were color coded by year of isolation using a greyscale. (c) Maximum likelihood phylogenetic tree based on 744 full-length HMPV F gene sequences. The tree was reconstructed using the GTR +G +I substitution model with 1000 bootstraps. The tree is color coded according to the colors used in the map shown in (a). The tree with bootstrap values and isolate names is shown in Figure A5. Markers on the right indicate virus lineages and sublineages.

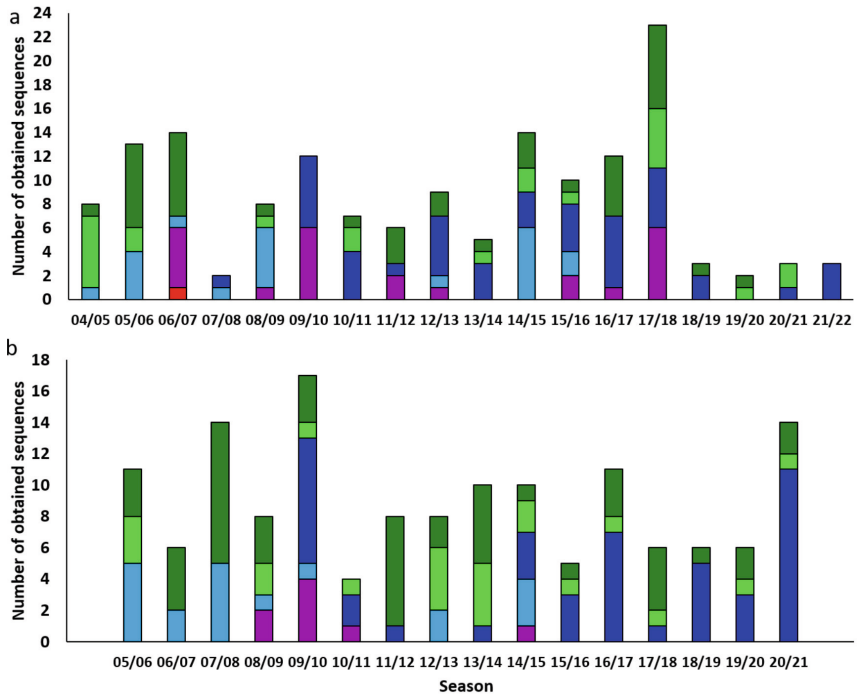

Figure 4. (a) The number of obtained sequences from each lineage of viruses isolated from hospitalized patients suffering from RTI per epidemiologic season. Seasons started in week 40 and ended in week 39 of the next year. Samples were selected based on a Ct value <=25.0, with exceptions as described in the Methods section, and genotyped by phylogenetic analyses of whole genome sequences. (b) Clustering of viruses isolated from patients suffering from RTI visiting general practitioners per year. Samples were selected as described in the Methods section and genotyped based on phylogenetic analyses of partial F and G gene sequences. Bars are color coded based on the map shown in Figure 3a.

To propose a robust HMPV classification system, genetic evolution was analyzed based on alignment of full-length F gene sequences obtained in this study combined with those from GenBank (n=744). Analysis of a genetic map and phylogenetic tree reconstructed from this alignment demonstrated that the viruses clustered in six distinct lineages (Figure 3a-3c, Figure A5), identical to described above. The A2.2 lineage displayed gradual evolution over time, while in other lineages directional evolution is not as clear (Figure 3b). In the genetic map, there appeared to be a segregation within the B2 lineage, although the border between these two lineages was not clear. This was in agreement with the phylogenetic tree, in which the distance between these two lineages was relatively small (Figure 3c). In order to accurately designate the different sublineages, the ranges of nucleotide substitutions between viruses

within and between lineages were calculated (Table 2). Overall, the genetic distances within the main lineages A and B were comparable (0-129 and 0-126 nucleotide substitutions between viruses within lineage A and B, respectively). Between lineage A1 and A2, the genetic distance ranged from 68-129 nucleotide substitutions. The genetic differences between viruses within the B1 and B2 lineage ranged from 0-88 and 0-73 nucleotide substitutions, respectively, while between B1 and B2 the genetic distance ranged between 62-126 nucleotide substitutions. The genetic distances between viruses within the lineage A2.1, A2.2.1 and A2.2.2 ranged between 0 and 59 nucleotide substitutions, while between A2.1 and the two A2.2 lineages (A2.2.1 and A.2.2.2), this distance was 21-75 and 38-87 for A2.2.1 and A.2.2.2 lineage viruses respectively. The distance between viruses from lineage A2.2.1 and A.2.2.2 ranged between 26 and 70 nucleotide substitutions. Although genetic distances within lineage A and B were comparable, two new lineages had evolved within lineage A while no new lineages have evolved in lineage B.

Based on this analysis, we suggest that the nucleotide substitutions between a newly sequenced virus and viruses from each known lineage can be used to determine to which lineage the new virus belongs. For example, a virus from lineage A2.2.2 should contain between 0-41 nucleotide substitutions compared to other lineage A2.2.2 viruses, between 26-70 nucleotide substitutions compared to A2.2.1 lineage viruses, etc. If the number of nucleotide substitutions fall within the ranges of each lineage as described in Table 2, the newly sequenced can be classified accordingly. Alternatively, if the genetic distance of a newly isolated virus exceeds the ranges of nucleotide substitutions between lineages as described in Table 2, this virus might be considered part of a new lineage. These calculations provide a means to determine which lineage a newly isolated virus belongs to.

Table 3. The number of viruses belonging to lineage A or lineage B sorted by Ct values (<=25.0 and >25.0) from both hospitalized patients and people visiting general practitioners.

	Ct <=25.0		**Ct >25.0**		**Total**	
Virus lineage	A	B	A	B	A	B
Hospitalized patients	81/130 (62.3%)	49/130 (37.6%)	11/33 (33.3%)	22/33 (66.7%)	92/163 (56.4%)	71/163 (43.5%)
General practitioners	20/34 (58.8%)	14/34 (41.2%)	52/110 (47.2%)	58/110 (52.8%)	72/144 (50.0%)	72/144 (50.0%)
Total	101/164 (61.6%)	63/164 (38.4%)	62/143 (43.4%)	80/143 (56.6%)		

Circulation of virus lineages over time

Among viruses obtained from hospitalized individuals between 2005 and 2021, one virus belonged to lineage A1, 15 to lineage A2.1, 21 to lineage A2.2.1, 44 to lineage A2.2.2, 14 to B1, and 35 to the B2 lineage (Figure 4a). The earliest virus of lineage A2.2.2 was obtained in 2008, similar to described by others (Nao et al., 2020). The last virus belonging to the A1 lineage was collected in 2006. In this data set, a significantly higher number of lineage A viruses (81/130, 62.3%) were detected than lineage B viruses (49/130, 37.7%) (Chi^2, p=0.046) (Table 3). It is possible that this is due to the selection bias of samples based on a cutoff qRT-PCR Ct-value <=25.0. To investigate whether the underrepresentation of B lineage viruses was due to this Ct cutoff value, 33 additional samples with a Ct value >25.0 (Ct range: 25.3-30.7) were sequenced and genotyped based on lineage specific amino acid residues of partial F gene sequences (Van Den Hoogen et al., 2004). Eleven of these viruses (33.3%) belonged to lineage A (one A1 virus from 2006 and ten A2 viruses) and 22 (66.6%) to lineage B (eight B1 and 14 B2). Thus, a higher number of lineage B viruses than lineage A viruses was detected in samples with a Ct value >25.0.

Prevalence of HMPV lineages in patients with RTI consulting general practitioners

To address circulation of HMPV lineages among patients with RTI consulting general practitioners, 144 viruses collected from samples obtained from patients with RTI consulting general practitioners in the Netherlands from 2005 through 2021 were genotyped by sequencing of partial F and G genes. The Ct value of these samples determined by qRT-PCR ranged from 18.6 to 38.1. Phylogenetic analysis of these sequences indicated clustering of the viruses in the six lineages similar to the viruses obtained from hospitalized patients (Figure 4b, Figure 5, Figure A6). Viruses belonging to lineage A1 were not detected. From the 144 viruses, 71 (49.3%) clustered in lineage A and 73 (50.7%) in lineage B (Table 3). In the samples with Ct value <=25.0 the number of A and B lineage viruses were not significantly different (20/34 (58.8%) lineage A and 14/34 (41.2%) lineage B, p=0.4651). In samples with a Ct >25.0, the number of lineage A (52/110, 47.2%) and lineage B viruses (58/110, 52.8%) were not significantly different (p=>0.05), although a slightly higher number of lineage B viruses was detected. This contrasted that of samples isolated from hospitalized patients, in which a significantly higher number of lineage B viruses was detected among samples with a Ct value >25.0 (Table 3).

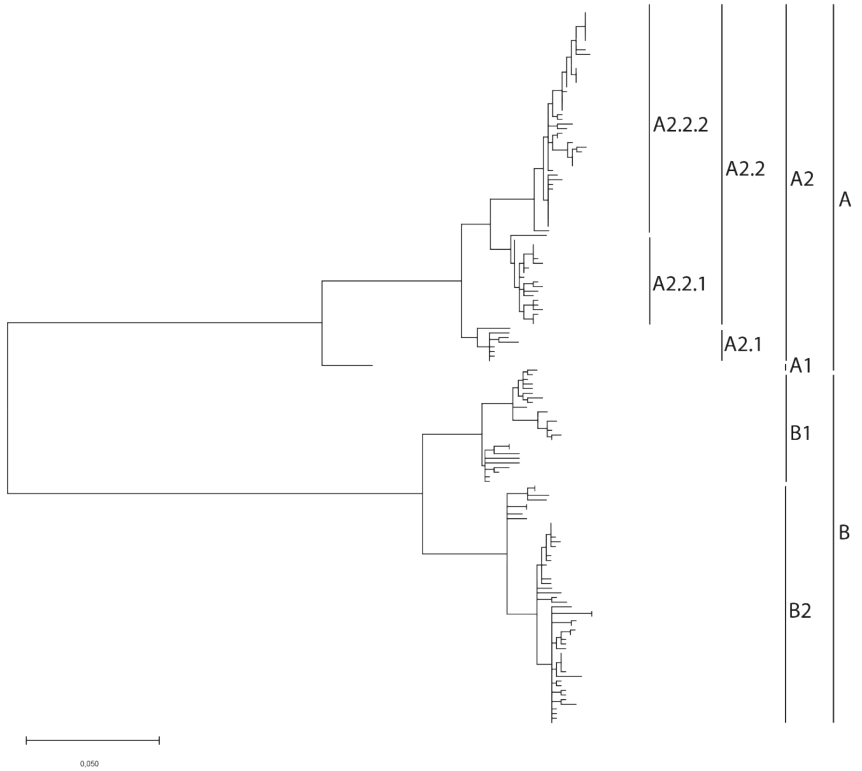

Figure 5. Maximum likelihood phylogenetic tree reconstructed from partial F gene sequences from viruses obtained from patients with RTI visiting general practitioners combined with those of six viruses obtained from hospitalized individuals. The tree was reconstructed using the GTR +G +I substitution model with 1000 bootstraps. The tree with bootstrap values and isolate names is shown in Figure A6. Lines indicate virus lineages (e.g. A2).

Discussion

After the identification of HMPV in 2001, it was reported that worldwide viruses clustered into two genetic lineages that were also antigenically distinct (A and B), which both split into two genetic lineages (A1, A2, B1, B2) (10). Here we investigated the evolution of HMPV over the last decades in the Netherlands using phylogenetic analysis of full genome sequences. In this study, phylogenetic analysis of 130 full-length genomes of viruses collected from hospitalized patients with respiratory tract infection from 2005 through 2021 indicated that viruses within our sample set clustered in six genetic lineages: A1, A2.1, A2.2.1, A2.2.2, B1, and B2. Additionally, this data indicates that since 2003, a split in the A2 lineage into lineages A2.1 and A2.2 was observed, and since 2008

lineages A2.2 split into lineages A2.2.1 and A2.2.2. All viruses in lineage A2.2.2 were relatively recent viruses, with the first collected in 2008, and since 2015 this lineage is primarily defined by viruses with a duplication in the G gene. A gradual evolution over time was only clear for lineage A2.2.2 and not so much for the other lineages.

In this study, HMPV evolution based on full genome sequences was studied using viruses circulating in the Netherlands between 2005 and 2021. However, analysis of the F gene sequences of these Dutch isolates together with those circulating worldwide (figures A1-3 and fig 2), demonstrated that the Dutch strain cluster among those collected worldwide, indicating that the circulation of different genotypes is not specific for the Netherlands.

Viruses clustering in the A2.2.2 lineage with a 111-nucleotide or 180-nucleotide duplication in the G gene have been reported to circulate worldwide since 2014 and 2017, respectively, and the prevalence of viruses carrying a duplication in the G gene has increased over the years (Saikusa, Kawakami, et al., 2017; Saikusa, Nao, et al., 2017; Piñana et al., 2017; Saikusa, Kawakami, et al., 2017; Saikusa, Nao, et al., 2017; Pinana et al., 2020; Saikusa et al., 2019). In our study, although the number of viruses were limited, all A2.2.2 viruses circulating between 2018-2021 carried a 111-nucleotide or 180-nucleotide duplication in the G gene.

In line with other studies, no viruses belonging to lineage A1 were detected after 2006. As most RT-qPCR assays used for HMPV diagnostics target the N gene, one explanation for this could be that viruses from this lineage are still circulating but became undetectable due to mutations in the region used in diagnostic assays. More likely, this virus lineage is now extinct or circulating in an area without surveillance.

The samples for the study in hospitalized patients were selected on basis of Ct values <=25 and a maximum of 10 samples per year, therefore no conclusions can be drawn on the yearly incidence of viruses from the different lineages. However, our study does show that viruses from the different lineages circulate in the same year. Among viruses obtained from hospitalized patients in the Netherlands, a higher number of lineage A than lineage B viruses was detected for most years. This in contrast to the study among patients with RTI visiting general practitioners, where lineage A and B viruses were equally often detected. This could be explained by the selection bias of samples from hospitalized patients, with a Ct value <=25.0, as in samples with a Ct >25.0 a higher number of lineage B than lineage A viruses was detected. Additionally, among all samples obtained in this study (from both hospitalized individuals and people visiting general practitioners combined), there was a significantly lower numbers of B lineage viruses among samples with a Ct value <25.0 (101/164 (61.6%) lineage A, 63/164 (38.4%) lineage B, (p=0.0347)). This indicates that, in general, in samples with a Ct value <=25.0, lineage A viruses are more often

detected than lineage B viruses. Whether this difference in Ct values between lineage A and B viruses corresponds to differences in clinical impact remains to be investigated. Of note, since 2019, diagnostics for detection of HMPV for hospitalized patients has switched from in-house primers and probe to the Panther Fusion System (Hologic), of which the primer and probe sequences are unknown. Primers and probes used to detect HMPV in samples from patients consulting general practitioners were similar to those used to detect HMPV in samples from hospitalized individuals before the introduction of the Panther Fusion System. These differences in assays used for virus diagnostics might result in different sensitivities to detect A or B lineage viruses after 2019.

One of the challenges of comparing HMPV molecular evolution studies is the use of different classification criteria for designating lineages. For other viruses, criteria have been used according to a more unified system, such as for SARS-CoV-2 and influenza virus. For SARS-CoV2, the Pangolin nomenclature system provides detailed cluster information (29), similar to the GISAID nomenclature system (https://www.gisaid.org/resources/statements-clarifications/clade-and-lineage-nomenclature-aids-in-genomic-epidemiology-of-active-hcov-19-viruses/), while the Nextstrain nomenclature system offers a more large-scale view of clade trends (https://nextstrain.org/blog/2020-06-02-SARSCoV2-clade-naming). The influenza A(H5) nomenclature system designates new lineages based on monophyletic clusters with bootstrap support values >70% with defined average pairwise *p*-distances within and between clades (30). Since 2016, a nomenclature system was proposed for swine influenza A viruses that is in concordance with the nomenclature system for Influenza A(H5) viruses (31). While a robust nomenclature system for these viruses is in place, attempts to unify a nomenclature system for RSV have recently started (32). Here, we propose a simple, yet robust HMPV classification system based on genetic clustering of F gene sequences. The number of nucleotide substitutions of a newly sequenced virus compared to the ranges of nucleotide substitutions within and between the known virus lineages can be used to determine to which lineage a virus belongs. A newly sequenced virus belonging to lineage A2.2.2 should fall within the range of nucleotide substitutions compared to A2.2.1, A2.1, A1, B1, and B2 as described in this study. Alternatively, a virus of which the number of nucleotide substitutions exceeds the ranges of nucleotide substitutions between each of these lineages could be considered part of a new lineage. In addition to this proposed numerical system, to achieve a uniform system for naming new HMPV isolates we suggest using the guidelines of the ICTV for other viruses, including country codes according to the ISO 3166-1 alpha-2 standards, i.e. HMPV/Country/IsolateNumber/Year/Lineage (e.g. HMPV/NL/17/06/A).

The proposed classification system described above supports the split between the A2.2.1 and A2.2.2 lineages. Although a split within lineage B2

seems to be developing, the data thus far does not support this split yet. These findings are in accordance with a study reporting division of the A2.2 lineage into A2.2.1 and A2.2.2 (13), which were referred to as A2b1 and A2b2. However, for HMPV nomenclature, the A and B lineages were initially named as such to define two lineages that were antigenically distinct. The A and B lineages both split into two phylogenetic lineages, which were not antigenically different, named A1, A2, B1, and B2. To prevent confusion about antigenic differences in HMPV nomenclature, we propose to use the nomenclature that follows the guidelines of the ICTV for other viruses, e.g. A2.1 instead of A2a and A2.2 instead of A2b (30, 33). There have been reports about the presence of a A2.3 lineage (named A2c in other reports (14), however viruses from this proposed lineage cluster within the A2.2.2 lineage in other studies as well as in ours.

Monitoring HMPV evolution is generally done by analyzing sequences of (partial) F or G genes (10, 11, 13, 16, 17, 20, 21, 34). More recently, analyzing whole genome sequences is being explored as it adds important information as compared to partial genome sequences and the cost-efficiencies of obtaining full genomes by next-generation sequencing have increased considerably (22). Here, we show that phylogenetic clustering based on whole genome sequences is similar to that of full-length F or partial F gene sequences, although trees reconstructed from partial F gene sequences are slightly more variable.

In conclusion, this study reports on the emergence and potential extinction of genetic HMPV lineages throughout recent decades in the Netherlands. This study suggests that using whole genome sequences of HMPV captures similar phylogenetic information as the use of full-length F gene sequences. However, new evolutionary events, such as the reported duplication in the G gene, will be missed when only the full-length F gene is analyzed. Finally, phylogenetic analyses were used to propose robust classification criteria for future HMPV lineage designation and virus nomenclature.

Methods

Sample selections from hospitalized patients

HMPV-positive samples obtained from patients hospitalized for RTI between 2005 and 2021 with a qRT-PCR Ct value of ≤25.0 were selected. For samples obtained before the year 2019, qRT-PCR was performed as described previously (35). For samples obtained after 2019, qRT-PCR was performed using a Panther Fusion system (Hologic), of which the primers and probe sequences are unknown. To obtain an even distribution throughout the years, ten samples were selected from each year. For seasons with more than ten samples with a Ct value of ≤25.0, the samples with the lowest Ct values were selected. For seasons with less than ten samples with a Ct value of ≤25.0, additional samples were selected with a Ct value between 25.0 and 29.0. For some years, either a

total number of 10 samples could not be obtained or 10 full genome sequences could not be obtained. Nine additional samples obtained between 1993 and 2004 were selected based on available materials. Already available full-length genome sequences of prototype viruses for each lineage (e.g. NL/1/00 for lineage A1, CAN83-97 for lineage A2.1) were also included for references. Patient data was anonymized prior to receiving the samples and as a consequence, additional medical ethics review was not needed as consented by the Erasmus MC Medical Ethical Board (MEC-2015-306).

Selection of samples obtained from patients with RTI consulting general practitioners

The General Practitioner (GP) sentinel surveillance by the Nivel Netherlands Institute for Health Services Research Primary Care Database and the RIVM reference laboratory (about 40 GP practices spread throughout the Netherlands representing about 0.7% of the Dutch population) collected nasopharyngeal and oropharyngeal swabs combined in one tube virus transport medium from patients consulting the GP for an RTI (including influenza-like illness). Based on weekly virological records of about 20 clinical diagnostic laboratories in the Netherlands under the auspices of the Dutch Working Group for Clinical Virology (https://www.rivm.nl/virologische-weekstaten) the HMPV epidemic period for each season 2005-2020 was determined. From these periods a mean 95 samples (range 84-100) per epidemic period evenly spread over the epidemic period were selected from the GP sentinel surveillance biobank that were negative by RT-qPCR for influenza virus, RSV, rhinovirus and enterovirus. These samples were subjected to RT-qPCR for HMPV as described previously (10), following nucleic acid isolation by MagNA Pure 96 (Roche) extraction of 200 **µ**l specimen using DNA and Viral NA Small Volume Kit (Roche). A mean 10 (range 4-19) samples per epidemic period were found positive for HMPV. In 2020/2021 there was no hMPV season due to COVID-19 measures. From January 2021 onwards all collected samples in the GP sentinel surveillance were prospectively tested for HMPV by RT-qPCR. A total of 15 HMPV positive samples were detected up to October 2021 that were included in the study. Due to lower viral loads in the GP sentinel surveillance patients than in hospitalized patients, all RT-qPCR HMPV positive specimens irrespective of Ct value (median Ct value 29; range 19-39) were subjected to partial F-gene and G-gene PCR and Sanger sequencing. For these samples, a nested PCR was performed to increase efficiency for lower viral load specimens (F PCR: forward primer 5'- TGTTGTGCGGCARTTTTCAGAC-3', reverse primers 5'GCACTGCTTAGGATTCTGTTTGA-3' and 5'TGCACTGTTYAGRATTTTGTTTGAC-3'. Nested F PCR: forward primers 5'TGGAATAACACCAGCAATATCCTT-3' and 5'-AATGCAGGGATAACACCAGCAAT-3', reverse primer 5'CTGTTCRCCYTCAACTTTGCT-3'. G PCR: forward primer 5'TACAAAACAAGAACATGGGACAAG3',

reverse primers 5'GTTTCACTGAAAGATATTACTCCTTT3' and 5'-GTCTCACTAAAAGAAATCACTCCTTT-3'. Nested G PCR: forward primers 5'ATGGAGGTGAAAGTGGAGAACATTC3' and 5'ATGGAAGTAAGAGTGGAGAACATTC3', reverse primer 5'GAGATAGACATTAACAGTGGATTC3'). The primers used for Sanger sequencing of PCR products were the same as those used for the nested PCR.

Virus nomenclature

Nomenclature of viruses followed the guidelines of the ICTV for other viruses, e.g. HMPV/Country/IsolateNumber/Year/lineage (i.e. HMPV/NL/17/06/A) (33).

MinION sequencing and PCR of the G gene and partial HMPV F gene

HMPV-positive samples were used for RNA isolation and MinION sequencing as described previously (27). PCR of HMPV F gene was performed as described previously (27). The presence or absence of 111-nucleotide and 180-nucleotide duplications was confirmed by Sanger sequencing as described previously (27). Gaps in consensus sequences were resolved by PCR amplification of the missing amplicon followed by Sanger sequencing as described previously (27). Sequencing of partial F genes (nucleotide position 778-1226 of the F ORF) for genotyping of samples obtained from hospitalized individuals with a Ct value >25.0 was performed as described previously (10). All full-length F gene sequences available from GenBank were downloaded as a FASTA alignment file.

Phylogenetic analysis

Nucleotide sequence alignments were generated using MAFFT (https://mafft.cbrc.jp/alignment/server/). Maximum likelihood phylogenetic analyses were conducted using the MEGA-X software with the best fit DNA model as determined by the MEGA-X software with 1000 bootstraps. The best fit model for each phylogenetic tree is described in the figure legends. Pairwise distances were generated by MEGA-X software.

Clustering of HMPV in genetic maps

To visualize the clustering of HMPV sequences based on the number of nucleotide substitutions between them, genetic maps representing HMPV nucleotide sequences were generated essentially as described (36, 37). Nucleotide sequence alignments were generated for various HMPV open reading frames using MAFFT and a genetic distance matrix was generated with all pairwise numbers of nucleotide substitutions. A multidimensional scaling algorithm was employed to generate two-dimensional representations of the matrices with Euclidian distances (36).

Data availability

All full genome sequences from viruses isolated from hospitalized individuals generated in this study were submitted to GenBank with accession numbers OL794355-OL794483. Partial F and G gene sequences form viruses isolated from patients visiting general practitioners were submitted to GenBank with accession numbers ON461481-ON461747.

Acknowledgement

The authors would like to thank Euníce Then for helping with qRT-PCRs on clinical specimens and sequencing of viruses obtained from specimens from patients visiting general practitioners, Gé Donker, Mariëtte Hooiveld and Janneke Hendriksen from Nivel and the Nivel Primary Care Database GP's for collecting specimens from patients consulting the GP's with RTI, and the Erasmus MC virology diagnostics department for performing qRT-PCRs on clinical specimens from hospitalized patients. The authors thank the Dutch Working Group for Clinical Virology for the opportunity to use the virology weekly records database to determine HMPV epidemic periods in The Netherlands.

Funding

This work was supported in part by Horizon 2020 research and innovation program grant No. 874735 (VEO) from the European Union. The Dutch Ministry of Health, Welfare and Sport funded the GP sentinel surveillance.

References

1. Van Den Hoogen BG, De Jong JC, Groen J, Kuiken T, De Groot R, Fouchier RAM, Osterhaus ADME. 2001. A newly discovered human pneumovirus isolated from young children with respiratory tract disease. Nat Med 7:719–724.
2. Williams JV, Wang CK, Yang C, Tollefson SJ, House FS, Heck JM, Chu M, Brown JB, Lintao LD, Quinto JD, Chu D, Spaete RR, Edwards KM, Wright PF, Crowe, Jr. JE. 2006. The Role of Human Metapneumovirus in Upper Respiratory Tract Infections in Children: A 20-Year Experience. J Infect Dis 193:387–395.
3. Jain S, Self WH, Wunderink RG, Fakhran S, Balk R, Bramley AM, Reed C, Grijalva CG, Anderson EJ, Courtney DM, Chappell JD, Qi C, Hart EM, Carroll F, Trabue C, Donnelly HK, Williams DJ, Zhu Y, Arnold SR, Ampofo K, Waterer GW, Levine M, Lindstrom S, Winchell JM, Katz JM, Erdman D, Schneider E, Hicks LA, McCullers JA, Pavia AT, Edwards KM, Finelli L. 2015. Community-Acquired Pneumonia Requiring Hospitalization among U.S. Adults. N Engl J Med 373:415–427.
4. O'Brien KL, Baggett HC, Brooks WA, Feikin DR, Hammitt LL, Higdon MM, Howie SRC, Deloria Knoll M, Kotloff KL, Levine OS, Madhi SA, Murdoch DR, Prosperi C, Scott JAG, Shi Q, Thea DM, Wu Z, Zeger SL, Adrian P V., Akarasewi P, Anderson TP, Antonio M, Awori JO, Baillie VL, Bunthi C, Chipeta J, Chisti MJ, Crawley J, DeLuca AN, Driscoll AJ, Ebruke BE, Endtz HP, Fancourt N, Fu W, Goswami D, Groome MJ, Haddix M, Hossain L, Jahan Y, Kagucia EW, Kamau A, Karron RA, Kazungu S, Kourouma N, Kuwanda L, Kwenda G, Li M, Machuka EM, Mackenzie G, Mahomed N, Maloney SA, McLellan JL, Mitchell JL, Moore DP, Morpeth SC, Mudau A, Mwananyanda L, Mwansa J, Silaba Ominde M, Onwuchekwa U, Park DE, Rhodes J, Sawatwong P, Seidenberg P, Shamsul A, Simões EAF, Sissoko S, Wa Somwe S, Sow SO, Sylla M, Tamboura B, Tapia MD, Thamthitiwat S, Toure A, Watson NL, Zaman K, Zaman SMA. 2019. Causes of severe pneumonia requiring hospital admission in children without HIV infection from Africa and Asia: the PERCH multi-country case-control study. Lancet 394:757–779.
5. O'Bryant SC, Momin Z, Camp E, Jones J, Meskill S. 2022. Longitudinal evaluation of pediatric respiratory infections. J Clin Virol 148:105084.
6. Loubet P, Mathieu P, Lenzi N, Galtier F, Lainé F, Lesieur Z, Vanhems P, Duval X, Postil D, Amour S, Rogez S, Lagathu G, L'Honneur AS, Foulongne V, Houhou N, Lina B, Carrat F, Launay O. 2021. Characteristics of human metapneumovirus infection in adults hospitalized for community-acquired influenza-like illness in France, 2012–2018: a retrospective observational study. Clin Microbiol Infect 27:127.e1-127.e6.
7. Barrera-Badillo G, Olivares-Flores B, Ruiz-López A, Fierro-Valdez MÁ, Gutiérrez-Vargas RI, López-Martínez I. 2020. Human metapneumovirus: Etiological agent of severe acute respiratory infections in hospitalized and deceased patients with a negative diagnosis of influenza. Pathogens 9.

8. Wang X, Li Y, Deloria-Knoll M, Madhi SA, Cohen C, Ali A, Basnet S, Bassat Q, Brooks WA, Chittaganpitch M, Echavarria M, Fasce RA, Goswami D, Hirve S, Homaira N, Howie SRC, Kotloff KL, Khuri-Bulos N, Krishnan A, Lucero MG, Lupisan S, Mira-Iglesias A, Moore DP, Moraleda C, Nunes M, Oshitani H, Owor BE, Polack FP, O'Brien KL, Rasmussen ZA, Rath BA, Salimi V, Scott JAG, Simões EAF, Strand TA, Thea DM, Treurnicht FK, Vaccari LC, Yoshida LM, Zar HJ, Campbell H, Nair H, Libster R, Otieno G, Joundi I, Broor S, Nicol M, Amarchand R, Shi T, López-Labrador FX, Baker JM, Jamison A, Choudekar A, Juvekar S, Obermeier P, Schweiger B, Madrid L, Thomas E, Lanaspa M, Nohynek H, Nokes J, Werner M, Danhg A, Chadha M, Puig-Barberà J, Caballero MT, Mathisen M, Walaza S, Hellferscee O, Laubscher M, Higdon MM, Haddix M, Sawatwong P, Baggett HC, Seidenberg P, Mwanayanda L, Antonio M, Ebruke BE, Adams T, Rahman M, Rahman MZ, Sow SO, Baillie VL, Workman L, Toizumi M, Tapia MD, Nguyen T hien anh, Morpeth S. 2021. Global burden of acute lower respiratory infection associated with human metapneumovirus in children under 5 years in 2018: a systematic review and modelling study. Lancet Glob Heal 9:e33–e43.
9. Shafagati N, Williams J. 2018. Human metapneumovirus - what we know now. F1000Research 7:135.
10. Van Den Hoogen BG, Herfst S, Sprong L, Cane PA, Forleo-Neto E, De Swart RL, Osterhaus ADME, Fouchier RAM. 2004. Antigenic and Genetic Variability of Human Metapneumoviruses. Emerg Infect Dis 10:658–666.
11. Williams J V., Harris PA, Tollefson SJ, Halburnt-Rush LL, Pingsterhaus JM, Edwards KM, Wright PF, Crowe JE. 2004. Human Metapneumovirus and Lower Respiratory Tract Disease in Otherwise Healthy Infants and Children. N Engl J Med 350:687–696.
12. Huck B, Scharf G, Neumann-Haefelin D, Puppe W, Weigl J, Falcone V. 2006. Novel human metapneumovirus sublineage. Emerg Infect Dis 12:147–150.
13. Nao N, Saikusa M, Sato K, Sekizuka T, Usuku S, Tanaka N, Nishimura H, Takeda M. 2020. Recent molecular evolution of human metapneumovirus (HMPV): Subdivision of HMPV a2b strains. Microorganisms 8:1–14.
14. Nidaira M, Taira K, Hamabata H, Kawaki T, Gushi K, Mahoe Y, Maeshiro N, Azama Y, Okano S, Kyan H, Kudaka J, Hiroyuki T, Noda M, Kimura H. 2013. Molecular Epidemiology of Human Metapneumovirus from 2009 to 2011 in Okinawa, Japan. Jpn J Infect Dis 66:56–59.
15. Carr MJ, Waters A, Fenwick F, Toms GL, Hall WW, O'Kelly E. 2008. Molecular Epidemiology of Human Metapneumovirus in Ireland Michael. J Med Virol 80:510–516.
16. Saikusa M, Nao N, Kawakami C, Usuku S, Sasao T, Toyozawa T, Takeda M, Okubo I. 2017. A novel 111-nucleotide duplication in the G gene of human metapneumovirus. Microbiol Immunol 61:507–512.
17. Saikusa M, Kawakami C, Nao N, Takeda M, Usuku S, Sasao T, Nishimoto K, Toyozawa T. 2017. 180-nucleotide duplication in the G Gene of Human metapneumovirus A2b subgroup strains circulating in Yokohama City, Japan, since 2014. Front Microbiol 8:1–11.
18. Piñana M, Vila J, Gimferrer L, Valls M, Andrés C, Codina MG, Ramón J, Martín MC, Fuentes F, Saiz R, Rodrigo PAC, Pumarola T, Antón A. 2017. Novel human metapneumovirus with a 180-nucleotide duplication in the G gene. Future Microbiol 12:565–571.
19. Boivin G, Mackay I, Sloots TP, Madhi S, Freymuth F, Wolf D, Shemer-Avni Y, Ludewick H, Gray GC, LeBlanc É. 2004. Global genetic diversity of human metapneumovirus fusion gene. Emerg Infect Dis 10:1154–1157.

20. Saikusa M, Nao N, Kawakami C, Usuku S, Tanaka N, Tahara M, Takeda M, Okubo I. 2019. Predominant detection of the subgroup a2b human metapneumovirus strain with a 111-nucleotide duplication in the g gene in Yokohama city, Japan in 2018. Jpn J Infect Dis 72:350–352.
21. Arshad Y, Rana MS, Ikram A, Salman M, Aamir UB, Zaidi SSZ, Alam MM, Sharif S, Shaukat S, Khurshid A, Hakim R, Mujtaba G, Umair M, Sattar S, Bostan N. 2022. Molecular detection and genetic characterization of human metapneumovirus strains circulating in Islamabad, Pakistan. Sci Rep 12:1–7.
22. Dudas G, Bedford T. 2019. The ability of single genes vs full genomes to resolve time and space in outbreak analysis. BMC Evol Biol 19:1–27.
23. Pollett S, Trovão NS, Tan Y, Eden JS, Halpin RA, Bera J, Das SR, Wentworth D, Ocaña V, Mendocilla SM, Álvarez C, Calisto ME, Garcia J, Halsey E, Ampuero JS, Nelson MI, Leguia M. 2018. The transmission dynamics and diversity of human metapneumovirus in Peru. Influenza Other Respi Viruses 12:508–513.
24. Xu Y, Lewandowski K, Jeffery K, Downs LO, Foster D, Sanderson ND, Kavanagh J, Vaughan A, Salvagno C, Vipond R, Carroll M, Danby R, Peto T, Crook D, Walker AS, Matthews PC, Pullan ST. 2020. Nanopore metagenomic sequencing to investigate nosocomial transmission of human metapneumovirus from a unique genetic group among haematology patients in the United Kingdom. J Infect 80:571–577.
25. Xu Y, Lewandowski K, Lumley S, Sanderson N, Ali V, Vipond R, Carroll M, Jeffery K, Foster D, Walker AS, Peto T, Crook D, Pullan ST, Matthews PC. 2018. Nanopore metagenomic sequencing of full length human metapneumovirus (HMPV) within a unique sub-lineage. bioRxiv.
26. Kamau E, Oketch JW, De Laurent ZR, Phan MVT, Agoti CN, Nokes DJ, Cotten M. 2020. Whole genome sequencing and phylogenetic analysis of human metapneumovirus strains from Kenya and Zambia. BMC Genomics 21:1–10.
27. Groen K, van Nieuwkoop S, Bestebroer TM, Fraaij PL, Fouchier RAM, van den Hoogen BG. 2021. Whole genome sequencing of human metapneumoviruses from clinical specimens using MinION nanopore technology. Virus Res 302:198490.
28. Pinana M, Vila J, Maldonado C, Galano-Frutos JJ, Valls M, Sancho J, Andres FXNC, Martín-Gomez MT, Esperalba J, Codina MG, Pumarola T, Anton A. 2020. Insights into immune evasion of human metapneumovirus: novel 180- and 111-nucleotide duplications within viral G gene throughout 2014-2017 seasons in Barcelona, Spain. J Clin Virol 132.
29. Rambaut A, Holmes EC, O'Toole Á, Hill V, McCrone JT, Ruis C, du Plessis L, Pybus OG. 2020. A dynamic nomenclature proposal for SARS-CoV-2 lineages to assist genomic epidemiology. Nat Microbiol 5:1403–1407.
30. Smith GJD, Donis RO. 2015. Nomenclature updates resulting from the evolution of avian influenza A(H5) virus clades 2.1.3.2a, 2.2.1, and 2.3.4 during 2013-2014. Influenza Other Respi Viruses 9:271–276.
31. Anderson TK, Macken C, Lewis NS, Scheuermann RH, Reeth K Van, Brown IH, Swenon S, Simon G, Saito T, Berhane Y, Ciacci-Zanella J, Pereda A, Davis CT, Donis RO, Webby RJ, Vincent L. 2016. A Phylogeny-Based Global System and Automated Annotation Tool for H1 Influenza A Viruses. mSphere 1:1–14.
32. Ramaekers K, Rector A, Cuypers L, Lemey P, Keyaerts E, van Ranst M. 2020. Towards a unified classification for human respiratory syncytial virus genotypes. Virus Evol 6:1–11.
33. Lefkowitz EJ, Dempsey DM, Hendrickson RC, Orton RJ, Siddell SG, Smith DB. 2018. Virus taxonomy: The database of the International Committee on Taxonomy of Viruses (ICTV). Nucleic Acids Res 46:D708–D717.

34. Perchetti GA, Wilcox N, Chu HY, Katz J, Khatry SK, LeClerq SC, Tielsch JM, Jerome KR, Englund JA, Kuypers J. 2021. Human Metapneumovirus Infection and Genotyping of Infants in Rural Nepal. J Pediatric Infect Dis Soc 10:408–416.
35. Hoek RAS, Paats MS, Pas SD, Bakker M, Hoogsteden HC, Boucher CAB, Van Der Eerden MM. 2013. Incidence of viral respiratory pathogens causing exacerbations in adult cystic fibrosis patients. Scand J Infect Dis 45:65–69.
36. Smith DJ, Lapedes AS, de Jong JC, Bestebroer TM, Rimmelzwaan GF, Osterhaus ADME, Fouchier RAM. 2004. Mapping the Antigenic and Genetic Evolution of Influenza Virus. Science (80-) 305:371–376.
37. Higgins DG. 1992. Sequence ordinations: a multivariate analysis approach to analysing large sequence data sets. Bioinformatics 8:15–22.


MAUS
MDA-5
PKR
RIG-1
INTERFERON
IFNAR
G
sh

5

Evidence against the human metapneumovirus G, SH, and M2-2 proteins as bonafide interferon antagonists

K. Groen[1], S. van Nieuwkoop[1], M. M. Lamers[1], R.A.M. Fouchier[1], B.G. van den Hoogen*[1]

[1] Department of Viroscience, Erasmus Medical Center, Rotterdam, The Netherlands.

J Virol. 2022 Sep 14;96(17):e0072322.

Abstract

The production of type I interferon (IFN) is the hallmark of the innate immune response. Most, if not all, mammalian viruses have a way to circumvent this response. Fundamental knowledge on viral evasion of innate immune responses may facilitate design of novel antiviral therapies. To investigate how human metapneumovirus (HMPV) interacts with the innate immune response, recombinant viruses lacking G, SH, or M2-2 protein expression were assessed for IFN induction in A549 cells. HMPV lacking G or SH protein expression induced asimilarly low levels of IFN as wild type virus, whereas HMPV lacking M2-2 expression induced significantly more IFN than the wild type virus. However, sequence analysis of the genomes of M2-2 mutant viruses revealed high numbers of mutations throughout the genome. Over 70% of these nucleotide substitutions were A-to-G and T-to-C mutations, consistent with the properties of the adenosine deaminase acting on RNA (ADAR) protein family. Knockdown of ADAR1 by CRISPR-interference confirmed the role of ADAR1 in editing of M2-2 deletion mutant virus genomes. More importantly, Northern blot analyses revealed the presence of defective interfering RNAs (DIs) in M2-2 mutant viruses and not in in wild type or G and SH deletion mutant viruses. DIs are known to be potent inducers of the IFN response. The presence of DIs in M2-2 mutant virus stocks, as well as hyper mutated virus genomes, interfere with studies on HMPV and the innate immune response and should be addressed in future studies.

Importance

Understanding the interaction between viruses and the innate immune response is one of the barriers towards the design of antiviral therapies. Here, we investigated the role of the G, SH, and M2-2 proteins of the human metapneumovirus (HMPV) as type-I interferon-antagonists. In contrast to other studies, no interferon antagonistic functions could be observed for the G and SH proteins. HMPV with a deletion of the M2-2 protein did induce type I interferon production upon infection of airway epithelial cells. However, during generation of virus stocks, these viruses rapidly accumulated defective interfering RNAs, which are strong activators of the type-I interferon response. Additionally, the genomes of these viruses were hypermutated, which was prevented by generating stocks in ADAR knockdown cells, confirming a role for ADAR in hypermutation of HMPV genomes or defective interfering RNAs. These data indicate that a role of the HMPV M2-2 protein as bona fide interferon-antagonist remains elusive.

Introduction

Human metapneumovirus (HMPV), a member of the *Pneumoviridae* family, is a major cause of respiratory tract illness, primarily in young children, immunocompromised individuals, and the elderly (1–3). Clinical symptoms caused by an HMPV infection are similar to those caused by infection with human respiratory syncytial virus (HRSV), ranging from mild respiratory illness to severe pneumonia (1, 4–6).

The innate immune system is pivotal in the host defense against virus infections. Antiviral immunity is initiated by sensing and recognition of pathogen-associated molecular patterns (PAMPs) by pattern-recognition receptors (PRRs). The main cytosolic sensors for RNA viruses include the retinoic acid-inducible gene I (RIG-I)-like receptors (RLRs), such as RIG-I and melanoma differentiation associated factor 5 (MDA5) (7–12). Activation of PRRs triggers expression of a myriad of downstream effectors, such as stimulator of interferon genes (STING), mitochondrial antiviral signaling protein (MAVS), and type-I and type-III interferons (IFN), ultimately resulting in an antiviral state (13, 14). Protein Kinase R (PKR) can amplify this IFN response and has shown to be important for defense against many viruses (reviewed in (15)). In addition, the Toll-like receptor (TLR) protein family contains extracellular viral sensors which signal through Myeloid differentiation primary response 88 (MyD88) and the TNF receptor associated factor (TRAF) protein family to induce IFN production (reviewed in (16)). Most, if not all, mammalian viruses have ways to antagonize this innate immune response and therefore HMPV, being a human pathogen, must possess mechanisms to avoid or suppress IFN production as well.

Since the identification of HMPV in 2001 (17), the interaction between HMPV and the innate immune system has been investigated by several research groups. Studies have suggested that the HMPV attachment glycoprotein (G) inhibits IFN production by physically interacting with RIG-I in A549 cells. Additional studies reported that G interfered with TLR4 mediated signaling in monocyte-derived dendritic cells (moDCs)(18, 19). However, a study using siRNA knockdown of the HMPV G protein reported that G was not an IFN antagonist (20). Another viral glycoprotein, the short hydrophobic (SH) protein, for which the function is not completely understood, was found to block IFN production by inhibiting the TLR7/MyD88/TRAF6 signaling pathway in plasmacytoid dendritic cells (pDCs)(21). Additionally, the SH protein was shown to downregulate IFN signaling by affecting STAT1 expression and phosphorylation in A549 cells (22). However, de Graaf et al., using a genomics approach, did not find an interaction between the SH protein and the IFN pathway (23). The HMPV M2-2 protein, encoded as second open reading frame (ORF) of the M2 gene, is involved in the regulation of viral mRNA and genome synthesis (24–28). A virus lacking M2-2 protein expression, generated by deletion of the part of the M2-2 ORF

that does not overlap with the M2-1 ORF, was found to be attenuated in hamsters. However, deleting this part of the M2-2 ORF resulted in insertions of U nucleotides in poly-U tracts of the genomic RNA and high mutation rates in the part of the genome that was investigated, showing that viruses without M2-2 are genetically unstable (26). Based on this data, another study employed a virus with ablated M2-2 protein expression by the introduction of nucleotide substitutions leading to stop codons in the ORF, thereby keeping the genome length intact. In studies with this virus, it was suggested that M2-2 had a role as IFN antagonist in A549 cells (25). The same research group reported that the PDZ-binding motifs of the M2-2 protein were important for the interaction with MAVS (29). However, in these studies the genetic stability of the M2-2 mutant viruses was not determined. Another study suggesting an IFN antagonistic role for the M2-2 protein, by inhibiting TLR7/9 dependent signaling, also did not assess the genetic stability of the mutant virus (30).

Previously, we have shown that, upon passaging of HMPV with a high multiplicity of infection (m.o.i), defective interfering particles (DIs) rapidly accumulated in these virus stocks, which are potent inducers of IFN production (31). This finding might explain inconsistencies between previously reported studies, in which virus stocks could have contained DIs. Alternatively, discrepancies in previous reported studies might relate to the methods of viral gene deletion, as deleting parts of the genome will alter genome length. Non-segmented, negative-sense RNA virus gene expression is a polar transcriptional gradient (reviewed in (32)). Therefore, deletion of complete genes, including gene-start and gene-end signals, could disrupt the transcriptional gradient leading to altered gene expression.

To examine the role of the G, SH, and M2-2 proteins as IFN antagonist, as well as the effect of genome length and the presence or absence of gene-start and gene-end signals, recombinant viruses were generated that lacked HMPV G, SH, or M2-2 protein expression by 1) deletion of the ORF, 2) deletion of the ORF including gene-start and gene-end signals, or 3) by the introduction of nucleotide substitutions leading to stop codons throughout the ORF. Using viruses that were generated at low MOI and with a maximum of two passages to limit formation of DIs, we re-examined the roles of the HMPV G, SH, and M2-2 proteins as potential IFN antagonists in A549 cells.

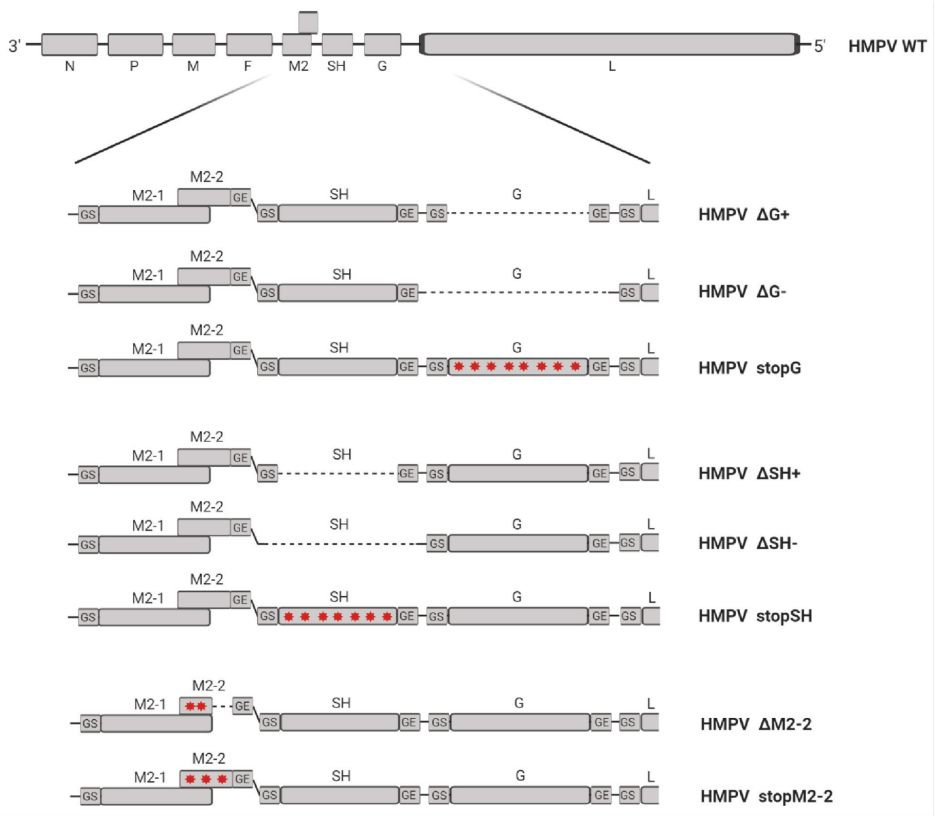

Figure 1. Schematic overview of HMPV NL/1/00 genomes lacking G, SH, or M2-2 protein expression. Protein expression was ablated either by deletion (dashed line) of the open reading frame (e.g. $HMPV_{\Delta G\text{-}ORF}$) or deletion of the ORF, gene-start, and gene-end signals (e.g. $HMPV_{\Delta G}$) or through the introduction of several mutations leading to stop codons in the open reading frame (e.g. $HMPV_{StopG}$) (red stars). The figure was generated using BioRender (https://biorender.com/). Image generated with Biorender.

Results

Phenotypic characterization of HMPV lacking G, SH, or M2-2 protein expression

Recombinant viruses lacking expression of the G, SH, or M2-2 proteins were generated using three different approaches (Figure 1): deletion of only the ORFs ($HMPV_{\Delta SH\text{-}ORF}$; $HMPV_{\Delta G\text{-}ORF}$; $HMPV_{\Delta M2\text{-}2}$), deletion of ORFs including GS and GE signals ($HMPV_{\Delta SH}$; $HMPV_{\Delta G}$), and introduction of mutations leading to stop codons throughout the ORFs ($HMPV_{StopSH}$; $HMPV_{StopG}$; $HMPV_{StopM2\text{-}2}$). These deletions and mutations in the viral genomes were confirmed by Sanger sequencing (data not

shown). Recombinant viruses were phenotypically characterized by assessing the replication kinetics in both IFN deficient (Vero-118) and IFN competent (A549) cells. These replication kinetics demonstrated that all three SH mutant viruses replicated similar as the wild type virus ($HMPV_{WT}$) in both Vero-118 and A549 cells (Figure 2a, 2b). The three G mutant viruses showed attenuated replication in both Vero-118 and A549 cells (Figure 2c, 2d). The replication of M2-2 mutant viruses was attenuated in A549 cells but not in Vero-118 cells (Figure 2e, 2f). Only minimal differences in replication were observed between viruses with a deletion of the ORF, deletion of the ORF including gene-start and gene-end signals or viruses in which expression of the protein was ablated by introduction of mutations throughout the ORF.

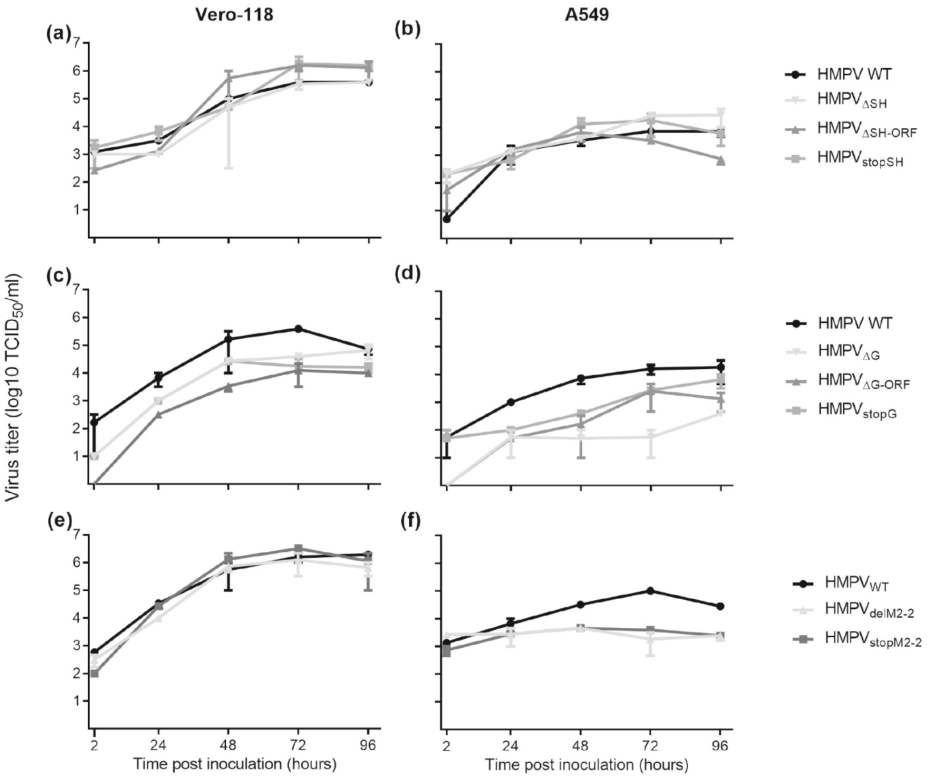

Figure 2. Replication kinetics of HMPV lacking (a, b) SH, (c, d) G, or (e, f) M2-2 protein expression in Vero-118 and A549 cells. Samples were collected at indicated time points. Data shown is representative of three individual experiments. Error bars indicate standard deviations (n=2).

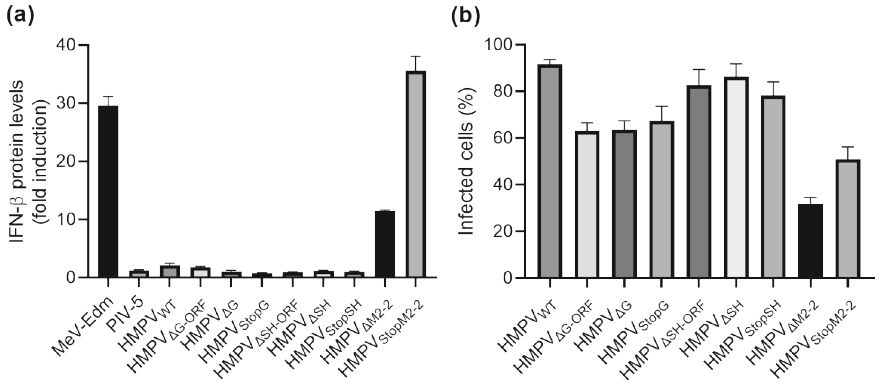

Figure 3. Fold increase in IFN production of A549 cells inoculated with HMPV mutants. (a) IFN-*β* expression levels were indirectly quantified by a luciferase-based bioassay and plotted as fold induction compared to mock inoculated cells and (b) infection percentages were determined by FACS analysis. Data shown is representative of three individual experiments. Error bars indicate standard deviations (n=3).

Induction of IFN-β production upon inoculation with HMPV mutants

Upon inoculation of A549 cells, the G and SH mutant viruses induced similarly low levels of IFN-β as the HMPV$_{WT}$ and negative control Parainfluenza virus type 5 (PIV-5)(Figure 3a), while infection efficiencies of SH and G mutant viruses were above 60% (Figure 3b). Inoculation of A549 cells with HMPV$_{\Delta M2\text{-}2}$ and HMPV$_{StopM2\text{-}2}$ induced significantly more IFN-β production than inoculation with HMPV$_{WT}$ or PIV-5 ($p=<0.0001$ for both viruses). However, inoculation of A549 cells with HMPV$_{StopM2\text{-}2}$ induced more IFN-β production than inoculation with HMPV$_{\Delta M2\text{-}2}$ (Figure 3a), while this was not observed for G or SH mutant viruses with an altered genome length. The differences between the M2-2 mutant viruses probably relates to difference in infection efficiency, being substantially lower for HMPV$_{\Delta M2\text{-}2}$ than that of HMPV$_{StopM2\text{-}2}$ (Figure 3b). Consistent with the attenuated replication in A549 cells, these data suggest that the M2-2 protein could play a role as IFN antagonist.

The role of RIG-I, PKR, and MAVS in sensing of HMPV mutants during infection of A549 cells

To investigate which part of the IFN pathway was involved during HMPV infection, A549 cells with a knockout of the RIG-I, PKR or MAVS genes were generated using CRISPR/Cas9 technology (Figure A1). Inoculation of these knockout (or wild type) cells with viruses lacking SH, G or M2-2 protein expression resulted in infection

efficiencies above 85% for the $HMPV_{WT}$ and SH mutant viruses, above 60% for the G mutant viruses, and 25-50% for the M2-2 mutant viruses. Inoculation of A549ΔPKR cells with the M2-2 mutant viruses resulted in similar IFN-β expression levels as inoculation of A549 WT cells, indicating that PKR did not play a role in the interaction between M2-2 mutant viruses and the IFN pathway (Figure 4a).

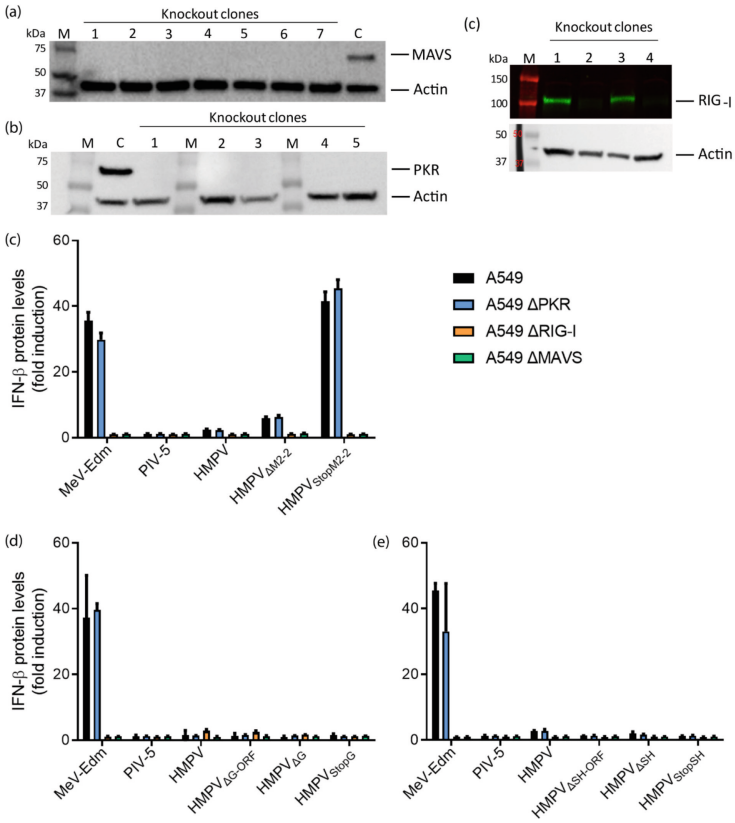

Figure 4. IFN induction in A549WT, A549ΔRIG-I, A549ΔPKR, and A549ΔMAVS upon inoculation with HMPV mutants. Western blot analysis of clonal A549 cells with a knockout of (a) MAVS, (b) PKR, (c) RIG-I M: marker, C: control (A549 WT cells). All analyzed clones for MAVS or PKR contained a knockout and two out of four clones for RIG-I had a knockout. IFN-*β* levels produced by cells inoculated with HMPV lacking (c) M2-2 (d) G or (e) SH protein expression in (knockout) A549 cells. Each virus was used to inoculate three replicates which were used to quantify IFN-*β* production in the supernatant and three replicates to determine the percentage of infected cells by FACS analysis. IFN-*β* production was quantified by a luciferase-based bioassay at 18 h.p.i. in (knockout) A549 cells inoculated with HMPV mutants at an m.o.i. of 3. Data shown is representative of three individual experiments. Error bars indicate standard deviations (n=3). Asterix indicate significance (**** =P>0.0001) as calculated by an unpaired t-test.

However, inoculation of A549ΔRIG-I and A549ΔMAVS cells with the M2-2 mutant viruses resulted in significantly lower IFN production compared to inoculation of A549 WT cells with these viruses ($HMPV_{\Delta M22}$: p=<0.0001 for both A549ΔRIG-I and A549ΔMAVS, $HMPV_{StopM2-2}$: p=<0.0001 for both A549ΔRIG-I and A549ΔMAVS). No differences in IFN-β expression levels were observed between cells inoculated with the $HMPV_{WT}$ and the G or SH mutant viruses (Figure 4b, 4c). This indicated that the RIG-I – MAVS signaling pathway is involved in activation of the IFN pathway by HMPV lacking M2-2 protein expression, which is in line with previous reported findings (25, 29).

Next-generation sequencing analysis reveals hyper mutation of $HMPV_{\Delta M2-2}$ and $HMPV_{StopM2-2}$ genomes

To assess whether the G, SH, and M2-2 mutant viruses were genetically stable, mutation frequencies in the viral genomes of passage 2 viruses were analyzed. To this end, RNA was directly isolated from virus stocks and used for illumina sequencing. In the $HMPV_{WT}$ genome, 32 minor variants were observed (Figure 5a). Between 30 and 60 minor variants were observed in the genomes of the G and SH mutant viruses, which is in the same range as detected in the $HMPV_{WT}$ genome (Figure 5b-5g). The viral genomes of the M2-2 mutants displayed significantly more minor variants than the genome of $HMPV_{WT}$, with 205 minor variants for $HMPV_{\Delta M2-2}$ (Chi^2: p=<0.0001, Figure 5h) and 135 for $HMPV_{StopM2-2}$ (Chi^2: p=<0.0001, Figure 5i). None of the G, SH, or M2-2 mutant virus genomes contained an increased number of insertions of deletions in the genome as compared to $HMPV_{WT}$. The $HMPV_{StopM2-2}$ and $HMPV_{\Delta M2-2}$ genomes contained hotspots of mutations between nucleotide 4000-7000 of the genome, and the $HMPV_{\Delta M2-2}$ genome also contained a mutation hotspot at the 5' end of the genome. Mutations in these hotspots were present in 10-15% of the reads. Notably, 71.5% of the 135 mutations of $HMPV_{StopM2-2}$ and 72.6% of the 205 mutations of $HMPV_{\Delta M2-2}$ were either A-to-G or T-to-C substitutions. This mutation pattern was similar to a previous report for viruses that were passaged 5 times at m.o.i. 3 (P5H) (31). This mutation pattern is consistent with the properties of the adenosine deaminase acting on RNA (ADAR) protein family (41, 42). The ADAR protein family consists of two catalytically active proteins, ADAR1 and ADAR2 (42). ADAR2 is primarily expressed in neurons, therefore ADAR1 is most likely responsible for the A-to-G and T-to-C mutation patterns observed in M2-2 mutant virus genomes. ADAR1 consists of isoforms ADAR1-p110, which is expressed in the nucleus, and ADAR1-p150 which is expressed in both the cytoplasm and the nucleus and is IFN-inducible (42). Since HMPV replication is restricted to the cytoplasm, we hypothesized that ADAR1-p150 was responsible for editing of M2-2 mutant virus genomes.

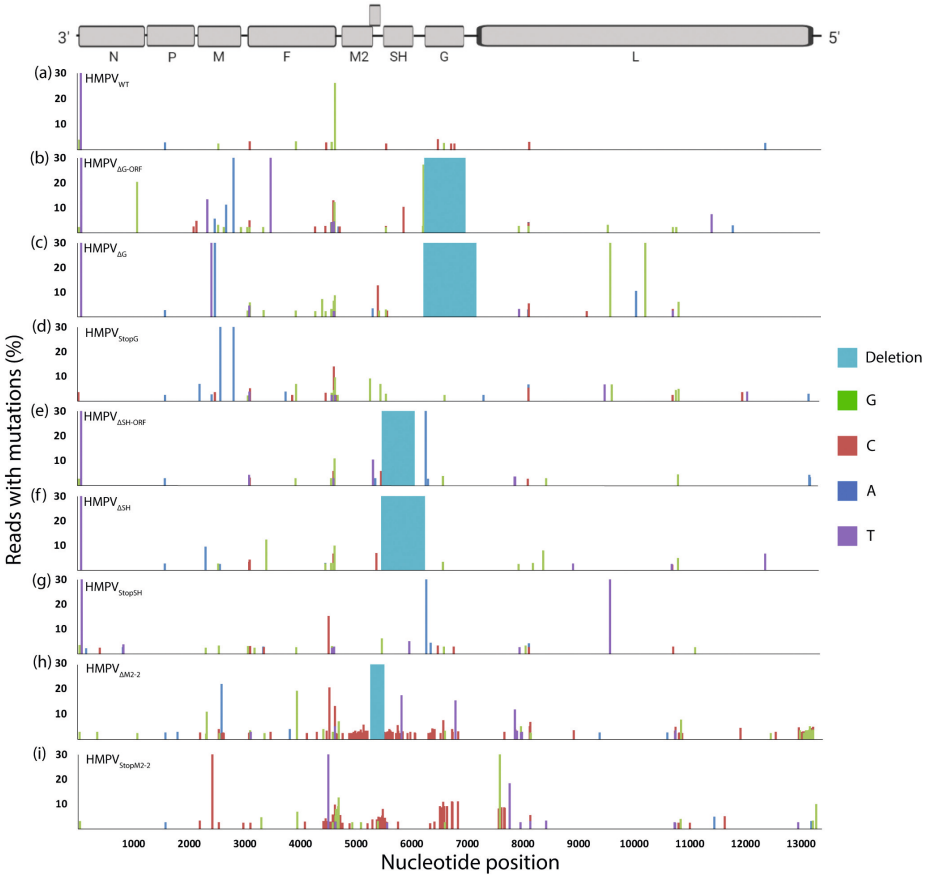

Figure 5. Mutations in HMPV$_{WT}$ and mutant genomes detected by Illumina next generation sequencing. The percentages of reads with specific mutations are shown. A schematic presentation of the genome drawn to scale is shown at the top. A variant analysis with a minimum coverage of 100 reads per nucleotide and a 2% cut off value was performed using the CLC genomic workbench software. Image generated with Biorender.

ADAR1 is responsible for mutations in M2-2 mutant virus genomes

To investigate the role of ADAR1 in editing of M2-2 mutant viral genomes, we used CRISPR-interference to knockdown ADAR1 expression (43). Two different guide RNAs (gRNAs), controlled by a doxycycline-inducible promoter, were used to knockdown ADAR1 in Vero-118 cells. As compared to the non-induced counterparts (from here on referred to as control cells), cell line 1 had a 60% knockdown of ADAR1-p150 and a 54% knockdown of ADAR1-p110, while cell line two had a 85% knockdown of ADAR1-p150 and a 67% knockdown of ADAR1-p110 (Figure 6a). After validation of ADAR1 knockdown, these cell lines were used to

generate new $HMPV_{WT}$ and $HMPV_{StopM2-2}$ stocks. In order to magnify the effect of an ADAR1 knockdown, passage three virus stocks were generated and genomes were sequenced to assess the number of A-to-G and T-to-C substitutions throughout the genomes (Figure 6b-e).

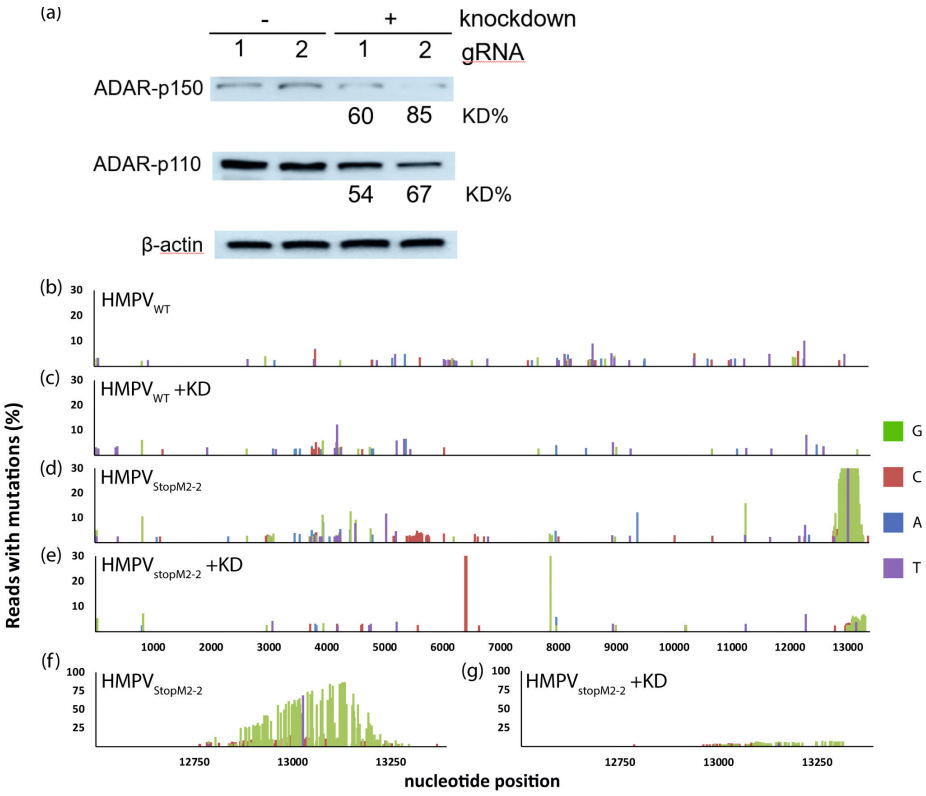

Figure 6. ADAR1 editing of M2-2 mutant virus genomes. (a) Percentages of ADAR1 knockdown (KD%) by CRISPR-interference in Vero-118 cells quantified by western blot. Two different gRNAs were used for knockdown of ADAR1 (gRNA1, gRNA2). Different exposure times were used to visualize the ADAR-p110 and ADAR-p150 bands. (b-e) Mutation maps of viral genomes generated in Vero-118 cells expressing gRNA 2 are shown. (f-g) Zoom in of nucleotide positions 12.500-13.378 from the $HMPV_{StopM2-2}$ virus genomes, to highlight mutation hotspots. Control cells used in these experiments (b, d, f) were transduced cells that were not treated with doxycycline. A variant analysis with a minimum coverage of 100 reads per nucleotide and a 2% cut off value was performed using the CLC genomic workbench software.

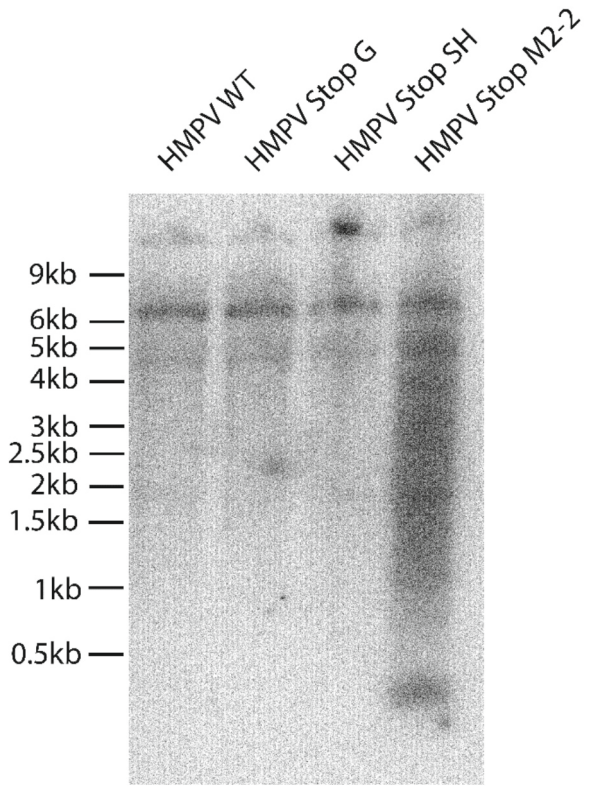

Figure 7. Northern blot analysis of RNA isolated from virus stocks of HMPV mutants. An RNA equivalent of 10^7 $TCID_{50}$ was loaded as input in each gel lane. The probe was complementary to a 180-nucleotide stretch of the trailer region.

$HMPV_{WT}$ generated in control cells displayed 97 minor variants (Figure 6b) as compared to 78 minor variants in the viruses generated in cells with ADAR1 knockdown (Figure 6c). $HMPV_{StopM2\text{-}2}$ generated in control cells displayed 291 minor variants, of which 222 (76,3%) were A-to-G or T-to-C (Figure 6d). In contrast, $HMPV_{StopM2\text{-}2}$ generated in cells with ADAR1 knockdown displayed a significantly lower rate with 89 minor variants (Figure 6e, Chi^2: p=<0.0001), which is similar to observed in the genomes of $HMPV_{WT}$ generated in control cells. In addition, the genomes of $HMPV_{StopM2\text{-}2}$ generated in control cells contained a hotspot of mutations at the 5′ end of the genome, in which up to 80% of the reads contained A-to-G and T-to-C mutations (Figure 6f). The mutation rate at this hotspot was drastically lower in the genome of $HMPV_{StopM2\text{-}2}$ generated in cells with ADAR1 knockdown (Figure 6g), with A-to-G and T-to-C mutations present in only 10% of the reads. This data confirms the role of ADAR1 in editing of $HMPV_{StopM2\text{-}2}$ viral genomes.

Northern blot analysis of HMPV mutants reveals DIs in M2-2 mutant virus stocks

The mutation patterns observed in the genomes of $HMPV_{\Delta M2\text{-}2}$ and $HMPV_{StopM2\text{-}2}$ were similar to those observed in the genomes of the P5H virus, described in our previous study, where it was demonstrated that this virus stock contained DIs (31). To assess the presence of DIs in the $HMPV_{StopG}$, $HMPV_{StopSH}$, and $HMPV_{StopM2\text{-}2}$ stocks, the presence of DIs was assessed by means of Northern blot analysis uing RNA directly isolated from passage two virus stocks. This analysis showed that each HMPV stock contained the full-length viral genome (Figure 7, top bands), and two additional bands with a size of approximately 7 kb and 4.5 kb of unknown origin. In addition, the $HMPV_{StopM2\text{-}2}$ stock contained a large amount of smaller RNA molecules with a size range from <0.5 to 4.5 kb, similar to previously reported for the P5H stock, demonstrating the presence of DIs in this virus stock. These smaller RNA molecules were far less abundant in the $HMPV_{WT}$, or $HMPV_{StopG}$ and $HMPV_{StopSH}$ stocks. These data demonstrate the presence of large amounts of DIs in M2-2 mutant virus stock, but not G or SH mutant virus stock.

Discussion

This study was set out to explore the role of the HMPV G, SH, and M2-2 proteins as IFN antagonist during infection. Overall, these data indicate that the HMPV G and SH proteins are no interferon antagonists and that the role of the M2-2 protein as bonafide interferon antagonist needs further investigation.

A number of studies reported on the mechanisms used by HMPV to subvert cellular innate immune responses (18, 19, 21, 22, 25, 29, 30), however data from these reports were sometimes contradictive. For HMPV, it has been shown that the method for generation of virus stocks is important for studies regarding the interaction with the innate immune system, as HMPV rapidly accumulates snapback DIs upon passaging at high m.o.i. (31). Double-stranded RNA snapback DIs in virus stocks results in production of IFN upon inoculation of cells (44, 45). The presence of snapback DIs in virus stocks could explain inconsistencies between previously reported studies. Therefore, we aimed to investigate the role of the G, SH, and M2-2 proteins in activation or subversion of the type I IFN pathway using viruses generated in a way to prevent DI accumulation. All viruses used in this study were passaged two times at an m.o.i. of 0.01. While the NL/1/00 virus used in this study did contain two mutations that resulted in trypsinindependent virus replication, these mutations did not alter the IFN-antagonistic phenotype, as the wild type virus did not induce the type-I IFN response upon infection of A549 cells.

Additionally, we aimed to address whether the design of knocking out protein expression affected the interaction of the virus with the type I IFN pathway.

To this end, G, SH, or M2-2 protein expression was ablated either by deletion of the ORF, deletion of the ORF including the gene-start and gene-end signals or by the introduction of multiple stop codons throughout the ORF, keeping the genome length and transcriptional gradient intact. An effect of genome length or accumulation of gene-start and gene-end signals on replication or IFN inducing capabilities of G, SH, or M2-2 mutant viruses was not observed. The attenuated replication of the mutant viruses in IFN-competent cells (A549) in contrast to IFN-deficient cells (Vero-118) indicated a role for the M2-2 protein in inhibiting interferon induction. In contrast to previous reports, we did not observe induction of IFN-β production by HMPV lacking G or SH protein expression upon inoculation of A549 cells (18, 19, 21, 22). The finding that the M2-2 mutant viruses induced IFN-β production upon inoculation of A549 cells was in agreement with other studies (25, 29). However, infection with $HMPV_{StopM2\text{-}2}$ induced more IFN than infection with $HMPV_{\Delta M2\text{-}2}$, which is most likely related to the lower infection rates of $HMPV_{\Delta M2\text{-}2}$ infection. Whether this is due to differences in genome length needs further investigation, although a similar effect was not observed for G or SH mutants.

Analysis of virus induced IFN-β production in A549 cells with a knockout of the RIG-I, MAVS, or PKR gene revealed a role of the RIG-I – MAVS signaling pathway in sensing of $HMPV_{\Delta M2\text{-}2}$ and $HMPV_{StopM22}$, consistent with previous reported studies (25, 29, 30). A role for PKR in induction of IFN-β production upon inoculation with M2-2 mutant viruses was not observed. However, PKR could still play a role during HMPV infection, which requires further investigation.

As previously mentioned, all the G mutant viruses, used at passage two, did not induce IFN-β production in inoculated A549 cells, contrary to previous reports (18, 19). All G mutant viruses displayed attenuated replication in Vero-118 cells, which resulted in low titers of produced virus stocks. To obtain high titers, virus stocks could be generated with a higher m.o.i., or by multiple passages. The use of a higher m.o.i. during generation of G mutant virus stocks or multiple passaging of the virus could result in the production of snapback DIs, as shown in our previous study (31). This might explain the contradictory results on the IFN inducing capacity of G mutants in other studies, which used virus stocks up to passage 5 (18). In addition, the contradicting results might be due to the use of different virus strains. Previously, we have shown that inoculation of A549 cells with NL/1/99 (genotype B1) did not induce the production of IFN. Additional experiments with inoculation of A549 cells with G and SH deletion mutants of NL/199 also demonstrated the absence of induction of IFN production (data not shown). In addition, *IFN-antagonists are often, if not always, shared within virus families (e.g. V proteins of paramyxoviruses, NS1 proteins from influenza viruses). Therefore, we do not expect different results when different virus strains are used.*

Previously, Schickli *et al*. reported on a high mutation frequency and an increased number of insertions in a part of the genomes of a M2-2 mutant

virus, which was generated by deletion of the part of the M2-2 ORF that does not overlap with the M2-1 ORF (26). In our study, both $HMPV_{StopM2-2}$ and $HMPV_{\Delta M2-2}$ contained increased mutation frequency throughout the whole genome as compared to that of $HMPV_{WT}$, but an increased frequency of insertions or deletions was not observed. This might be due to the method used to assess genetic stability. Schickli *et al*. used Sanger sequencing of cloned PCR fragment of a region surrounding the M2-2 ORF (26), while in our study illumina next-generation sequencing of the complete genome was used. Hyper mutation in the $HMPV_{\Delta M2-2}$ and $HMPV_{StopM2-2}$ genomes in this study was present in 10-15% of all reads in passage 2 virus stocks. Sanger sequencing will most likely not detect these hyper mutated genomes, as the mutation detection limit of Sanger sequencing is between 15-20% (46). The high rate of mutations in the viral genome may lead to the loss of function of other HMPV proteins or could disrupt secondary RNA structures, causing the virus to be sensed differently by the infected cell. However, viral protein expression levels during infection were not assessed in this study.

Previously, we showed that repeated passaging of HMPV at a high m.o.i. (P5H) resulted in the generation of snapback DIs (31), and substantial A-to-G and T-to-C editing of DIs or viral genomes. The observed mutation patterns were consistent with the properties of ADAR proteins, which deaminate adenosine residues to inosines in double-stranded RNA (41, 42). Inosines are then recognized as guanosines by polymerases during replication, leading to A-to-G mutations during replication of RNA viruses. The observed high rates of A-to-G or T-to-C mutations in $HMPV_{\Delta M2-2}$ and $HMPV_{StopM2-2}$ genomes suggested a role for ADAR editing. This was confirmed by generating M2-2 mutant virus stocks in ADAR1 knockdown Vero-118 cells. Since the A-to-G and T-to-C hyper mutation was observed in both $HMPV_{\Delta M2-2}$ and $HMPV_{StopM2-2}$ genomes, this editing is independent of the genome length. More importantly, similarities in mutation patterns as well as the percentage of A-to-G and T-to-C mutations between $HMPV_{\Delta M2-2}$ and $HMPV_{StopM2-2}$ and the P5H virus in our previous studies suggested that the M2-2 mutant virus stocks contained DIs (31). Northern blot analysis of RNA isolated from the $HMPV_{StopM2-2}$ stock confirmed the presence of DIs, which were absent in the wild type, SH, or G mutant virus stocks. As snapback DIs are potent inducers of the interferon response, the presence of DIs complicates studies regarding interaction between the innate immune system and HMPV M2-2 mutants. The M2-2 protein is involved in the regulation of viral mRNA and genome synthesis (24, 25), therefore deletion of the M2-2 protein might affect viral transcription or replication which could result in production of snapback DIs. Since snapback DIs are double-stranded RNAs, which are a template for ADAR1, the A-to-G and T-to-C mutations observed in M2-2 mutant viruses might be hyper mutated DIs rather than viral genomes. ADAR1 editing of viral genomes can either be antiviral or proviral (reviewed in (42, 47)), however

editing of M22 mutant virus genomes could be an artefact of the DIs rather than a natural interaction between HMPV and ADAR1. This issue will require further investigation.

Ideally, to confirm the role of the M2-2 protein as a bonafide IFN antagonist, M2-2 mutant virus stocks should be generated in cells stably expressing the M2-2 protein. This could result in M2-2 mutant virus stocks without of DIs. Unfortunately, using various expression systems we have failed to stably express the M2-2 protein in Vero-118 cells due to protein expression and degradation issues.

In conclusion, in contrast to reported studies, this study showed that the HMPV G and SH proteins do not function as IFN antagonist. HMPV lacking M2-2 protein expression did induce IFN production, which is in agreement with reported studies. However, the role of DIs and hyper mutated genomes in M22 mutants needs to be further elucidated before the M2-2 protein is defined as a bonafide IFN antagonist.

Materials and Methods

Cloning and rescue of recombinant HMPV

For cloning of all recombinant viruses lacking G, SH, or M2-2 protein expression, synthetic DNA fragments spanning nucleotide 4460-7438 of the HMPV NL/1/00 (genotype A1) genome (GenBank accession no. AF371337.2) containing deletions of- or mutations in- the G, SH, or M2-2 genes to ablate protein expression were obtained from IDT (www.idtdna.com). Synthetic fragments were PCR amplified and cloned into the full length HMPV NL1/00 genome using restriction enzymes StuI (nt 4463-4468) and BsrGI (nt 7430-7435) (33). The following mutant viruses were generated: $HMPV_{\Delta G\text{-}ORF}$ and $HMPV_{\Delta SH\text{-}ORF}$, where only the ORF of the gene was deleted (from start-codon to stop-codon); $HMPV_{\Delta G}$ and $HMPV_{\Delta SH}$, where both the ORF and the gene-start and gene-end signals of the gene were deleted; $HMPV_{\Delta M2\text{-}2}$, where the non-overlapping sequence of the M2-2 ORF with the M2-1 ORF was deleted and nucleotide substitutions leading to stop codons were introduced in the overlapping sequence with the M2-1 ORF without changing the amino acids of the M2-1 protein; $HMPV_{StopG,}$ $HMPV_{StopSH}$ and $HMPV_{StopM2\text{-}2}$, nucleotide substitutions leading to stop codons were introduced that resulted in coding potential of less than 20 amino acids of the ORF of the gene (Figure 1). Virus rescue was performed as described previously (34).

Cells and viruses

Vero-118, A549 and 293-T cells were cultured as previously described (31, 33). HMPV NL/1/00 (genotype A1) virus stocks were generated as previously reported using a trypsin-independent virus strain (31). All virus stocks used in this study were generated as previously described and used at a maximum passage of

two using trypsin-free medium (31). Measles virus strain Edmonston (MeV-Edm) and Parainfluenza virus type 5 (PIV-5) strain W3 were generated as previously described (31, 35, 36). Titers of virus stocks, expressed as $TCID_{50}$ ml^{-1}, were determined by end-point dilution in Vero-118 cells. Virus inoculation of Vero-118 and A549 cells was performed as previously described (31).

Replication kinetics

10^6 Vero-118 and A549 cells were seeded in 25 cm^2 cell culture. Sixteen hours after seeding, cells were inoculated with HMPV at an m.o.i. of 0.1 for two hours. Cells were washed three times with PBS and inoculated in 5 ml infection medium as described previously (31, 33). At each time-point, 100 µl supernatant was diluted in 100 µl 50% sucrose in PBS and stored at -80°C until further use. The titer of each sample, expressed as$TCID_{50}$ ml^{-1}, was determined as described above.

RNA isolation and quantitative PCR

RNA was isolated with the use of the High Pure RNA Isolation kit (Roche) according to the manufacturer's instructions. Quantitative PCR was performed using the Taqman Fast Virus 1-Step Master Mix (Applied Biosystems) according to the manufacturer's instructions. Input RNA was normalized using the β-actin housekeeping gene (forward primer 5'-ggcatccacgaaactacctt-3', reverse primer 5'-agcactgtgttggcgtacag-3' and probe 5'-FAM-atcatgaagtgtgacgtggacatccg-TAMRA-3'). IFN-β primers and probe were purchased from Applied Biosystems (HS00277188_s1). IFN-β mRNA was quantified by calculating the fold induction as compared to mock-infected cells using the $\Delta\Delta C_t$ method (37).

FACS analysis of HMPV infected cells and Interferon-β bioassay

At specified time points, cells were harvested and were washed in 2% fetal calf serum (FCS) in PBS. Immunostaining was performed using a 1:100 dilution of an in-house generated mouse anti-HMPV F hybridoma antibody followed by a 1:100 diluted secondary polyclonal rabbit-anti-mouse immunoglobulins/FITC (DAKO). Cells were fixed with 2% paraformaldehyde (PFA) in PBS and the percentage of cells infected with HMPV was analyzed using a FACSLyric machine (BD Biosciences). IFN-β levels were quantified by a firefly luciferase reporter assay as previously described (38).

CRISPR/Cas9 knock-out cell lines

To generate A549 knock-out cells, plasmid px458 (Addgene #48138) was used. Synthetic guide RNA (gRNA) sequences targeting the exons of RIG-I (5'-GGGTCTTCCGGATATAATCC-3'), PKR (5'-TAATACATACCGTCAGAAGC-3') and MAVS (5'-AGTTGATCTCGCGGACGAAG-3') were obtained as complementary primers with an additional 5'-CACC sequence for the forward primer and an

additional 5'-TTTG sequence for the reverse primer. The px458 plasmid was digested by BbsI (New England Biolabs), primers were annealed and 5' overhang sequences were used to ligate the gRNA fragment into the px458 vector. A549 cells were transfected overnight using FuGENE HD Transfection Reagent (Promega) according to the manufacturer's instructions and FACS sorted for eGFP expression. Sorted cells were subjected to limiting-dilution in a 96-wells plate and monitored to obtain clonal eGFP positive cell lines. The knockout of RIG-I (A549ΔRIG-I), PKR (A549ΔPKR) and MAVS (A549ΔMAVS) was validated by western blot analysis as described below.

CRISPR-interference knockdown of ADAR1

To generate Vero-118 knockdown cells, lentiviral plasmids pHAGE TRE dCAS9-KRAB (Addgene #50917) and pKLV-U6gRNA(BbsI)-PKGpuro2ABFP (Addgene #50946) were used. Plasmids containing gRNA 1 (5'-GCCAAACTTTCCGGAGGGGA-3') or 2 (5'-GCGGAGTTTCCCGTGCCGAC-3') targeting the promoter region of ADAR1-p150 were a kind gift by Mart Lamers (Department of Virology, Erasmus MC). Lentiviruses were produced by transfection of pHAGE TRE dCAS9-KRAB or pKLV-U6gRNA(BbsI)-PKGpuro2ABFP containing a gRNA sequence together with plasmid pLenti1 (a kind gift from Didier Trono, Laboratory of Virology and Genetics, École polytechnique fédérale de Lausanne) and plasmid pCMV-VSV-G (Addgene #8454). After two days, the lentivirus-containing supernatant was harvested and used for transduction of target cells. Geneticin (Invitrogen), puromycin (Invivogen) and doxycycline (Sigma-Aldrich) was added to the medium according to the manufacturer's instructions 48 hours post transduction to select for transduced cells and to induce the expression of the CRISPR-interference knockdown system. Fresh doxycycline was added to the medium every other day. After two weeks of selection and induction, ADAR1 knockdown percentages were validated by western blot as described below.

Western blot analysis

(Knock out) cells were grown until confluent in a 6-wells plate, washed twice with cold PBS and lysed in RIPA lysis and extraction buffer (Thermo Scientific) supplemented with phosphatase inhibitors (PhosSTOP EASYpack, Roche) and protease inhibitors (EASYpack Protease Inhibitor Cocktail, Roche). After 5 minutes of incubation at 4°C, cells were scraped, transferred into Eppendorf tubes and incubated in a tube revolver (Thermofisher Scientific) for 1 hour at 4°C. Samples were centrifuged for 15 minutes at 15.000x*g* at 4°C. The supernatants were diluted in NuPAGE LDS Sample Buffer (4X) and analyzed by western blot analysis as described previously (39). Monoclonal antibodies targeting RIG-I (Bio-Connect, AG-20B-0009-C100), PKR (Abcam, ab226819), and MAVS (Abcam, ab89825) were used according to the manufacturer's instructions. Secondary polyclonal rabbit-**α**-mouse-HRP (Agilent, P0260) and polyclonal swine-**α**-Rabbit-

HRP (Agilent, P0217) antibodies were used at a 1:1000 dilution. Imaging was performed using an Amersham Imager 600 (GE Healthcare).

Next-generation sequencing of virus genomes and data analysis

For detection of mutated viral genomes in virus stocks, from here on referred to as minor variants, RNA of virus stocks was isolated as described above. Random cDNA synthesis was performed by Superscript IV reverse transcriptase (Invitrogen) according to the manufacturer's instructions using random hexamer primers with a specific tail sequence (RF2596, 5'-CCCACCACCAGAGAGAAANNNNNN-3' and RF2597, 5'-ACCAGAGAGAAACCCACCNNNNNN-3') in individual reactions. After the RT reaction samples were treated with Klenow DNA polymerase (Thermo Scientific) according to the manufacturer's instructions to repair 5' overhangs of the cDNA. Two separate PCRs were performed with Amplitaq Gold DNA polymerase (Applied Biosystems) using primer RF2602 (5'-CCCACCACCAGAGAGAAA-3') for cDNA synthesized with primer RF2596 and primer RF2603 (5'-ACCAGAGAGAAACCCACC-3') for cDNA synthesized with primer RF2597 in a total volume of 50 µl. The cDNA's were PCR amplified (2 min. 95°C, 40 cycles of 20 sec. 95°C, 1 min. 56°C, 2 min. 72°C, followed by 10 min. 72°C) and gel purified. Library preparation, Illumina sequencing and data analysis was performed as previously described (40).

Northern blot and subsequent blot analysis

RNA was isolated from 1 ml virus stocks by TRIzol RNA isolation according to the manufacturer's instructions. Northern blotting was performed using the NorthernMax-Gly kit according to the manufacturer's instructions. A ^{32}P-labeled radioactive RNA probe was generated using the MAXIscript T7 Transcription Kit according to the Manufacturer's instructions. A PCR product containing a T7 minimal promoter sequence followed by a 180 nucleotide stretch of the HMPV trailer was used as template DNA to generate the probe, as described previously (31). The activity of the probe was determined using a Beta counter (which acted as a surrogate for the probe concentration). A probe concentration of 5x10^7 cpm/ml of radiolabeled probe was used for hybridization. The Northern blot was exposed to a phosphor-imager screen for three days and images were generated using an Amersham Typhoon laser-scanner platform.

Statistics. Statistical analyses were conducted using GraphPad Prism5 software. All comparisons were done using tests indicated at figure legends.

Acknowledgements

The authors would like to thank Ron Voorwald for quantifying the Northern blot probe concentrations using a beta counter.

Funding
This study was supported by the Marie Sklodowska-Curie Actions 2020 Innovative Training Networks (H2020-MSCA-ITN-813343-INITIATE)

References

1. Hoogen BG van den, Doornum GJJ van, Fockens JC, Cornelissen JJ, Beyer WEP, Groot R de, Osterhaus ADME, Fouchier and RAM. 2003. Prevalence and clinical symptoms of human metapneumovirus infection in hospitalized patients. Infect Dis Clin Pract 12:207–208.
2. Van Den Hoogen BG, De Jong JC, Groen J, Kuiken T, De Groot R, Fouchier RAM, Osterhaus ADME. 2001. A newly discovered human pneumovirus isolated from young children with respiratory tract disease. Nat Med 7:719–724.
3. Williams J V., Harris PA, Tollefson SJ, Halburnt-Rush LL, Pingsterhaus JM, Edwards KM, Wright PF, Crowe JE. 2004. Human Metapneumovirus and Lower Respiratory Tract Disease in Otherwise Healthy Infants and Children. N Engl J Med 350:687–696.
4. Williams JV, Wang CK, Yang C, Tollefson SJ, House FS, Heck JM, Chu M, Brown JB, Lintao LD, Quinto JD, Chu D, Spaete RR, Edwards KM, Wright PF, Crowe, Jr. JE. 2006. The Role of Human Metapneumovirus in Upper Respiratory Tract Infections in Children: A 20-Year Experience. J Infect Dis 193:387–395.
5. Jain S, Self WH, Wunderink RG, Fakhran S, Balk R, Bramley AM, Reed C, Grijalva CG, Anderson EJ, Courtney DM, Chappell JD, Qi C, Hart EM, Carroll F, Trabue C, Donnelly HK, Williams DJ, Zhu Y, Arnold SR, Ampofo K, Waterer GW, Levine M, Lindstrom S, Winchell JM, Katz JM, Erdman D, Schneider E, Hicks LA, McCullers JA, Pavia AT, Edwards KM, Finelli L. 2015. Community-Acquired Pneumonia Requiring Hospitalization among U.S. Adults. N Engl J Med 373:415–427.
6. O'Brien KL, Baggett HC, Brooks WA, Feikin DR, Hammitt LL, Higdon MM, Howie SRC, Deloria Knoll M, Kotloff KL, Levine OS, Madhi SA, Murdoch DR, Prosperi C, Scott JAG, Shi Q, Thea DM, Wu Z, Zeger SL, Adrian P V., Akarasewi P, Anderson TP, Antonio M, Awori JO, Baillie VL, Bunthi C, Chipeta J, Chisti MJ, Crawley J, DeLuca AN, Driscoll AJ, Ebruke BE, Endtz HP, Fancourt N, Fu W, Goswami D, Groome MJ, Haddix M, Hossain L, Jahan Y, Kagucia EW, Kamau A, Karron RA, Kazungu S, Kourouma N, Kuwanda L, Kwenda G, Li M, Machuka EM, Mackenzie G, Mahomed N, Maloney SA, McLellan JL, Mitchell JL, Moore DP, Morpeth SC, Mudau A, Mwananyanda L, Mwansa J, Silaba Ominde M, Onwuchekwa U, Park DE, Rhodes J, Sawatwong P, Seidenberg P, Shamsul A, Simões EAF, Sissoko S, Wa Somwe S, Sow SO, Sylla M, Tamboura B, Tapia MD, Thamthitiwat S, Toure A, Watson NL, Zaman K, Zaman SMA. 2019. Causes of severe pneumonia requiring hospital admission in children without HIV infection from Africa and Asia: the PERCH multi-country case-control study. Lancet 394:757–779.
7. Jensen S, Thomsen AR. 2012. Sensing of RNA Viruses: a Review of Innate Immune Receptors Involved in Recognizing RNA Virus Invasion. J Virol 86:2900–2910.
8. Kell AM, Gale M. 2015. Since January 2020 Elsevier has created a COVID-19 resource centre with free information in English and Mandarin on the novel coronavirus COVID- 19 . The COVID-19 resource centre is hosted on Elsevier Connect , the company ' s public news and information. Virology 479–480:110–121.
9. Rehwinkel J, Gack MU. 2020. RIG-I-like receptors: their regulation and roles in RNA sensing. Immunity 34:680–692.
10. Loo YM, Gale M. 2011. Immune Signaling by RIG-I-like Receptors. Immunity 34:680–692.
11. Yoneyama M, Kikuchi M, Matsumoto K, Imaizumi T, Miyagishi M, Taira K, Foy E, Loo Y-M, Gale M, Akira S, Yonehara S, Kato A, Fujita T. 2005. Shared and Unique Functions of the DExD/H-Box Helicases RIG-I, MDA5, and LGP2 in Antiviral Innate Immunity. J Immunol 175:2851–2858.

12. Patel JR, García-Sastre A. 2014. Activation and regulation of pathogen sensor RIG-I. Cytokine Growth Factor Rev 25:513–523.
13. Goubau D, Deddouche S, Reis e Sousa C. 2013. Cytosolic Sensing of Viruses. Immunity 38:855–869.
14. Hartmann G. 2017. Nucleic Acid Immunity. Adv Immunol 133:121–169.
15. Gal-Ben-Ari S, Barrera I, Ehrlich M, Rosenblum K. 2019. PKR: A kinase to remember. Front Mol Neurosci 11:1–20.
16. Kawasaki T, Kawai T. 2014. Toll-like receptor signaling pathways. Front Immunol 5:1–8.
17. Van Den Hoogen BG, De Jong JC, Groen J, Kuiken T, De Groot R, Fouchier RAM, Osterhaus ADME. 2001. A newly discovered human pneumovirus isolated from young children with respiratory tract disease. Nat Med 7:719–724.
18. Bao X, Liu T, Shan Y, Li K, Garofalo RP, Casola A. 2008. Human metapneumovirus glycoprotein G inhibits innate immune responses. PLoS Pathog 4.
19. Kolli D, Bao X, Liu T, Hong C, Wang T, Garofalo RP, Casola A. 2011. Human Metapneumovirus Glycoprotein G Inhibits TLR4-Dependent Signaling in Monocyte-Derived Dendritic Cells. J Immunol 187:47–54.
20. Preston FM, Straub CP, Ramirez R, Mahalingam S, Spann KM. 2012. SiRNA against the G gene of human metapneumovirus. Virol J 9:1–5.
21. Bao X, Kolli D, Esham D, Velayutham TS, Casola A. 2018. Human metapneumovirus small hydrophobic protein inhibits interferon induction in plasmacytoid dendritic cells. Viruses 10.
22. Hastings AK, Amato KR, Wen SC, Peterson LS, Williams V. 2017. Human metapneumovirus small hydrophobic (SH) protein downregulates type I IFN pathway signaling by affecting STAT1 expression and phosphorylation 248–256.
23. de Graaf M, Herfst S, Aarbiou J, Burgers PC, Zaaraoui-Boutahar F, Bijl M, van IJcken W, Schrauwen EJA, Osterhaus ADME, Luider TM, Scholte BJ, Fouchier RAM, Andeweg AC. 2013. Small Hydrophobic Protein of Human Metapneumovirus Does Not Affect Virus Replication and Host Gene Expression In Vitro. PLoS One 8:1–10.
24. Buchholz UJ, Biacchesi S, Pham QN, Tran KC, Yang L, Luongo CL, Skiadopoulos MH, Murphy BR, Collins PL. 2005. Deletion of M2 Gene Open Reading Frames 1 and 2 of Human Metapneumovirus: Effects on RNA Synthesis, Attenuation, and Immunogenicity. J Virol 79:6588–6597.
25. Ren J, Wang Q, Kolli D, Prusak DJ, Tseng C-TK, Chen ZJ, Li K, Wood TG, Bao X. 2012. Human Metapneumovirus M2-2 Protein Inhibits Innate Cellular Signaling by Targeting MAVS. J Virol 86:13049–13061.
26. Schickli JH, Kaur J, MacPhail M, Guzzetta JM, Spaete RR, Tang RS. 2008. Deletion of human metapneumovirus M2-2 increases mutation frequency and attenuates growth in hamsters. Virol J 5:1–14.
27. Kitagawa Y, Zhou M, Yamaguchi M, Komatsu T, Takeuchi K, Itoh M, Gotoh B. 2010. Human metapneumovirus M2-2 protein inhibits viral transcription and replication. Microbes Infect 12:135–145.
28. Biacchesi S, Pham QN, Skiadopoulos MH, Murphy BR, Collins PL, Buchholz UJ. 2005. Infection of Nonhuman Primates with Recombinant Human Metapneumovirus Lacking the SH, G, or M2-2 Protein Categorizes Each as a Nonessential Accessory Protein and Identifies Vaccine Candidates. J Virol 79:12608–12613.
29. Chen Y, Deng X, Deng J, Zhou J, Ren Y, Prusak DJ, Wood TG, Bao X, Hospital T, First T, Hospital A. 2017. Functional Motifs Responsible for Human Metapneumovirus M2-2-mediated Innate Immune Evasion. Virology 361–368.

30. Kitagawa Y, Sakai M, Funayama M, Itoh M, Gotoh B. 2017. Human Metapneumovirus M2-2 Protein Acts as a Negative Regulator of Alpha Interferon Production by Plasmacytoid Dendritic Cells 91:1–15.
31. van den Hoogen BG, van Boheemen S, de Rijck J, van Nieuwkoop S, Smith DJ, Laksono B, Gultyaev A, Osterhaus ADME, Fouchier RAM. 2014. Excessive production and extreme editing of human metapneumovirus defective interfering RNA is associated with type I IFN induction. J Gen Virol 95:1625–1633.
32. Pfaller CK, Cattaneo R, Schnell MJ. 2015. Reverse genetics of Mononegavirales: How they work, new vaccines, and new cancer therapeutics. Virology 479–480:331–344.
33. Herfst S, de Graaf M, Schickli JH, Tang RS, Kaur J, Yang C-F, Spaete RR, Haller AA, van den Hoogen BG, Osterhaus ADME, Fouchier RAM. 2004. Recovery of Human Metapneumovirus Genetic Lineages A and B from Cloned cDNA. J Virol 78:8264–8270.
34. Herfst S, de Graaf M, Schickli JH, Tang RS, Kaur J, Yang C-F, Spaete RR, Haller AA, van den Hoogen BG, Osterhaus ADME, Fouchier RAM. 2004. Recovery of Human Metapneumovirus Genetic Lineages A and B from Cloned cDNA. J Virol 78:8264–8270.
35. Shingai M, Ebihara T, Begum NA, Kato A, Honma T, Matsumoto K, Saito H, Ogura H, Matsumoto M, Seya T. 2007. Differential Type I IFN-Inducing Abilities of Wild-Type versus Vaccine Strains of Measles Virus. J Immunol 179:6123–6133.
36. Childs K, Randall R, Goodbourn S. 2012. Paramyxovirus V Proteins Interact with the RNA Helicase LGP2 To Inhibit RIG-I-Dependent Interferon Induction. J Virol 86:3411–3421.
37. Livak KJ, Schmittgen TD. 2001. Analysis of Relative Gene Expression Data Using Real-Time Quantitative PCR and the 2-△△Ct Method. Methods.
38. Patel JR, Jain A, Chou YY, Baum A, Ha T, García-Sastre A. 2013. ATPase-driven oligomerization of RIG-I on RNA allows optimal activation of type-I interferon. EMBO Rep 14:780–787.
39. Mykytyn AZ, Breugem TI, Riesebosch S, Schipper D, van den Doel PB, Rottier RJ, Lamers MM, Haagmans BL. 2021. Sars-cov-2 entry into human airway organoids is serine protease-mediated and facilitated by the multibasic cleavage site. Elife 10:1–23.
40. Oude Munnink BB, Kik M, de Bruijn ND, Kohl R, van der Linden A, Reusken CBEM, Koopmans M. 2019. Towards high quality real-time whole genome sequencing during outbreaks using Usutu virus as example. Infect Genet Evol 73:49–54.
41. George CX, Gan Z, Liu Y, Samuel CE. 2011. Adenosine deaminases acting on RNA, RNA editing, and interferon action. J Interf Cytokine Res 31:99–117.
42. Lamers MM, van den Hoogen BG, Haagmans BL. 2019. ADAR1: "Editor-in-Chief" of Cytoplasmic Innate Immunity. Front Immunol 10:1763.
43. Larson MH, Gilbert LA, Wang X, Lim WA, Weissman JS, Qi LS. 2013. CRISPR interference (CRISPRi) for sequence-specific control of gene expression. Nat Protoc 8:2180–2196.
44. Strahle L, Garcin D, Kolakofsky D. 2006. Sendai virus defective-interfering genomes and the activation of interferon-beta. Virology 351:101–111.
45. Sekellick J, Marcus I. 1978. Persistent Infection 1. Interferon-inducing Defective-Interfering Particles as Mediators of Cell Sparing: Possible Role in Persisten Infection by Vesucular Stomatitis Virus. Virology 85:175–186.
46. Rohlin A, Wernersson J, Engwall Y, Wiklund L, Björk J, Nordling M. 2009. Parallel sequencing used in detection of mosaic mutations: Comparison with four diagnostic DNA screening techniques. Hum Mutat 30:1012–1020.
47. Samuel CE. 2011. Adenosine deaminases acting on RNA (ADARs) are both antiviral and proviral. Virology 411:180–193.

7

Summarizing discussion

Human metapneumovirus (HMPV), identified in the Netherlands in 2001, has been circulating worldwide for at least 50 years (1). Primarily young children, immunocompromised individuals, and the elderly population are susceptible to HMPV induced severe disease. In young children, HMPV is one of the leading causative agents of respiratory illness, next to respiratory syncytial virus (RSV), another member of the *Pneumoviridae* family, and influenza virus (2). The clinical impact of RSV has resulted in the decision by the world health organization (WHO) to focus efforts on RSV vaccines (3), for which in the last decades significant progress has been made. For instance, a phase 3 clinical trial of Pfizer's bivalent vaccine candidate, composed of a stabilized fusion (F) protein in its pre-fusion state (RSVpreF) from viruses from lineage A and B, has shown promising results (4). In addition, the Food and Drug Administration (FDA) has accepted priority review for the biologics license application for this vaccine candidate. With a potential RSV vaccine on its way, it seems logical that HMPV is the next vaccine target, given that HMPV and RSV share seasonality, susceptible population, and the clinical impact of HMPV ranks after that of Influenza and RSV. To develop a vaccine against HMPV, similar approaches can be used as those used for an RSV vaccine, as RSV and HMPV are genetically closely related. It might even be feasible to develop a quadrivalent vaccine that is composed of lineage A and B viruses from both RSV and HMPV, similar to the approach of the quadrivalent influenza vaccine (5).

For the development of HMPV vaccines, knowledge on epidemiology, evolution and virus-host interactions are indispensable. Even though significant progress has been made towards understanding these viral properties, many aspects remain relatively understudied.

Evolution of HMPV

To study virus evolution, it is crucial to have access to a solid whole genome sequencing (WGS) pipeline. WGS provides unmatched insights for studying virus evolution as compared to sequencing of partial genomes. For example, the use of whole genome sequences has led to a better temporal resolution of the West African Ebola virus epidemic of 2013-2015 (6), as well as the Zika virus outbreak in 2015 in Brazil (7). More recently, an unprecedented number of SARSCoV2 whole genome sequences has been generated that were used to track transmission, detect the emergence of new variants, and aid public health decision-making (8). Despite the advantages of whole genome sequencing compared to sequencing of partial genomes, it has not been implemented for other circulating viruses. For HMPV, the fusion protein (F) is most often sequenced and used to study virus evolution (9–14). The main reason for this is that the F protein is the main target for neutralizing antibodies and is therefore under the highest selection pressure (15). However, the attachment protein G is more variable between strains (9), and sequencing of this gene might provide

more details on evolution. Ideally, whole genome sequencing would provide information on both the F and G gene, along all other genes. Methods for whole genome sequencing of HPMV strains have been reported, but generating good coverage of the highly variable G with these methods gene has been challenging (16–19). **Chapter 2** describes an HMPV whole genome sequencing method that generates good coverage of the entire genome, including the G gene, from all circulating HMPV lineages. This method was subsequently used to study HMPV evolution in hospitalized and non-hospitalized individuals between 2005-2021 in **Chapter 3**. This study showed that viruses clustered into six genetic lineages (A1, A2.1, A2.2.1, A2.2.2, B1, B2) and that multiple lineages cocirculate each year. The circulation of different genetic lineages was similar between hospitalized and nonhospitalized individuals for respiratory tract infections (RTI) throughout the years. This could indicate equal hospitalization rates of people infected with viruses from each lineage. Finally, a robust HMPV classification and nomenclature system was proposed based on the number of nucleotide substitutions between viral F gene sequences, which could provide a solution for comparing data between several reports.

Similar to other research groups (20–24), our study reported on viruses with a duplication in the G gene and all these viruses clustered together within lineage A2.2.2. We detected the first virus containing a duplication in the G gene in the Netherlands in 2015. From 2018 onwards, all of the viruses carrying a duplication in the G gene contained a 111-nucleotide duplication rather than a 180-nucleotide duplication. Interestingly, the 111nucleotide and 180nucleotide duplicated sequences were copied from the same part of the G gene, i.e. the 111nucleotide duplication is a shortened version of the 180nucleotide duplication. This suggests that the 180-nucleotide duplicationcontaining virus could be the parental strain from which 111nucleotide duplicationcontaining viruses emerged. This could explain why no more viruses containing a 180nucleotide duplication in the G gene were detected after 2018, not only by us but also by others (11).

The rapid global distribution and dominance of these viruses with duplications in the G gene suggests a fitness advantage over viruses without a duplication in the G gene. It is notable that similar duplication events in the G gene of RSV have occurred (25). Most RSVs from lineage Buenos Aires (BA, subtype B viruses) and Ontario 1 (ON1, subtype A viruses) carry a 60nucelotide and 72nucleotide duplication in the G gene, respectively (26, 27). After their initial detection, these duplication-containing viruses have rapidly spread globally and have become the predominant circulating viruses in many countries (28, 29). One of these isolates, a BA virus containing a 60-nucleotide duplication in the G gene, was suggested to have increased attachment capacity which resulted in increased fitness *in vitro* (30). However, evidence for increased virulence of RSV carrying duplication in the G gene is lacking (31, 32). For HMPV, one study

suggested that an increased glycoprotein length, combined with additional glycosylation sites, might result in a G protein that protrudes further over the F protein, therefore further limiting the accessibility of neutralizing antibodies against the F protein (33). However, experimental evidence for this hypothesis is lacking, therefore the clinical relevance of this duplication event in the G gene remains unknown.

Waning immunity against pneumoviruses could explain the reported reinfections with these viruses, sometimes even with homologous viruses (34). Therefore, once a vaccine has been developed, it is possible that this vaccine has to be administered every year. Vaccines for respiratory viruses, like the influenza virus, are usually administered before the winter season, as most respiratory viruses, including HMPV, tend to have a winter seasonality. This was previously thought to be explained by winter temperature and humidity, a generally lower immune status of the host population due to a lack of sunlight and vitamins, or that people were more likely to be inside together which facilitates viral spread (reviewed in (35)). However, alleviating the lockdown measures which were in place for the SARS-CoV-2 pandemic has caused several respiratory viruses to resurge out of the regular winter season (36–38), including HMPV (**Chapter 4** and (39)). This might have resulted in a relatively naïve immune status against many of these viruses on a population level with a relatively large size, resulting in increased population spread of respiratory viruses regardless of the current season. It is unclear how long it will take for respiratory viruses to assume their regular winter seasonality, however this altered virus seasonality is important to monitor, as the timing of vaccination might require adjustment.

Interaction between HMPV and the innate immune system

Several approaches to develop an RSV vaccine are currently being employed. Stabilized F proteins are being used for maternal immunization (4), and a clinical trial using live-attenuated vaccines to vaccinate infants and toddlers is currently ongoing (clinicaltrials.gov identifier NCT04491877). For development of live-attenuated vaccines, different approaches have been employed. One of the approaches comprises the generation of viruses lacking expression of their interferon-antagonists (40, 41). For HMPV, a clear consensus on how the virus subverts the type-I IFN response is thus far lacking, therefore studying the interaction between HMPV and the host innate immune system would provide fundamental knowledge that can be used for the rational design of liveattenuated vaccines.

Previously, we showed that HMPV rapidly accumulates defective interfering particles (DIs) upon passaging at a high multiplicity of infection (MOI). This complicates studies between HMPV and the innate immune response, as DIs are potent inducers of the type-I IFN response (42, 43). In **Chapter 5**, we investigated the role of the G, SH, and M2-2 proteins as IFNantagonists using virus stocks

generated in a way to prevent DI accumulation (44). We demonstrated that the G and SH proteins of HMPV did not function as IFNantagonist in epithelial (A549) cells. The findings that the G protein did not act as IFN antagonist was in contrast with other studies (45–48), but in line with a study utilizing siRNA knockdown of the G gene (49). The finding that the SH protein did not function as IFN antagonist was in contrast with one study (50), but in agreement with another study using a genomics approach (51). Additionally, the SH protein was suggested to inhibit IFN-signaling by inhibiting STAT1 phosphorylation and signaling (52). Our study in chapter 5 was limited to the assessment of proteins involved in inhibiting IFN production, therefore we cannot confirm this observation. In line with other reports (53–55), our studies demonstrated that M2-2 deletion mutants induced IFN production upon infection of A549 cells. However, we showed that M22 deletion mutant virus stocks contained DIs. The results suggested a function for the M22 protein in preventing production and accumulation of DIs during infection, which in turn activate the IFN response (Figure 1). Therefore, future studies on HMPV and the innate immune system should assess whether the virus stocks contain DIs.

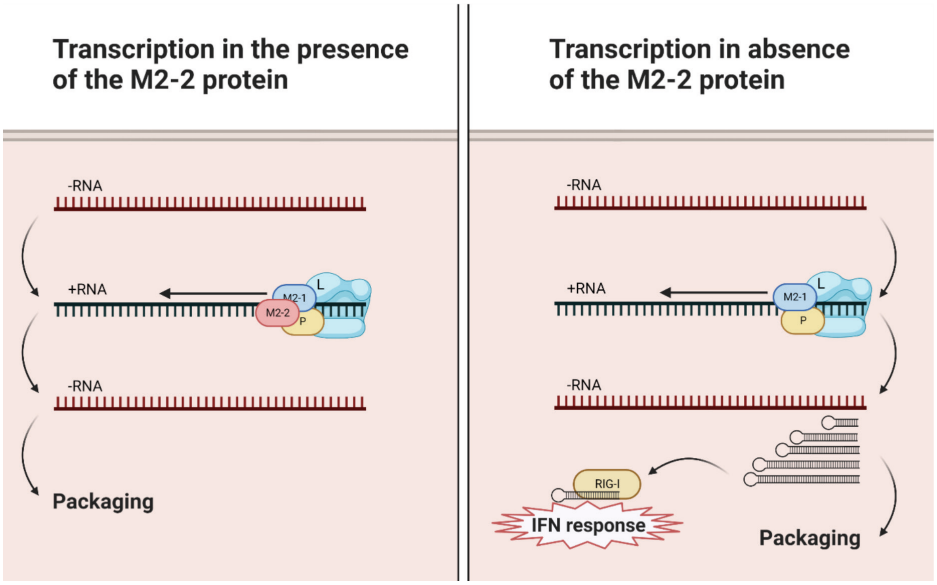

Figure 1. A model for induction of IFN production by cells infected with M2-2 deletion mutant viruses. During infection of cells with $HMPV_{WT}$ (left side of the image), after release of the genome into the cytoplasm, the viral negative sense RNA (RNA) is transcribed into a fulllength positive sense RNA (+RNA) copy of the genome by the viral polymerase complex. This +RNA (also called the antigenome) then serves as template for transcription of –RNA genome copies that are packaged into new virions. However, during transcription of +RNA in absence of the M2-2 protein (right side of the image), snapback DIs are generated. These DIs potently activate RIG-I that leads to induction of IFN production. Image generated with Biorender.

The finding that M2-2 deletion mutants contained hypermutated genomes and DIs complicates studies on the interaction between HMPV and the innate immunity. To generate a M22 deletion mutant virus stock without mutated genomes or DIs, we attempted to generate Vero118 cells stably expressing the M2-2 protein in which M2-2 deletion mutants could be generated without genomic hypermutations or DIs. Retroviral vectors encoding the M22 gene were used to transduce Vero-118 cells. Initially, we found that splicing prevented M2-2 protein expression. Addition of a woodchuck hepatitis virus post-transcriptional regulatory element (WPRE), a sequence known to promote nuclear export of unspliced RNAs (56), to the retroviral vector solved the issues of spicing. However, upon transduction of Vero-118 cells, M22 protein expression could not be confirmed, even though the mRNA was expressed, presumably due to degradation of the protein. Therefore, we were unable to generate cells stably expressing the M22 protein. The mechanism for this degradation still needs to be elucidated.

The observation that genomes of M2-2 deletion mutants were edited by ADAR1, as shown in **Chapter 5**, raised the hypothesis that the M2-2 protein inhibits ADAR1 activity. Preliminary experiments, such as coimmunoprecipitation assays, showed no interaction between the M2-2 protein and ADAR1 and suggested that the M22 protein does not actively inhibit ADAR1 editing (data not shown). Previously, the DIs in a high MOI passaged virus stock (P5H) were shown to be double-stranded hairpin RNAs, which is the template for ADAR1 (44). However, whether viral genomes or DIs in either wild-type or M22 deletion mutant virus stocks are edited by ADAR1 remains unclear.

The pneumovirus M2-1 and M2-2 proteins have been described to play a role in virus transcription and replication (57–61). In **Chapter 6** we show that homologous M2-1 and M2-2 proteins act in a concerted manner to maintain virus transcription, thereby preventing the production of DIs. This transcription mechanism was maintained when both HMPV M2 proteins were exchanged for that or RSV or APV-C, but was disrupted when only the M2-2 protein was exchanged.

The function of the M2-2 protein in preventing accumulation of DIs, and thereby induction of type-I IFN production, is similar to what has been described for the C protein of several paramyxoviruses. Deletion of C protein expression from the genome of parainfluenza virus type 1 (PIV-1), measles virus (MeV), and Sendai virus (SeV) leads to the production of dsRNAs, which in turn activate the innate immune response (62–65). Notably, both paramyxovirus C proteins and the HPMV M2-2 protein have been described to function in the transcription process. These data indicate a shared transcriptional function of these viral proteins that is important to prevent accumulation of DIs in virus stocks.

Similar to other non-segmented single-stranded negative-sense RNA viruses, HMPV gene expression is a polar transcriptional gradient (57, 66).

Genes expressed from a more promoter-distal location of the genome therefore have lower expression levels. The M2 gene is encoded as the 5th most promoterproximal gene of HMPV, therefore the M2-1 and M2-2 proteins have relatively low expression levels. In addition, expression of the M2-2 protein by $HMPV_{WT}$ is regulated by a ribosomal termination reinitiation process (67), which further reduces M2-2 protein expression levels. The viruses expressing the M2-2 protein from the 3rd position of the genome as an individual gene bypass this mechanism and are expressed from a more promoter-proximal position of the genome. Therefore, the levels of M2-2 protein expression are expected to be higher. The virus expressing the HMPV M22 protein from the 3rd position of the genome was phenotypically identical to $HMPV_{WT}$, indicating that M2-2 protein levels, as well as expression by a ribosomal termination re-initiation mechanism, might not be of critical importance *in vitro*. As the production of type-I IFN is detrimental for virus infections, counteracting this response is critical. Therefore, expression levels of a virus' IFN-antagonist should be sufficiently high to prevent production of type-I IFNs. For example, the RSV NS1 and NS2 proteins that function as IFN antagonists are the two most promoter-proximal genes (68). The Paramyxovirus V proteins, which function as IFN-antagonists (69, 70), are encoded as second ORF within the P gene that are expressed from the second most promoter-proximal gene position. The relatively low expression levels of the HMPV M22 protein should be taken into mind when considering the M2-2 protein as IFNantagonist.

Additionally, in **Chapter 6**, we demonstrated that the HMPV M2-2 protein was not able to substitute the function of the RSV NS1 and NS2 proteins as IFNantagonist, indicating that the M22 protein of HMPV is not a potent IFNantagonist. However, it cannot be ruled out that it might still function as a relatively weak IFNantagonist.

Most, if not all, viruses that cause disease in humans encode active IFN-antagonists. While some viruses encode nonstructural proteins as active IFN antagonist, such as influenza viruses, RSV, and members of the *Paramyxoviridae* family (70–73), some viruses encode essential proteins that function as active IFNantagonist, such as the SARS-CoV-2 matrix protein and nucleoprotein (74–76). Therefore, while the non-essential proteins of HMPV (G, SH, M2-2) might not function as active IFNantagonist, other proteins that are essential for virus replication, for which deletion mutants cannot be rescued, could function as active IFNantagonist. Alternatively, none of the known proteins of HMPV function as active IFN-antagonist and the virus passively avoids detection by innate immune responses. However, to our knowledge, a virus that causes disease in humans without an active IFNantagonist has not been described yet. Therefore, it is likely that another protein of HMPV, possibly one that has not been discovered yet, or a concerted action of multiple proteins, act as HMPVs IFN-antagonist.

Future perspectives

In the two decades after identification of HMPV, many advances have been made in knowledge regarding epidemiology, evolution, and molecular biology of HMPV. While immortalized cell lines are useful for studying certain aspects of viral-host interactions, these models do not resemble the physiological complexity of human airways. Over the past few years, induced pluripotent stem cells (iPSCs) and primary cell models have been developed and used to study several respiratory viruses (reviewed in (77)). iPSCs or human respiratory tissues have been used to generate organoid models *in vitro* that can be cultured and differentiated in transwell inserts as air-liquid interface (ALI) models, which better resemble the physiological complexity of human airway tissue. These models have led to rapid advances in virus research. For example, using this model, the RSV CX3CR1 receptor has been implicated to function as the receptor for RSV (78, 79). Some studies have reported the use of primary human material to study HMPV infections (80, 81), but the use of organoid-derived airliquid interface models have not been described for HMPV studies yet. The development and use of these models for HMPV could aid towards a better understanding of virushost interactions in the future.

The reported duplication events in the G gene highlight the importance to monitor HMPV evolution, preferably using whole genome sequencing methods as sequencing of (partial) F genes will miss any important evolutionary event in other regions of the genome. While a duplication in G could result in better binding efficiency to target cells, or differences in antigenic properties of these viruses, experimental data that support these hypotheses are lacking. Elucidating the nature of the duplication events in the G gene could aid towards a better fundamental understanding of the virus life cycle or antigenic properties, which in turn could impact the development of vaccine candidates.

There is no consensus about which HMPV proteins function as IFN-antagonist. However, the wild-type virus does not induce IFN production upon inoculation of A549 cells (44), which suggests that it possesses mechanisms to block or avoid the IFN response. Studies thus far have focused on the interaction between the G, SH, and M22 proteins and the innate immune response, but data on other HMPV proteins as IFN-antagonists is lacking. Additionally, the IFNantagonist of HMPV might be encoded by a gene that has not been identified yet. For example, several new influenza A virus proteins have been identified since the early 2000s (82–87), from which some are known to regulate host immune responses. For example, analysis of peptides that are recognized by CD8+ T cells has led to the identification of the Influenza PB1-F2 protein (87), a ribosomal frameshift in segment 3 that results in production of the PA-X protein (86), and expression of the M42 protein as a result of alternative splicing of the M2 protein (85). For HMPV, the alignment of whole genome sequences generated in Chapter 3 can be used to search for conserved putative ORFs. Knockout of these putative ORFs

could then serve as alternative approach to identify a possible IFN-antagonist of HMPV. Second, tagging viral genes at the Nterminus and C-terminus by reverse genetics, followed by western blot analysis of these tagged proteins, could be used to identify proteins that are expressed by a ribosomal frameshift or alternative start-codon usage. Nevertheless, identification of the new viral proteins for influenza viruses has been challenging, and this will also be the case for HMPV.

Several approaches were used to investigate the potential function of the M22 protein as IFNantagonist. In **Chapter** 6, we used RSV as model to determine whether heterologous proteins can function as IFNantagonist when expressed by RSVΔNS1+2. Using this model, the IAV protein, a potent IFNantagonist, only partially blocked the IFN response. Therefore, relatively weak interferon antagonists might not be able to inhibit IFN-responses when expressed in this model. This suggests that validating the HPMV M2-2 protein as IFNantagonist might require an alternative model. Previously, the IAV NS1 protein was shown to completely block induction of IFN production during infection with Newcastle disease virus (NDV), a virus that induces the IFN response (88). Therefore, NDV could be an alternative model to study the function of HMPV proteins as IFNantagonist. Additionally, **Chapter 6** demonstrated that the transcriptional function of the M2-2 protein requires the expression of the autologous M2-1 protein. Therefore, generation of NDV expressing both M2-1 and M2-2 proteins of HMPV might elucidate knowledge on the possible concerted action of the M2 proteins as active interferon-antagonists.

Analysis of RNAs present in HMPV stocks demonstrated the presence of DIs in M22 deletion mutant virus stocks (**Chapter 5**). Therefore, deletion of the transcriptional function of the HMPV M22 protein results in accumulation of DIs, and thereby induction of type-I IFN production. Interestingly, during detection of DIs by northern blot analyses, an RNA band with a size of approximately 7kb was observed in addition to the full-length 13kb genome fragment. This RNA species was present in all tested virus stocks and was also observed in our previous study (44). While this RNA could represent a partially deleted genome, the exact nature of this RNA is currently unknown. Identification of the sequence and function of this RNA species may lead to a better understanding of HMPVs molecular biology.

In conclusion, knowledge on the molecular biology of viruses and the interactions with the host aids to the design of novel intervention strategies and vaccines. Together, the studies presented in this thesis contribute towards a better fundamental understanding of HMPV evolution and its interaction with the host innate immune response.

References

1. van den Hoogen BG, de Jong JC, Groen J, Kuiken T, de Groot R, Fouchier RAM, Osterhaus ADME. 2001. A newly discovered human pneumovirus isolated from young children with respiratory tract disease. Nat Med 7:719–724.
2. Bosis S, Esposito S, Niesters HGM, Crovari P, Osterhaus ADME, Principi N. 2005. Impact of human metapneumovirus in childhood: Comparison with respiratory syncytial virus and influenza viruses. J Med Virol 75:101–104.
3. World Health Organization. 2021. https://www.who.int/publications/i/item/9789240021853. WHO preferred product characteristics of monoclonal antibodies for passive immunization against respiratory syncytial virus (RSV) disease.
4. Pfizer. 2022. https://www.pfizer.com/news/press-release/press-release-detail/pfizer-announces-positive-top-line-data-phase-3-global. Pfizer Announces Positive Top-Line Data of Phase 3 Global Maternal Immunization Trial for its Bivalent Respiratory Syncytial Virus (RSV) Vaccine Candidate.
5. European Medicines Agency. 2023. https://www.ema.europa.eu/en/news/eu-recommendations-2022-2023-seasonal-flu-vaccine-composition. EU recommendations for the seasonal influenza vaccine composition for the season 2022/2023. Amended BWP Ad Hoc Infuenza Working Group.
6. Dudas G, Bedford T. 2019. The ability of single genes vs full genomes to resolve time and space in outbreak analysis. BMC Evol Biol 19:1–27.
7. Faria NR, do Socorro Da Silva Azevedo R, Kraemer MUG, Souza R, Cunha MS, Hill SC, Thézé J, Bonsall MB, Bowden TA, Rissanen I, Rocco IM, Nogueira JS, Maeda AY, da Silva Vasami FG, de Lima Macedo FL, Suzuki A, Rodrigues SG, Cruz ACR, Nunes BT, de Almeida Medeiros DB, Rodrigues DSG, Queiroz ALN, da Silva EVP, Henriques DF, da Rosa EST, de Oliveira CS, Martins LC, Vasconcelos HB, Casseb LMN, de Brito Simith D, Messina JP, Abade L, Lourenço J, Alcantara LC, de Lima MM, Giovanetti M, Hay SI, de Oliveira RS, da Silva Lemos P, de Oliveira LF, de Lima CPS, da Silva SP, de Vasconcelos JM, Franco L, Cardoso JF, da Silva Gonçalves Vianez-Júnior JL, Mir D, Bello G, Delatorre E, Khan K, Creatore M, Coelho GE, de Oliveira WK, Tesh R, Pybus OG, Nunes MRT, Vasconcelos PFC. 2016. Zika virus in the Americas: Early epidemiological and genetic findings. Science 352:345–349.

8. Oude Munnink BB, Nieuwenhuijse DF, Stein M, O'Toole Á, Haverkate M, Mollers M, Kamga SK, Schapendonk C, Pronk M, Lexmond P, van der Linden A, Bestebroer T, Chestakova I, Overmars RJ, van Nieuwkoop S, Molenkamp R, van der Eijk AA, GeurtsvanKessel C, Vennema H, Meijer A, Rambaut A, van Dissel J, Sikkema RS, Timen A, Koopmans M, Oudehuis GJAPM, Schinkel J, Kluytmans J, Kluytmans-van den Bergh M, van den Bijllaardt W, Berntvelsen RG, van Rijen MML, Schneeberger P, Pas S, Diederen BM, Bergmans AMC, van der Eijk PAV, Verweij J, Buiting AGN, Streefkerk R, Aldenkamp AP, de Man P, Koelemal JGM, Ong D, Paltansing S, Veassen N, Sleven J, Bakker L, Brockhoff H, Rietveld A, Slijkerman Megelink F, Cohen Stuart J, de Vries A, van der Reijden W, Ros A, Lodder E, Verspui-van der Eijk E, Huijskens I, Kraan EM, van der Linden MPM, Debast SB, Naiemi N Al, Kroes ACM, Damen M, Dinant S, Lekkerkerk S, Pontesilli O, Smit P, van Tienen C, Godschalk PCR, van Pelt J, Ott A, van der Weijden C, Wertheim H, Rahamat-Langendoen J, Reimerink J, Bodewes R, Duizer E, van der Veer B, Reusken C, Lutgens S, Schneeberger P, Hermans M, Wever P, Leenders A, ter Waarbeek H, Hoebe C. 2020. Rapid SARS-CoV-2 whole-genome sequencing and analysis for informed public health decision-making in the Netherlands. Nat Med 26:1405–1410.
9. van den Hoogen BG, Herfst S, Sprong L, Cane PA, Forleo-Neto E, de Swart RL, Osterhaus ADME, Fouchier RAM. 2004. Antigenic and Genetic Variability of Human Metapneumoviruses. Emerg Infect Dis 10:658–666.
10. Williams J v., Harris PA, Tollefson SJ, Halburnt-Rush LL, Pingsterhaus JM, Edwards KM, Wright PF, Crowe JE. 2004. Human Metapneumovirus and Lower Respiratory Tract Disease in Otherwise Healthy Infants and Children. N Engl J Med 350:687–696.
11. Nao N, Saikusa M, Sato K, Sekizuka T, Usuku S, Tanaka N, Nishimura H, Takeda M. 2020. Recent molecular evolution of human metapneumovirus (HMPV): Subdivision of HMPV a2b strains. Microorganisms 8:1–14.
12. Saikusa M, Nao N, Kawakami C, Usuku S, Tanaka N, Tahara M, Takeda M, Okubo I. 2019. Predominant detection of the subgroup a2b human metapneumovirus strain with a 111-nucleotide duplication in the g gene in Yokohama city, Japan in 2018. Jpn J Infect Dis 72:350–352.
13. Boivin G, Mackay I, Sloots TP, Madhi S, Freymuth F, Wolf D, Shemer-Avni Y, Ludewick H, Gray GC, LeBlanc É. 2004. Global genetic diversity of human metapneumovirus fusion gene. Emerg Infect Dis 10:1154–1157.
14. Arshad Y, Rana MS, Ikram A, Salman M, Aamir UB, Zaidi SSZ, Alam MM, Sharif S, Shaukat S, Khurshid A, Hakim R, Mujtaba G, Umair M, Sattar S, Bostan N. 2022. Molecular detection and genetic characterization of human metapneumovirus strains circulating in Islamabad, Pakistan. Sci Rep 12:1–7.
15. Skiadopoulos MH, Biacchesi S, Buchholz UJ, Amaro-Carambot E, Surman SR, Collins PL, Murphy BR. 2006. Individual contributions of the human metapneumovirus F, G, and SH surface glycoproteins to the induction of neutralizing antibodies and protective immunity. Virology 345:492–501.
16. Kamau E, Oketch JW, de Laurent ZR, Phan MVT, Agoti CN, Nokes DJ, Cotten M. 2020. Whole genome sequencing and phylogenetic analysis of human metapneumovirus strains from Kenya and Zambia. BMC Genomics 21:1–10.
17. Pollett S, Trovão NS, Tan Y, Eden JS, Halpin RA, Bera J, Das SR, Wentworth D, Ocaña V, Mendocilla SM, Álvarez C, Calisto ME, Garcia J, Halsey E, Ampuero JS, Nelson MI, Leguia M. 2018. The transmission dynamics and diversity of human metapneumovirus in Peru. Influenza Other Respir Viruses 12:508–513.

18. Xu Y, Lewandowski K, Jeffery K, Downs LO, Foster D, Sanderson ND, Kavanagh J, Vaughan A, Salvagno C, Vipond R, Carroll M, Danby R, Peto T, Crook D, Walker AS, Matthews PC, Pullan ST. 2020. Nanopore metagenomic sequencing to investigate nosocomial transmission of human metapneumovirus from a unique genetic group among haematology patients in the United Kingdom. J Infect 80:571–577.
19. Xu Y, Lewandowski K, Lumley S, Sanderson N, Ali V, Vipond R, Carroll M, Jeffery K, Foster D, Walker AS, Peto T, Crook D, Pullan ST, Matthews PC. 2018. Nanopore metagenomic sequencing of full length human metapneumovirus (HMPV) within a unique sub-lineage. J Infect. 80(5):571-577.
20. Piñana M, Vila J, Gimferrer L, Valls M, Andrés C, Codina MG, Ramón J, Martín MC, Fuentes F, Saiz R, Rodrigo PAC, Pumarola T, Antón A. 2017. Novel human metapneumovirus with a 180-nucleotide duplication in the G gene. Future Microbiol 12:565–571.
21. Saikusa M, Nao N, Kawakami C, Usuku S, Sasao T, Toyozawa T, Takeda M, Okubo I. 2017. A novel 111-nucleotide duplication in the G gene of human metapneumovirus. Microbiol Immunol 61:507–512.
22. Munoz-Escalante JC, Mata-Moreno G, Rivera-Alfaro G, Noyola DE. 2022. Global Extension and Predominance of Human Metapneumovirus A2 Genotype with Partial G Gene Duplication. Viruses 14(5):1058.
23. Saikusa M, Kawakami C, Nao N, Takeda M, Usuku S, Sasao T, Nishimoto K, Toyozawa T. 2017. 180-nucleotide duplication in the G Gene of Human metapneumovirus A2b subgroup strains circulating in Yokohama City, Japan, since 2014. Front Microbiol 8:1–11.
24. Parida P, Sudheesh N, Sanjay ER, Jagadesh A, Marate S, Arunkuman G. 2022. The emergence of Human Metapneumovirus G gene duplication in hospitalized patients with respiratory tract infection, India, 2016-2018. Mol Biol Rep 50:1109–1116.
25. Schobel SA, Stucker KM, Moore ML, Anderson LJ, Larkin EK, Shankar J, Bera J, Puri V, Shilts MH, Rosas-Salazar C, Halpin RA, Fedorova N, Shrivastava S, Stockwell TB, Peebles RS, Hartert T v., Das SR. 2016. Respiratory Syncytial Virus whole-genome sequencing identifies convergent evolution of sequence duplication in the C-terminus of the G gene. Sci Rep 6:1–11.
26. Trento A, Galiano M, Videla C, Carballal G, García-Barreno B, Melero JA, Palomo C. 2003. Major changes in the G protein of human respiratory syncytial virus isolates introduced by a duplication of 60 nucleotides. J Gen Virol 84:3115–3120.
27. Eshaghi AR, Duvvuri VR, Lai R, Nadarajah JT, Li A, Patel SN, Low DE, Gubbay JB. 2012. Genetic variability of human respiratory syncytial virus A strains circulating in Ontario: A novel genotype with a 72 nucleotide G gene duplication. PLoS One 7(3):e32807.
28. Trento A, Viegas M, Galiano M, Videla C, Carballal G, Mistchenko AS, Melero JA. 2006. Natural History of Human Respiratory Syncytial Virus Inferred from Phylogenetic Analysis of the Attachment (G) Glycoprotein with a 60-Nucleotide Duplication. J Virol 80:975–984.
29. Kim YJ, Kim DW, Lee WJ, Yun MR, Lee HY, Lee HS, Jung HD, Kim K. 2014. Rapid replacement of human respiratory syncytial virus A with the ON1 genotype having 72 nucleotide duplication in G gene. Infec Genet Evol 26:103–112.
30. Hotard AL, Laikhter E, Brooks K, Hartert T v., Moore ML. 2015. Functional Analysis of the 60-Nucleotide Duplication in the Respiratory Syncytial Virus Buenos Aires Strain Attachment Glycoprotein. J Virol 89:8258–8266.

31. Sato M, Saito R, Sakai T, Sano Y, Nishikawa M, Sasaki A, Shobugawa Y, Gejyo F, Suzuki H. 2005. Molecular epidemiology of respiratory syncytial virus infections among children with acute respiratory symptoms in a community over three seasons. J Clin Microbiol 43:36–40.
32. Tabatabai J, Prifert C, Pfeil J, Grulich-Henn J, Schnitzler P. 2014. Novel respiratory syncytial virus (RSV) genotype ON1 predominates in germany during winter season 2012-13. PLoS One 9(10):e109191.
33. Pinana M, Vila J, Maldonado C, Galano-Frutos JJ, Valls M, Sancho J, Andres FXNC, Martín-Gomez MT, Esperalba J, Codina MG, Pumarola T, Anton A. 2020. Insights into immune evasion of human metapneumovirus: novel 180- and 111-nucleotide duplications within viral G gene throughout 2014-2017 seasons in Barcelona, Spain. J Clin Virol 132:104590.
34. van den Hoogen BG, Herfst S, de Graaf M, Sprong L, van Lavieren R, van Amerongen G, Yüksel S, Fouchier RAM, Osterhaus ADME, de Swart RL. 2007. Experimental infection of macaques with human metapneumovirus induces transient protective immunity. J Gen Virol 88:1251–1259.
35. Moriyama M, Hugentobler WJ, Iwasaki A. 2020. Seasonality of Respiratory Viral Infections. Annu Rev Virol 7:83–101.
36. Nott R, Fuller TL, Brasil P, Nielsen-Saines K. 2022. Out-of-Season Influenza during a COVID-19 Void in the State of Rio de Janeiro, Brazil: Temperature Matters. Vaccines (Basel) 10:821.
37. Eden J-S, Sikazwe C, Xie R, Deng Y-M, Sullivan SG, Michie A, Levy A, Cutmore E, Blyth CC, Britton PN, Crawford N, Dong X, Dwyer DE, Edwards KM, Horsburgh BA, Foley D, Kennedy K, Minney-Smith C, Speers D, Tulloch RL, Holmes EC, Dhanasekaran V, Smith DW, Kok J, Barr IG, Alafaci A, Carter I, Daley A, Francis M, Kesson A, Moore H, Ngo C, Tran T. 2022. Off-season RSV epidemics in Australia after easing of COVID-19 restrictions. Nat Commun 13:1–9.
38. Jones N. 2020. How COVID-19 is changing the cold and flu season. Nature 588:388–390.
39. Stein M, Cohen H, Nemet I, Atari N, Kliker L, Fratty IS, Bucris E, Geva M, Mendelson E, Zuckerman N, Mandelboim M. 2022. Human metapneumovirus prevalence during 2019-2021 in Israel is influenced by the COVID-19 pandemic. Int J Infect Dis 120:205–209.
40. Karron RA, Buchholz UJ, Collins PL. 2013. Live-attenuated respiratory syncytial virus vaccines. Curr Top Microbiol Immunol 372:259–284.
41. Nogales A, DeDiego ML, Martínez-Sobrido L. 2022. Live attenuated influenza A virus vaccines with modified NS1 proteins for veterinary use. Front Cell Infect Microbiol. 12:954811.
42. Strahle L, Garcin D, Kolakofsky D. 2006. Sendai virus defective-interfering genomes and the activation of interferon-beta. Virology 351:101–111.
43. Sekellick MJ, Marcus PI. 1978. Interferon-inducing Defective-Interfering Particles as Mediators of Cell Sparing: Possible Role in Persistent Infection by Vesicular Stomatitis Virus. Virology 85:175–186.
44. van den Hoogen BG, van Boheemen S, de Rijck J, van Nieuwkoop S, Smith DJ, Laksono B, Gultyaev A, Osterhaus ADME, Fouchier RAM. 2014. Excessive production and extreme editing of human metapneumovirus defective interfering RNA is associated with type I IFN induction. J Gen Virol 95:1625–1633.
45. Bao X, Kolli D, Ren J, Liu T, Garofalo RP, Casola A. 2013. Human Metapneumovirus Glycoprotein G Disrupts Mitochondrial Signaling in Airway Epithelial Cells. PLoS One 8(4):e62586.

46. Bao X, Liu T, Shan Y, Li K, Garofalo RP, Casola A. 2008. Human metapneumovirus glycoprotein G inhibits innate immune responses. PLoS Pathog 4(5):e1000077.
47. Kolli D, Bao X, Liu T, Hong C, Wang T, Garofalo RP, Casola A. 2011. Human Metapneumovirus Glycoprotein G Inhibits TLR4-Dependent Signaling in Monocyte-Derived Dendritic Cells. J Immunol 187:47–54.
48. Kolli D, Bao X, Liu T, Hong C, Wang T, Roberto P. 2011. Human Metapneumovirus Glycoprotein G Inhibits TLR4-Dependent Signaling in Monocyte-Derived Dendritic Cells. J Immunol 187:47–54.
49. Preston FM, Straub CP, Ramirez R, Mahalingam S, Spann KM. 2012. SiRNA against the G gene of human metapneumovirus. Virol J 9:1–5.
50. Bao X, Kolli D, Esham D, Velayutham TS, Casola A. 2018. Human metapneumovirus small hydrophobic protein inhibits interferon induction in plasmacytoid dendritic cells. Viruses 10(6):278.
51. de Graaf M, Herfst S, Aarbiou J, Burgers PC, Zaaraoui-Boutahar F, Bijl M, van IJcken W, Schrauwen EJA, Osterhaus ADME, Luider TM, Scholte BJ, Fouchier RAM, Andeweg AC. 2013. Small Hydrophobic Protein of Human Metapneumovirus Does Not Affect Virus Replication and Host Gene Expression In Vitro. PLoS One 8:1–10.
52. Hastings AK, Amato KR, Wen SC, Peterson LS, Williams V. 2016. Human metapneumovirus small hydrophobic (SH) protein downregulates type I IFN pathway signaling by affecting STAT1 expression and phosphorylation. Virology 494:248–256.
53. Ren J, Wang Q, Kolli D, Prusak DJ, Tseng C-TK, Chen ZJ, Li K, Wood TG, Bao X. 2012. Human Metapneumovirus M2-2 Protein Inhibits Innate Cellular Signaling by Targeting MAVS. J Virol 86:13049–13061.
54. Ren J, Liu G, Go J, Kolli D, Zhang G, Bao X. 2014. Human metapneumovirus M2-2 protein inhibits innate immune response in monocyte-derived dendritic cells. PLoS One 9:1–9.
55. Kitagawa Y, Sakai M, Funayama M, Itoh M, Gotoh B. 2017. Human Metapneumovirus M2-2 Protein Acts as a Negative Regulator of Alpha Interferon Production by Plasmacytoid Dendritic Cells. J Virol 91:1–15.
56. Lim CS, Brown CM. 2016. Hepatitis B virus nuclear export elements: RNA stem-loop α and β, key parts of the HBV post-transcriptional regulatory element. RNA Biol 13:743–747.
57. Fearns R, Collins PL. 1999. Role of the M2-1 Transcription Antitermination Protein of Respiratory Syncytial Virus in Sequential Transcription. J Virol 73:5852–5864.
58. Kitagawa Y, Zhou M, Yamaguchi M, Komatsu T, Takeuchi K, Itoh M, Gotoh B. 2010. Human metapneumovirus M2-2 protein inhibits viral transcription and replication. Microbes Infect 12:135–145.
59. Cheng X, Park H, Zhou H, Jin H. 2005. Overexpression of the M2-2 Protein of Respiratory Syncytial Virus Inhibits Viral Replication. J Virol 79:13943–13952.
60. Schickli JH, Kaur J, MacPhail M, Guzzetta JM, Spaete RR, Tang RS. 2008. Deletion of human metapneumovirus M2-2 increases mutation frequency and attenuates growth in hamsters. Virol J 5:1–14.
61. Bermingham A, Collins PL. 1999. The M2-2 protein of human respiratory syncytial virus is a regulatory factor involved in the balance between RNA replication and transcription. Proc Natl Acad Sci U S A 96:11259–11264.
62. Boonyaratanakornkit J, Bartlett E, Schomacker H, Surman S, Akira S, Bae Y-S, Collins P, Murphy B, Schmidt A. 2011. The C Proteins of Human Parainfluenza Virus Type 1 Limit Double-Stranded RNA Accumulation That Would Otherwise Trigger Activation of MDA5 and Protein Kinase R. J Virol 85:1495–1506.

63. Pfaller CK, Mastorakos GM, Matchett WE, Ma X, Samuel CE, Cattaneo R. 2015. Measles Virus Defective Interfering RNAs Are Generated Frequently and Early in the Absence of C Protein and Can Be Destabilized by Adenosine Deaminase Acting on RNA-1-Like Hypermutations. J Virol 89:7735–7747.
64. Sánchez-Aparicio MT, Garcin D, Rice CM, Kolakofsky D, García-Sastre A, Baum A. 2017. Loss of Sendai virus C protein leads to accumulation of RIG-I immunostimulatory defective interfering RNA. J Gen Virol 98:1282–1293.
65. Takeuchi K, Komatsu T, Kitagawa Y, Sada K, Gotoh B. 2008. Sendai Virus C Protein Plays a Role in Restricting PKR Activation by Limiting the Generation of Intracellular Double-Stranded RNA. J Virol 82:10102–10110.
66. Whelan SPJ, Barr JN, Wertz GW. 2004. Transcription and Replication of Nonsegmented Negative-Strand RNA Viruses. Curr Top Microbiol Immunol. 283:61-119.
67. Gould PS, Easton AJ. 2007. Coupled Translation of the Second Open Reading Frame of M2 mRNA Is Sequence Dependent and Differs Significantly within the Subfamily Pneumovirinae. J Virol 81:8488–8496.
68. Sedeyn K, Schepens B, Saelens X. 2019. Respiratory syncytial virus nonstructural proteins 1 and 2: Exceptional disrupters of innate immune responses. PLoS Pathog 15:1–18.
69. Andrejeva J, Childs KS, Young DF, Carlos TS, Stock N, Goodbourn S, Randall RE. 2004. The V proteins of paramyxoviruses bind the IFN-inducible RNA helicase, mda-5, and inhibit its activation of the IFN-β promoter. Proc Natl Acad Sci U S A 101:17264–17269.
70. Sanchez-Aparicio MT, Feinman LJ, Garcia-Sastre A, Shaw ML, Complex R, Signaling IR, Sánchez-aparicio MT, Feinman LJ, García-sastre A, Shaw L. 2018. Paramyxovirus V Proteins Interact with the RIG-I/TRIM25 Regulatory Complex and Inhibit RIG-I Signaling. J Virol 92:1–21.
71. Ban J, Lee NR, Lee NJ, Lee JK, Quan FS, Inn KS. 2018. Human respiratory syncytial virus NS1 targets TRIM25 to suppress RIG-I ubiquitination and subsequent RIG-I-mediated antiviral signaling. Viruses 10(12):716.
72. Ling Z, Tran KC, Teng MN. 2009. Human Respiratory Syncytial Virus Nonstructural Protein NS2 Antagonizes the Activation of Beta Interferon Transcription by Interacting with RIG-I. J Virol 83:3734–3742.
73. Ayllon J, Garcia-Sastre A. 2014. The NS1 Protein: A Multitasking Virulence Factor. Curr Top Microbiol Immunol 386:73–107.
74. Oh SJ, Shin OS. 2021. SARS-CoV-2 nucleocapsid protein targets RIG-I-like receptor pathways to inhibit the induction of interferon response. Cells 10:1–13.
75. Lei X, Dong X, Ma R, Wang W, Xiao X, Tian Z, Wang C, Wang Y, Li L, Ren L, Guo F, Zhao Z, Zhou Z, Xiang Z, Wang J. 2020. Activation and evasion of type I interferon responses by SARS-CoV-2. Nat Commun 11:1–12.
76. Hayn M, Hirschenberger M, Koepke L, Nchioua R, Straub JH, Klute S, Hunszinger V, Zech F, Prelli Bozzo C, Aftab W, Christensen MH, Conzelmann C, Müller JA, Srinivasachar Badarinarayan S, Stürzel CM, Forne I, Stenger S, Conzelmann KK, Münch J, Schmidt FI, Sauter D, Imhof A, Kirchhoff F, Sparrer KMJ. 2021. Systematic functional analysis of SARS-CoV-2 proteins uncovers viral innate immune antagonists and remaining vulnerabilities. Cell Rep 35(7):109126.
77. Rijsbergen LC, van Dijk LLA, Engel MFM, de Vries RD, de Swart RL. 2021. In Vitro Modelling of Respiratory Virus Infections in Human Airway Epithelial Cells – A Systematic Review. Front Immunol 12:1–18.

78. Anderson CS, Chu CY, Wang Q, Mereness JA, Ren Y, Donlon K, Bhattacharya S, Misra RS, Walsh EE, Pryhuber GS, Mariani TJ. 2020. CX3CR1 as a respiratory syncytial virus receptor in pediatric human lung. Pediatr Res 87:862–867.
79. Johnson SM, McNally BA, Ioannidis I, Flano E, Teng MN, Oomens AG, Walsh EE, Peeples ME. 2015. Respiratory Syncytial Virus Uses CX3CR1 as a Receptor on Primary Human Airway Epithelial Cultures. PLoS Pathog 11:1–16.
80. Kinder JT, Moncman CL, Barrett C, Jin H, Kallewaard N. 2020. Respiratory Syncytial Virus and Human Metapneumovirus an Interesting Dichotomy in Viral Replication, Spread, and Inhibition by Neutralizing Antibodies. J Virol 94:1–20.
81. Geiser J, Boivin G, Huang S, Constant S, Kaiser L, Tapparel C, Essaidi-Laziosi M. 2021. RSV and HMPV Infections in 3D Tissue Cultures: Mechanisms Involved in Virus-Host and Virus-Virus Interactions Johan. Viruses 13:1–15.
82. Muramoto Y, Noda T, Kawakami E, Akkina R, Kawaoka Y. 2013. Identification of Novel Influenza A Virus Proteins Translated from PA mRNA. J Virol 87:2455–2462.
83. Selman M, Dankar SK, Forbes NE, Jia JJ, Brown EG. 2012. Adaptive mutation in influenza A virus non-structural gene is linked to host switching and induces a novel protein by alternative splicing. Emerg Microbes Infect 1(11):e42.
84. Wise HM, Foeglein A, Sun J, Dalton RM, Patel S, Howard W, Anderson EC, Barclay WS, Digard P. 2009. A Complicated Message: Identification of a Novel PB1-Related Protein Translated from Influenza A Virus Segment 2 mRNA. J Virol 83:8021–8031.
85. Wise HM, Hutchinson EC, Jagger BW, Stuart AD, Kang ZH, Robb N, Schwartzman LM, Kash JC, Fodor E, Firth AE, Gog JR, Taubenberger JK, Digard P. 2012. Identification of a Novel Splice Variant Form of the Influenza A Virus M2 Ion Channel with an Antigenically Distinct Ectodomain. PLoS Pathog 8(11):e1002998.
86. B. W. Jagger, H. M. Wise, J. C. Kash, A. Walters, N. M. Wills, Y.-L. Xiao, R. L. Dunfee, L. M. Schwartzman, A. Ozinsky, G. L. Bell, R. M. Dalton, A. Lo, S. Efstathiou, J. F. Atkins, A. E. Firth, J. K. Taubenberger, P. Digard. 2012. An Overlapping Protein-Coding Region in Influenza A Virus Segment 3 Modulates the Host Response. Science 337:1999–204.
87. Chen W, Calvo PA, Malide D, Gibbs J, Schubert U, Bacik I, Basta S, O'Neill R, Schickli J, Palese P, Henklein P, Bennink JR, Yewdell JW. 2001. A novel influenza A virus mitochondrial protein that induces cell death. Nat Med 7:1306–1312.
88. Buijs P, van Nieuwkoop S, Vaes V, Fouchier R, van Eijck C, van den Hoogen B. 2015. Recombinant immunomodulating lentogenic or mesogenic oncolytic newcastle disease virus for treatment of pancreatic adenocarcinoma. Viruses 7:2980–2998.

8

Appendices

Nederlandse samenvatting

Het humaan metapneumvoirus (HMPV), een pneumovirus, is een belangrijke veroorzaker van luchtweginfecties met name in jonge kinderen. Tussen de 5-15% van luchtweginfecties in deze groep wordt veroorzaakt door HMPV. De piek van infecties is in kinderen in de leeftijd van 3 tot 6 maanden oud en zo goed als elk kind heeft een HMPV infectie doorstaan tegen de tijd dat ze 5 jaar zijn. Naast kinderen zijn ook ouderen en immuun gecompromitteerde mensen vatbaar voor ziekte die veroorzaakt wordt door HMPV infecties. De klinische symptomen van een HMPV infectie zijn vergelijkbaar met die veroorzaakt door een infectie met het respiratoir syncytieel virus (RSV), het enige andere humane pneumovirus, wat varieert van hoesten en keelpijn in milde gevallen tot bronchiolitis en pneumonie in ernstigere gevallen. HMPV wordt voornamelijk gedetecteerd in het winterseizoen, met over het algemeen een piek rond het einde van de winter en begin van de lente. Ondanks de morbiditeit die veroorzaakt wordt door HMPV is er op dit moment nog geen vaccin of antivirale therapie beschikbaar.

Het bestuderen van HMPV evolutie en epidemiologie is belangrijk voor het updaten van diagnostische testen en het rationeel ontwerpen van vaccins of antivirale behandelingen. Op basis van serologische studies zijn HMPV stammen geclassificeerd in twee serotypes, A en B, welke beide op basis van genetische verschillen onderverdeeld zijn in twee genotypes (A1, A2, B1, B2). Recent zijn er door verschillende groepen afsplitsingen gerapporteerd binnen genotype A2, waar verschillende naamgevingen voor zijn gebruikt. Ondanks dat er verschillende studies zijn gedaan naar de evolutie van HMPV, is er binnen het onderzoeksveld nog geen consensus over de classificatie of nomenclatuur van de verschillende nieuwe genotypes van het virus, en grootschalige evolutie studies voor HMPV zijn nog schaars.

De genotypes van HMPV worden voornamelijk geclassificeerd op basis van de sequenties van het fusie eiwit (F) gen of het glycoprotein (G) gen. Dit komt doordat G het meest variabele eiwit is, wat een groot onderscheidend vermogen geeft, en F onder druk staat van het immuunsysteem waardoor mutaties kunnen ontstaan die leiden tot nieuwe genotypes. Ondanks dat voornamelijk de F en G genen gesequenced worden in HMPV evolutie studies, kunnen door het sequencen van het complete HMPV genoom accuratere evolutie studies uitgevoerd worden. Technieken om complete virale genomen te sequencen zijn over de afgelopen jaren makkelijker in uitvoering en goedkoper geworden, maar er zijn maar weinig studies waarbij hele genomen van HMPV gesequenced zijn. In de meeste studies bleek het gevoelig detecteren van het G gen lastig, wat mede komt door de hoge variabiliteit van het gen.

In de studie in **hoofdstuk 2** is een methode opgezet voor het sequencen van hele HMPV genomen die geïsoleerd zijn uit klinische monsters. Deze methode had een goede detectie van het G gen en detecteerde de vier voorheen

beschreven HMPV genotypes met een gelijke gevoeligheid. In **hoofdstuk 3** is deze methode gebruikt voor het sequencen van de complete genomen van 130 HMPVs geisoleerd uit klinische monsters. Deze sequenties zijn gebruikt om de evolutie van HMPV in Nederland tussen 2005 en 2021 te bestuderen. Hieruit bleek dat er zes genotypes circuleerde (A1, A2.1, A2.2.1, A2.2.2, B1, en B2), waarvan genotype A1 niet meer gedetecteerd werd sinds 2006. Dit zou kunnen betekenen dat dit genotype uitgestorven is, of dat het virus circuleert in een populatie waar geen surveillance plaatsvindt. Net als door andere onderzoeksgroepen zijn binnen genotype A2.2.2 varianten gevonden met een duplicatie in het G gen, waarvan de functie tot dusver nog onbekend is. De varianten met een duplicatie in het G gen werden in Nederland voor het eerst gedetecteerd in 2015 en na 2018 hadden alle genotype A2.2.2 virussen een duplicatie in het G gen. Al eerder zijn er ook voor RSV virussen met duplicaties in het G gen gedetecteerd, welke zich snel wereldwijd verspreid hebben. Het feit dat er nu ook HMPVs met een duplicatie in het G gen zijn gedetecteerd suggereert dat pneumovirussen met een duplicatie in het G eiwit een voordeel hebben over virussen zonder duplicatie, maar op dit moment is er nog geen bewijs voor deze hypothese.

In **hoofdstuk 3** is vervolgens de circulatie van de verschillende genotypes in de klinische setting vergeleken met die in een niet-klinische setting. Voor deze laatste populatie zijn de F en G gen sequenties geanalyseerd van 144 HMPVs geïsoleerd uit patiënten die huisartsen bezoeken voor luchtwegklachten. Een vergelijking tussen de circulatie van de verschillende genotypes tussen de twee populaties liet zien dat alle genotypes in beide populaties even vaak voorkwamen. Dit suggereert dat er geen verschil is in pathogeniteit tussen de verschillende genotypes. Daarentegen is er in andere studies wel meer viraal RNA gevonden in monsters van ziekenhuispatiënten die geïnfecteerd waren met genotype A virussen dan in patiënten die geïnfecteerd waren met type B virussen. Of deze hogere hoeveelheid viraal RNA bijdraagt aan een ernstiger ziekteverloop is nog onduidelijk.

De meeste virussen die luchtweginfecties veroorzaken zijn voornamelijk prevalent in de winter. Dit werd voorheen verklaard door meerdere factoren, waaronder humaan gedrag, klimaatfactoren zoals luchtvochtigheid, of een minder functionerend immuunsysteem in de populatie door een gebrek aan zonlicht. Na het opheffen van de niet-medische interventiemaatregelen betreffende de SARSCoV2 pandemie zijn er echter meerdere respiratoire virussen gedetecteerd buiten het normale winterseizoen, waaronder het influenzavirus en RSV. Dit is ook zo gerapporteerd voor HMPV, waarvoor in **hoofdstuk 4** een HMPV uitbraak in het Zuyderland Medisch Centrum in Heerlen in de zomer van 2021 wordt beschreven. Detectie van deze virussen buiten het normale seizoen zou kunnen komen doordat mensen minder in contact zijn geweest met seizoensgebonden virussen tijdens de lockdown periodes,

waardoor de immuniteit op populatieniveau verminderde. Hierdoor zou men vatbaarder kunnen zijn voor respiratoire virussen, ongeacht het seizoen. Het is onduidelijk hoelang deze virusuitbraken in de zomer zullen blijven gebeuren nu dat de SARS-CoV-2 lockdown maatregelen voorbij zijn. Circulatie buiten het seizoen kan een gevolg hebben voor de timing van het toedienen van seizoensgebonden influenzavirus vaccinaties en andere seizoensgebonden vaccinaties in de toekomst.

Het aangeboren immuunsysteem is een belangrijke barrière in het menselijk lichaam dat een virus moet overkomen om de gastheer te infecteren. Deze immuunreactie wordt gekenmerkt door de productie van type-1 interferonen. De meeste virussen die ziekte veroorzaken in mensen kunnen deze reactie ontwijken. In de meeste gevallen gebruiken deze virussen eiwitten die ervoor zorgen dat interferonen niet worden aangemaakt. Deze eiwitten worden interferonantagonisten genoemd. Voor HMPV nog niet bekend welke eiwitten functioneren als interferon-antagonist. Fundamenteel onderzoek naar hoe virussen deze interferon reactie ontwijken kan leiden tot een rationeel ontwerp van levendverzwakte vaccins.

Voor HMPV hebben een aantal studies gesuggereerd dat de G, shorthydrophobic (SH), en matrix 2-2 (M2-2) eiwitten een rol spelen als interferon-antagonist. Echter is in deze studies voor alle drie de eiwitten dezelfde functie beschreven en in het onderzoeksveld is nog geen consensus bereikt over welk eiwit als interferon antagonist functioneert of over het mechanisme dat HMPV hiervoor gebruikt. Dit zou kunnen komen doordat het genereren en passeren van HMPV in cellen kan leiden tot de productie van defecte viruspartikels, welke bekend staan om het induceren van interferon productie. In **hoofdstuk 5** is de rol van het G, SH, en M2-2 eiwit als interferonantagonist onderzocht, waarvoor virussen zijn gegenereerd die geen G, SH, of M2-2 eiwitexpressie hebben. Deze virussen zijn geproduceerd door middel van een methode die de productie van defecte viruspartikels voorkomt. Uit deze studie bleek dat, in tegenstelling tot de gepubliceerde studies, de G en SH eiwitten geen rol spelen in het blokkeren van de interferon productie. Virussen die geen M2-2 eiwit tot expressie brachten induceerde wel interferon productie, maar deze virus stocks bleken toch ook defecte viruspartikels te hebben ondanks dat deze virus stocks zodanig waren geproduceerd waarbij het wildtype virus geen defecte viruspartikels produceerde. Daarnaast werd er in het genoom van deze M2-2 deletie virussen een hoog aantal mutaties gevonden. Hierdoor is het onduidelijk of de inductie van interferon door deze virussen komt door de afwezigheid van het M2-2 eiwit als interferon-antagonist, of door de defecte viruspartikels en mutaties in het genoom van deze virussen. Deze vraag is tot dusver nog onbeantwoord, waardoor het nog onzeker is of het M2-2 eiwit functioneert als een interferonantagonist.

De M2-1 en M2-2 eiwitten van pneumovirussen spelen een rol tijdens virus replicatie, maar hoe deze eiwitten daarin precies functioneren is nog onbekend. Ook is bekend dat de genen van pneumovirussen tot expressie worden gebracht door middel van een transcriptie gradient, waarbij de expressie van genen die dichter bij de promoter gelegen zijn hoger is dan dat van genen die verder weg van de promoter gelegen zijn. Het M2-1 eiwit bijdraagt bij aan het behouden van deze transcriptie gradient. In **hoofdstuk 6** is de functie van de M2-1 en M2-2 eiwitten van pneumovirussen tijdens transcriptie onderzocht. Hiervoor zijn chimere HMPVs gegenereerd waarbij het M2 gen, wat zowel M2-1 en M2-2 codeert, vervangen werd voor het M2 gen van RSV of avian pneumovirus type-C (APV-C). APV-C is ook een pneumovirus, maar heeft vogelsoorten als gastheer. Om de rol van het M2-2 eiwit los te koppelen van die van het M2-1 eiwit, zijn virussen gegenereerd waarin alleen het M2-2 gen werd vervangen voor dat van RSV of APV-C. Fenotypische karakterisatie van deze virussen toonde aan dat wanneer beide M2 eiwitten van HMPV werden vervangen door die van RSV of APV-C, deze virussen hetzelfde fenotype lieten zien als wildtype HMPV wat betreft inductie van interferon, afwezigheid van hypermutatie in de virale genomen en RNA transcriptie profielen in de eerste 48 uur na infectie. Dit was in tegenstelling tot de virussen waarin alleen het M2-2 eiwit was uitgewisseld. Deze virussen induceerde interferon productie, bevatte hypermutaties in hun genoom en hadden een andere RNA transcriptie gradiënt gedurende de eerste 48 uur na infectie dan het wild type HMPV. Deze resultaten laten zien dat het M2-2 eiwit van pneumovirussen, maar alleen in samenwerking met het homologe M2-1 eiwit, een functie heeft tijdens transcriptie elongatie en de productie van defectieve RNAs en hyper gemuteerde genomen voorkomt.

Als laatste is geprobeerd om de potentiële functie van het M2-2 eiwit als interferon-antagonist te onderzoeken. Hiervoor is een chimeer RSV gegenereerd waarin de NS1 en NS2 genen, welke coderen voor interferon-antagonisten, werden vervangen voor het HMPV M2-2 gen. Hiermee werd onderzocht of het HMPV M2-2 eiwit de functie kon overnemen van de RSV interferon-antagonisten. De resultaten in **hoofdstuk 6** laten zien dat het HMPV M2-2 eiwit de functie als interferon antagonist van de RSV NS1 en NS2 eiwitten niet kon overnemen, waardoor een functie van het HMPV M2-2 eiwit als interferon-antagonist als onwaarschijnlijk kan worden geacht.

Op dit moment is er nog geen vaccin of antivirale therapie beschikbaar voor HMPV. De fundamentele studies beschreven in dit proefschrift dragen bij aan het in kaart brengen van HMPV evolutie en het begrijpen van virale mechanismes voor het ontwijken van ons aangeboren immuunsysteem. Deze studies zijn belangrijk voor het rationeel ontwerpen van antivirale therapieën of vaccins, welke in de toekomst kunnen bijdragen aan het verminderen van de morbiditeit van HMPV.

Portfolio

Courses and certificates	**Year**
Department and workgroup meetings	2018-2022
Stem Cells, Organoids and Regenerative Medicine (SCORE)	2019
Scientific Integrity	2019
Biostatistical Methods I: Basic Principles Part A	2019
Introduction to GraphPad Prism Version 7	2019
Microscopic Image Analysis: From Theory to Practice	2019
Biomedical English Writing	2019
Advanced course on Applications in flow cytometry	2019
Course in Virology	2021

Teaching and supervision	
Alexander Havelaar, Bachelor student (9 months)	2019-2020
Master I&I lecture on innate immunity	2019, 2022

Conferences and Symposia	
Oral presentations	
Viruses – Novel Concepts in Virology	2020
12th International RSV Symposium	2022
Poster presentations	
Negative sense virus	2022
Attended	
European Conference on Virology	2019
Dutch Annual Virology Symposium	2019, 2020

Achievements	
Oral Presentation – 2nd place at the 12th International RSV Symposium	2022

List of publications

Groen K, van Nieuwkoop S, Meijer A, van der Veer B, van Kampen JJA, Fraaij PL, Fouchier RAM, van den Hoogen BG. Emergence and Potential Extinction of Genetic Lineages of Human Metapneumovirus between 2005 and 2021. mBio. 2023 Feb 28;14(1):e0228022. doi: 10.1128/mbio.02280-22.

Groen K, van Nieuwkoop S, Lamers MM, Fouchier RAM, van den Hoogen BG. Evidence against the Human Metapneumovirus G, SH, and M2-2 Proteins as Bona Fide Interferon Antagonists. J Virol. 2022 Aug 17:e0072322.

Kivit C, **Groen K**, Jongbloed M, Linssen C, van Loo A, van Gorp E, van Nieuwkoop S, den Hoogen BV, Kruif M. An off-season outbreak of human metapneumovirus infections after ending of a COVID-19 lockdown. J Infect. 2022 May;84(5):722-746.

Kevin Groen, Stefan van Nieuwkoop, Theo M Bestebroer, Pieter L Fraaij, Ron A M Fouchier, Bernadette G van den Hoogen. Whole genome sequencing of human metapneumoviruses from clinical specimens using MinION nanopore technology. Virus Res. 2021 Sep;302:198490.

Gilles Darcis, Neeltje A Kootstra, Berend Hooibrink, Thijs van Montfort, Irma Maurer, **Kevin Groen**, Suzanne Jurriaa, Margreet Bakker, Carine van Lint, Ben Berkhout, Alexander O Pasternak. CD32 + CD4 + T Cells Are Highly Enriched for HIV DNA and Can Support Transcriptional Latency. Cell Rep. 2020 Feb 18;30(7):2284-2296.e3.

Thijs van Montfort, Renée van der Sluis, Gilles Darcis, Doyle Beaty, **Kevin Groen**, Alexander O Pasternak, Georgios Pollakis, Monique Vink, Ellen M Westerhout, Mohamed Hamdi, Margreet Bakker, Boas van der Putten, Suzanne Jurriaans, Jan H Prins, Rienk Jeeninga, Adri A M Thomas, Dave Speijer, Ben Berkhout. Dendritic cells potently purge latent HIV-1 beyond TCR-stimulation, activating the PI3K-Akt-mTOR pathway. EBioMedicine. 2019 Apr;42:97-108.

Marilia Rita Pinzone, D Jake VanBelzen, Sam Weissman, Maria Paola Bertuccio, LaMont Cannon, Emmanuele Venanzi-Rullo, Stephen Migueles, R Brad Jones, Talia Mota, Sarah B Joseph, **Kevin Groen**, Alexander O Pasternak, Wei-Ting Hwang, Brad Sherman, Anastasios Vourekas, Giuseppe Nunnari, Una O'Doherty. Longitudinal HIV sequencing reveals reservoir expression leading to decay which is obscured by clonal expansion. Nat Commun. 2019 Feb 13;10(1):728.

Oudshoorn D, Rijs K, Limpens RWAL, **Groen K**, Koster AJ, Snijder EJ, Kikkert M, Bárcena M. Expression and Cleavage of Middle East Respiratory Syndrome Coronavirus nsp3-4 Polyprotein Induce the Formation of Double-Membrane Vesicles That Mimic Those Associated with Coronaviral RNA Replication. MBio. 2017 Nov 21;8(6). pii: e01658-17.

I very much appreciate everyone who supported me in over the past years:

Bernadette, Ron, Marion, Frederique, Pau, Susma, Daphne, Marco, Anne, Lex, Sander, Mathilde, Adinda, Miruna, Jasmine, Ilona, Anja, Mathis, Monique, Willemijn, Dennis, Theo, Pascal, Mark, Sacha, Rik, Rory, Katie, Daryl, Lennert, Laura, Yvette, Bernard, Bri, Lisa, Kristina, Feline, Shirley, Diana, Seyar, Werner, Mart, Tim, Peter, Bas, Gijs, Jeroen, Pieter, Danny, Claudia, Debbie, Petra, Nella, David, Chantal, Machteld, Simone, Anouk, Maria, Maarten, Monique, Ingrid, Wim, Helga, Wesley, Kim, Jan, Ria, Rie, Maarten, Teoman, Elmar, Rob, Robin, Max, Stelios

Stefan

Juha

Laurine


Mavs
Mda-5
Pkr
RIG-1
Interferon
Ifnar
Stat1
G
M2-2
sh